DISSECTING THE ROLE OF SUP-17/ADAM10 IN THE BONE MORPHOGENETIC PROTEIN SIGNALING PATHWAY IN *C. ELEGANS*

A Dissertation

Presented to the Faculty of the Graduate School

of Cornell University

In Partial Fulfillment of the Requirements for the Degree of

Doctor of Philosophy

by

Lin Wang

May 2018

DISSECTING THE ROLE OF SUP-17/ADAM10 IN THE BONE MORPHOGENETIC PROTEIN SIGNALING PATHWAY IN C. ELEGANS

Lin Wang, Ph. D.

Cornell University 2018

Bone morphogenetic proteins (BMPs) belong to the transforming growth factor (TGF-β) superfamily of ligands and mediate a highly conserved signal transduction cascade. Following ligand binding, the type I receptors are phosphorylated by the type II receptors on the cell surface. Then activated type I receptors phosphorylate and release the receptor mediated Smads (R-Smads), which subsequently complex with common mediator Smad (co-Smad) and shuttle into the nucleus to regulate target gene transcription. The BMP pathway plays multiple important roles in regulating development and tissue homeostasis. Abnormalities of the BMP signaling pathway are often associated with physiological disorders and diseases in human, which include, but are not limited to, skeleton diseases, cardiovascular disorders and cancers. Thus it is important to ensure tight regulations of BMP signaling. The Liu lab uses *C. elegans* as a model system to investigate regulations of a BMP-like signaling pathway. Using a genetic screen highly specific to the BMP pathway, many novel modulators of the pathway have been identified that function at the ligand-receptor level. Among them are two paralogous tetraspanins, TSP-12 and TSP-14, the netrin receptor UNC-40/Neogenin, and the RGM protein DRAG-1. However, how these new players

interact with the ligand-receptor complex or with other cell surface modulators to regulate BMP signaling is not fully understood.

SUP-17/ADAM10 belongs to the ADAM (a disintegrin and metalloprotease) family of transmembrane proteins that are known for cleaving many membrane and membrane-associated proteins through 'ectodomain shedding'. In this thesis, I reveal that SUP-17/ADAM10 is expressed and functions in the signal receiving cells to regulate BMP signaling. Endogenously tagged SUP-17 is localized both to the cell surface and to intracellular vesicles. In embryos, null mutations in *tsp-12,* but not in *tsp-14,* cause decreased SUP-17 localization at the cell surface, and show increased accumulated localization in early and late endosomes. TSP-12 may also facilitate the cleavage of SUP-17's pro-domain in gravid adults. Using genetic approaches, I identified UNC-40/Neogenin as one of the substrates of SUP-17 in BMP signaling. Using western blotting, I generated preliminary evidence suggesting that the endogenous UNC-40 may be cleaved by SUP-17, and that there is a slight increase in steady state protein level of UNC-40 in adult *tsp-12(0)* mutants and a decrease in *drag-1(0)* mutants. These results suggested a model for how these BMP modulators may function to regulate BMP signaling: tetraspanins TSP-12 and TSP-14 regulate the cell surface localization and maturation of SUP-17/ADAM10, which in turn cleaves UNC-40/neogenin and other proteins to regulate the signaling pathway. Future work will be needed to identify the additional substrates of SUP-17/ADAM10 in the BMP pathway.

BIOGRAPHICAL SKETCH

Lin Wang was born in Shenyang, China in 1990. Thanks to the scientific micro climate in her family, Lin gained her passion about biology and enrolled in China Agriculture University in Beijing in 2008, majoring Biological Sciences. The undergraduate training solidified her desire of doing cutting-edge research in this field, so she came to Cornell University in 2012 and became a graduate student in the department of Molecular Biology and Genetics.

ACKNOWLEDGMENTS

I am excited to express my gratitude to all the following individuals who have made this dissertation possible.

First and foremost, I would like to thank my advisor Jun (Kelly) Liu for her mentorship throughout my research experience at Cornell: her inspirations, her innovations, her critical thinking and her motherly kindness. She is always insightful in my experiment design and has devoted a lot of time to help me in the lab, which is extremely beneficial for the development of my fundamental scientific skills. She burnished not only my academic capability but also my well-round personality. None of the work would be possible without her help, and my gratitude is beyond my words.

I am fortunate to have Kenneth Kemphues and Mariana Wolfner on my committee. I benefited a lot from Ken's deep knowledge of *C. elegans* and from Mariana's explanation of profound genetics in a straightforward way. The incisive feedback and pinpointing advice from both of them have made my research more comprehensive.

I would like to express my warmest thanks to everyone in the Liu lab. I appreciate Zhiyu Liu and Herong Shi for taking indispensable roles in my project, as well as for being friends in and out of the lab. I also thank Erich Schwarz for sharing with the lab much of his expertise in genomics. Also, thanks to Melisa, Anthony, Alex, Gaby and Justin, our lab is made to a lively working place.

Special thanks to my parents for introducing me to science and always being understanding for every decision I make. Finally, upon his request, I would like to thank my husband Rusen Yan for his unconditional support of my career as well as his growing tolerance as I gradually filled up our bedroom with countless plush & stuffed animals from ToysRUs and Disney Stores.

TABLE OF CONTENT

LIST OF FIGURES

LIST OF TABLES

LIST OF ABBREVIATIONS

C. elegans: *Caenorhabditis elegans*

TGFβ: transforming growth factor-β

TβRI: type I TGF β receptor

TβRII: type II TGF β receptor

BMP: bone morphogenetic protein

ADAM: a disintegrin and metalloproteinase

TACE: tumor necrosis factor-alpha-converting enzyme

CCs: coelomocytes

Susm: suppression of the *sma-9* mesoderm phenotype

RAD-SMAD: reporter acting downstream of SMAD

CRISPR: clustered regularly interspaced short palindromic repeats

SS: secretion signal

EXD: extracellular domain

TMD: transmembrane domain

ICD: intracellular domain

ER: endoplasmic reticulum

UNC: uncoordinated

RGM: repulsive guidance molecule

LRIG: leucine-rich repeats and immunoglobulin-like domains protein

CR: cysteine-rich

PR: pathogenesis related

PC: proprotein convertase

GPI: glycosylphosphatidylinositol

CHAPTER 1

INTRODUCTION

1.1 The TGFβ signaling pathway

The transforming growth factor β (TGF-β) signaling pathway plays tremendously important roles in development. Mutations in the ligands, receptors or effectors are associated with cancers. Malfunction of the pathway causes widespread developmental disorders and human diseases [1]. TGF-β signals through a highly conserved transduction cascade [2] (Figure 1.1).

The TGF-β ligand is translated with a prodomain upstream of the mature domain. The prodomain prevents the ligand from binding to its receptors [3] and facilitates its targeting to the extracellular matrix [4]. Furin family proprotein convertases are involved in the removal of the prodomain in the secreted pathway, resulting in activated ligands. There are two cleavage sites in the prodomain of TGF-β ligands [5]. The first cleavage is right before the mature domain, however the cleaved prodomain still remains non-covalently associated with the mature domain. After the second cleavage, fully active TGF-βs are released and can bind to the receptors as dimers.

TGF-β receptors form a hetero-tetrameric complex comprised of two dimers of type I and type II receptors. Both type I and type II receptors are serine/threonine kinases each having a N-terminal extracellular ligand binding domain, a transmembrane domain and a C-terminal serine/threonine kinase domain. The TGF-

β type II receptors are constitutively phosphorylated and can bind to the TGF-β ligand dimer. Type I receptors can also bind to ligands in the presence of the type II receptors and are phosphorylated by type II receptors in the cytoplasmic GS domain. The GS domain has a characteristic SGSGSG sequence preceding the kinase domain of type I receptor, but this sequence is not present in the type II receptor [6].

Activated type I receptors recruit and phosphorylate the two C-terminal Serines in the SSXS motif of receptor mediated Smads (R-Smads) [7, 8]. The phosphorylated R-Smads are then released from the type I receptors and form a heteromeric complex with the common mediator Smad (Co-Smad) in the cytoplasm. The hetero-oligomerized Smad complex then translocates into the nucleus and regulates gene expression. Both R-Smads and co-Smad have an N-terminal Mad homolog domain-1(MH1) and a C-terminal Mad homolog domain-2(MH2), the two domains are connected by a proline-rich linker. The MH2 domain is involved in protein-protein interaction, while the MH1 domain binds to DNA at the 8 bp palindromic Smad binding element (SBE) [9]. However, Smads' binding to DNA is weak, and is assisted by DNA binding partners.

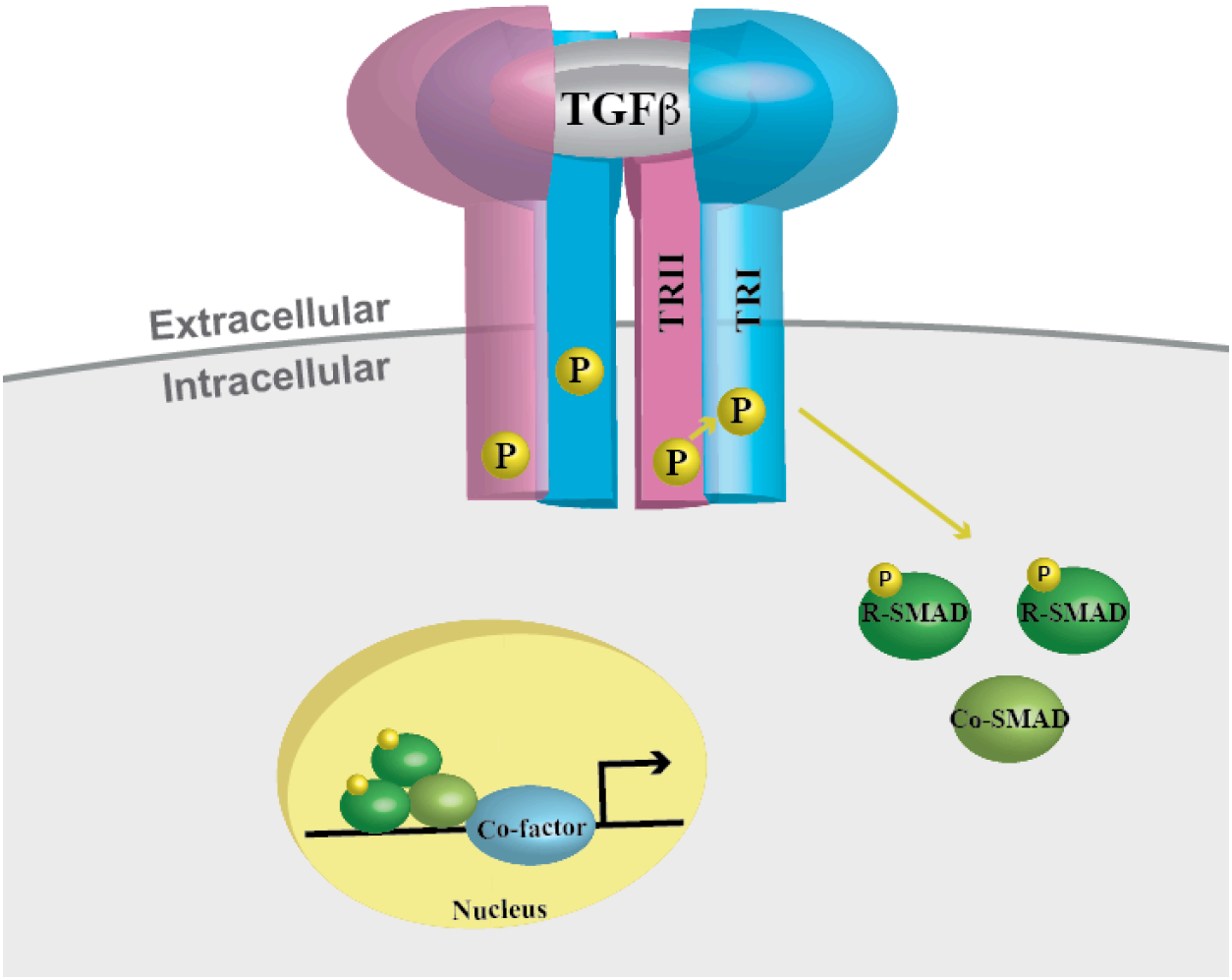

Figure 1.1 The TGF-β signaling pathway

TGFβs initiate the signaling cascade by binding to the type I and type II receptors on the cell surface. The receptors have serine/threonine kinase activity and can phosphorylate the receptor mediated Smads (R-SMADs), then the activated R-SMADs oligomerize with common mediator Smad (Co-SMAD) and translocate to the nucleus where they regulate gene expression with DNA-binding co-factors.

1.2 The BMP signaling pathway

1.2.1 The core BMP signaling pathway

Bone morphogenetic proteins (BMPs) were initially discovered in 1965 because of their inductive activity in ectopic bone formation [10]. Starting in the late 1980s, BMPs began to be characterized and cloned [11]. BMPs belong to the Transforming Growth Factor β (TGF-β) superfamily of ligands, which consists of TGF-β proteins, BMPs, growth differentiation factors (GDFs), glial derived neurotrophic factors (GDNFs), Activins, inhibins, Nodal and anti-Müllerian hormone (AMH) [1].

There are 15 known BMP ligands in mammals, namely BMP-1 to BMP-15 [12]. BMP-2 and BMP-7 have been approved by US Food and Drug Administration (FDA) for the treatment of fracture healing and spinal fusion [13]. Two BMP monomers form an antiparallel heterodimer, which is covalently linked by a disulfide bond, and each monomer interacts with both type I and type II receptors [14]. In mammals there are three type I receptors (BMPR-1A, BMPR-1B and ActR-1A) and three type II receptors (BMP-2, ActR-2A and ActR-2B) that can interact with BMPs. Distinct from the TGF-β type I receptors that cannot bind to ligands in the absence of type II receptors, type I receptors of BMP can bind to ligands even without type II receptors [15]. In the presence of type II receptors, the binding of type I receptor to ligands is enhanced. Smad-1,5,8 are R-Smads in the BMP signaling pathway, and the co-Smad is Smad-4. Crystallography at 2.5 Å showed that the co-SMAD Smad-4 forms a homotrimer with its MH2 domain [16].

1.2.2 Regulation of BMP signaling

BMPs have been characterized with essential roles in many developmental and physiological processes, such as embryogenesis, skeleton and limb formation, and cardiovascular and neuronal patterning [12]. Given its importance in establishing the body plan, it is critical that BMP signaling is regulated tightly at both extracellular and intracellular levels [17].

Extracellularly, Chordin is a BMP antagonist in *Xenopus*. Chordin can bind to BMP with its four cysteine-rich domains and inhibit the binding of BMP to the receptors. The inhibition of BMP by Chordin is reversible, BMP can be released by Tolloid, which is a metalloprotease that cleaves Chordin. Sizzled can inhibit Tolloid activity, resulting in elevated level of the BMP antagonist Chordin [18]. (Figure 1.2)

In *Xenopus*, another known antagonist of BMP is Noggin. In contrast to the BMP dimer that is formed in an overlapping antiparallel conformation, two Noggin monomers form a symmetric head-to-head dimer. The Noggin dimer interacts with BMPs at the same surface via which BMPs interact with its receptors, thus obstructing both type I and type II receptor binding of the BMPs [19].

Follistatin binds Activin with high affinity while binding to BMPs with low affinity. Follistatin binds to BMP with a C-clamp structure, a manner different from Noggin binding [20]. Despite the distinct binding structure, Follistatin also inhibits BMP signaling by blocking the molecular interfaces of BMP's binding to both type I and type II receptors.

The extracellular matrix (ECM) also play important roles in regulating BMP signaling. ECMs can function as passive barriers that bind to and sequester BMP ligands; inhibit diffusion of the BMP dimer; or bind to and facilitate regulatory complex formation to regulate BMP signaling [21]. For example, hyaluronic acid (HA) is a glycosaminoglycan in the ECM, whose receptor CD44 interacts with the R-Smad Smad1 [22]. HA facilitates the clustering of CD44, thus bringing Smad1 to the cell surface for phosphorylation by the BMP receptors [23].

The ECM also regulates long-range BMP signaling. In Drosophila, the BMP ligand Dpp is can undergo long distance shuttling due to the formation of a ternary complex with short gastrulation (Sog) and twisted gastrulation (Tsg) [24]. The Sog/Dpp/Tsg complex formation is assisted by the ECM component collagen IV, which acts as a scaffold [25]. After reaching a distant site, Dpp is then released from the ternary complex through the cleavage of Sog by the Tolloid metalloprotease. Collagen IV is also a scaffold for the interaction between Sog and Tolloid [26].

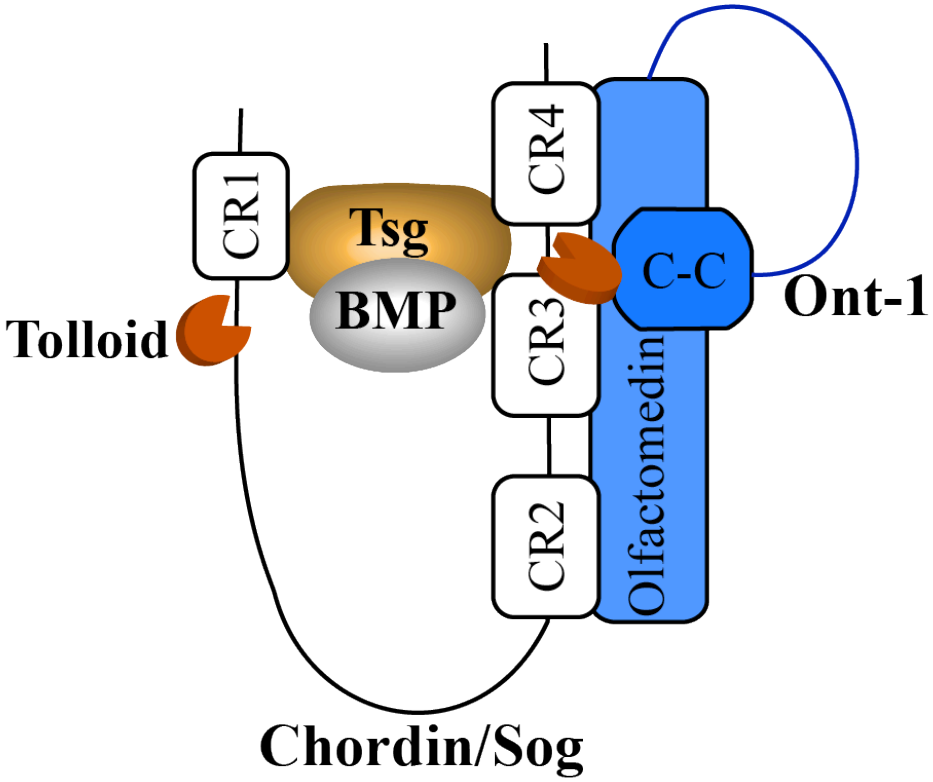

Figure 1.2 Reversible regulation of BMP signaling through the Chordin-BMP-Tsg-Tolloid-Ont-1 complex (modified from [18])

On one hand, Chordin binds to BMP through the four cysteine-rich domains (CR1-4), thus inhibiting BMP binding to its receptors. Twisted Gastrulation (Tsg) interacts with both Chordin/Sog and BMP, forming the Chordin-Tsg-BMP complex that can diffuse in the extracellular space. On the other hand, Tolloid releases BMP by cleaving Chordin at 2 different sites: one after CR1 and one between CR3 and CR4. The olfactomedin-related protein Ont-1 assists Chordin degradation by bringing together Chordin and Tolloid. The olfactomedin domain of Ont-1 binds to Chordin and the coiled-coil (C-C) domain of Ont-1 interacts with Tolloid.

1.2.3 The BMP-like signaling pathway in C. elegans

The BMP signaling pathway in *C. elegans* regulates body size, male tail patterning of sensory rays and copulatory spicules [27], and post embryonic mesoderm patterning [28]. The ligand is called DBL-1, type I and type II receptors are SMA-6 and DAF-4 respectively, SMA-2 and SMA-3 are the R-Smads, and SMA-4 is the co-Smad [29, 30]. In addition to these core pathway components, a few modulators have been previously identified to either positively or negatively regulate the signaling pathway at the level of the ligand-receptor complex. SMA-10 is a transmembrane protein that belongs to the family of leucine rich repeats and immunoglobulin-like domain-containing proteins (LRIG). SMA-10 positively regulates BMP signaling by binding to both type I and type II receptors SMA-6 and DAF-4 [31]. CRM-1 is predicted to be a transmembrane protein containing multiple extracellular cysteine-rich (CR) domains. CRM-1 is expressed in the ligand producing cells and can function non-autonomously to promote BMP signaling [32]. LON-2 belongs to the glypican family of heparin sulfate proteoglycans. LON-2 negatively regulates BMP signaling by interacting with and sequestering the ligand DBL-1 [33]. In addition to the modulators described above, LON-1 belongs to the pathogenesis related (PR) protein superfamily that regulates polyploidization and body length. LON-1 is a downstream target that is negatively regulated by the pathway [34, 35]. *sma-9* encodes the *C. elegans* homolog of Schnurri, is a downstream transcriptional cofactor required for BMP signaling [36]. (Figure 1.3)

Our lab also identified additional BMP modulators through a highly specific genetic screen based on suppression of the *sma-9* phenotype [28]. Mutations in *sma-9*

cause a dorsal-to-ventral fate transformation in the *C. elegans* postembryonic mesoderm, the M lineage, resulting in the loss of the two post embryonically derived coelomocytes (CCs), which are non-muscle mesodermal cells [28]. Mutations in each component of the BMP pathway can suppress the M lineage defects of *sma-9*, resulting in normal M lineage patterning [28]. However, mutations in the BMP pathway do not cause any M lineage defects on their own. Mutations in other signaling pathway, such as *daf-1*, the type I receptor in the TGFβ-like dauer pathway, cannot suppress the *sma-9* M lineage defect. Mutations that cause body size defects not through BMP signaling also cannot suppress the *sma-9* M lineage defects. So the *sma-9* M lineage suppression phenotype is specific to mutations in the BMP pathway [28]. Using this specific suppression assay, the Liu lab has found multiple new modulators in the BMP pathway, including DRAG-1/RGM, UNC-40/Neogenin, TSP-12/TSPAN5/TSPAN17, TSP-14/TSPAN10/CD63, TSP-21/TSPAN3 and SUP-17/ADAM10. DRAG-1 positively regulates BMP signaling by binding to both the ligand and receptors [37]. UNC-40 also positively regulates the signaling by binding to DRAG-1 [38]. TSP-12 and TSP-14 bind to TSP-21 and the type I receptor SMA-6, the three tetraspanins promote BMP signaling [39]. SUP-17/ADAM10 is the subject of Chapter 2 in this thesis.

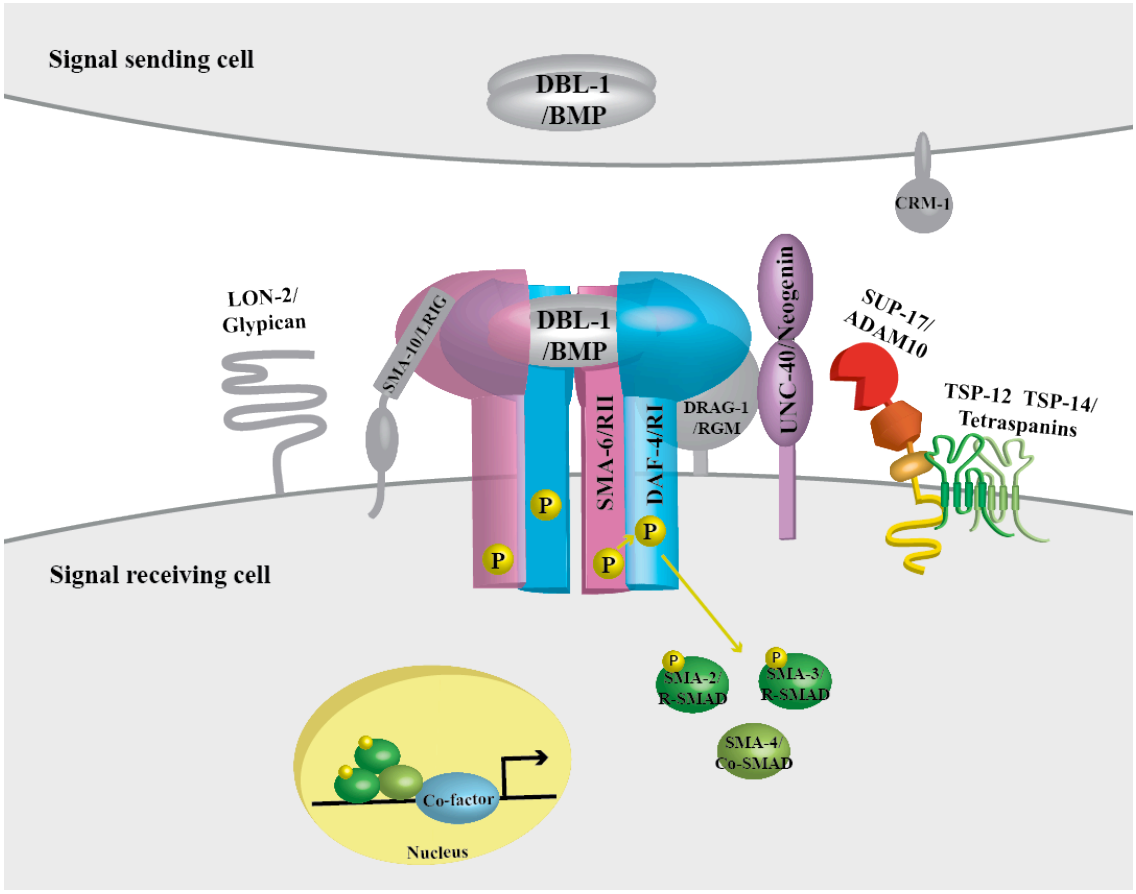

Figure 1.3 The BMP signaling pathway and its modulators in *C. elegans*.

Upon DBL-1 binding, SMA-6 phosphorylates DAF-4, which then phosphorylates SMA-2 and SMA-3. Activated SMA-2 and SMA-3 complex with SMA-4 and enter the nucleus to regulate downstream gene transcription. LON-2, SMA-10, DRAG-1, UNC-40, SUP-17, CRM-1, TSP-12 and TSP-14 are modulators of the pathway.

1.3 SUP-17/ADAM10

1.3.1 Overview of ADAM10

Proteins of a disintegrin and metalloprotease (ADAM) family are type I transmembrane proteins that belong to the zinc protease superfamily. “Disintegrins” describe a family of proteins from snake venom that inhibit integrin-dependent cell adhesion and platelet aggregation [40]. ADAMs are known to cleave many cell surface proteins through a process called ‘ectodomain shedding’ [41]. In humans, there are 19 *adam* genes, and as many as 34 in a variety of species [42]. ADAMs have a prodomain, a metalloprotease domain, a disintegrin domain, a cysteine-rich and EGF-like domain, a transmembrane domain, and a cytoplasmic tail [42]. Mammalian ADAM10 and ADAM17 (also known as TACE, tumor necrosis factor-α-converting enzyme) share functional redundancy in cleaving some of the substrates [43].

Mammalian ADAM10 is synthesized in the rough endoplasmic reticulum and matures in the late Golgi compartment. Maturation of bovine ADAM10 involves N-glycosylation on four arginines at position 267, 278, 439 and 551, and removal of the prodomain from the ADAM precursor protein, which is mediated by proprotein convertases (PCs) in the conserved Rx(R/K)R motif at position 210-213 [44]. The 195 amino acid-long prodomain of ADAM10 has two important roles, one is to keep the proprotein in a latent form through a “cysteine switch”. In the “cysteine switch” model, the critical cysteine residue at position 173 coordinates the zinc atom and sequesters the metalloprotease domain [45]. Another role of the prodomain is to chaperone the

proper folding of the ADAMs. ADAM10 lacking the prodomain is inactive *in vivo*, however this truncated ADAM10 becomes active after co-transfection with a construct that expresses the prodomain only [46]. Recently, another PC cleavage site, RAKR, was revealed in the N-terminus of prodomain at position 48-51 in mice. Mutations in this novel cleavage site do not affect the cleavage of the prodomain on the secondary site, but lead to reduced catalytic activity of ADAM10 [47].

The metalloprotease domain contains the active site of ADAMs, the conserved HExxHxxGxxH sequence. The three histidines coordinate a $Zinc^{2+}$ ion, which is required to catalyze the hydrolysis of the substrate peptide bond by withdrawing an electron from the oxygen. The glutamate is the key catalytic residue that is proposed to deprotonate a water molecule. Then the resultant hydroxide performs a nucleophilic attack to the carbonyl carbon on the peptide backbone, thus hydrolyzing the substrate [48, 49].

The disintegrin domain, cysteine-rich domain and the membrane-proximal region of ADAM10, co-immunoprecipitates with TapanC8 subfamily of tetraspanins. And the interactions of these regions with tetraspanins are required for the subcellular localization of ADAM10 protein in HEK293T cells [50].

The cytoplasmic tail of ADAMs is highly variable, and the intracellular domains of ADAM10 and ADAM17 can be removed without affecting the cleavage of the cell surface glycoprotein CD44, one of their substrates [51]. There is a ER retention motif, an arginine stretch at position 722-724, in the cytoplasmic tail that impedes ADAM10's export from the ER and slows down its trafficking to the cell surface [52]. This ER-retention motif controls the constitutive but not the stimulated

activity of ADAM10 [53]. Another important feature in the cytoplasmic tail is a proline-rich Src homology 3 (SH3)-binding domain located at position 708-711. This region is critical for the basolateral sorting of ADAM10 to cell junctions of epithelial cells and for E-cadherin processing in cell migration [54].

1.3.2 Biological roles of ADAM10

ADAM10 plays roles in many developmental processes of various species and human diseases due to the diversity of its substrates. ADAM10 is responsible for the proteolytic release of many cell surface proteins, including mouse Notch, human precursor of TNFα, mouse ephrin-A2, CD44, CDH2, amyloid precursor protein (APP), and the adhesion molecule L1 [42].

ADAM10 plays roles in cell fate determination and cell migration. In the Notch signaling pathway, the receptor Notch undergoes 2 sequential cleavages upon ligand binding. ADAM10 is required for the Site 2 cleavage of Notch at the juxtamembrane region of the extracellular domain. This cleavage site is mapped between the Ala^{1710}- Val^{1711} amide bond. Following this S2 cleavage, the remaining membrane bound C-terminal part of Notch is cleaved by γ-secretase at the S3 site, releasing the Notch intracellular domain (NICD). NICD then translocates to the nucleus and regulates gene transcription with the DNA binding protein CSL and co-activator Mastermind. In addition to the receptor Notch, the ligand Delta is also processed by ADAM10/Kuzbanian in Drosophila [55]. The adhesion molecule L1 can be released by ADAM10 cleavage in the Golgi apparatus and at the cell surface, and the soluble form of L1 promotes cell migration in HEK293 cells [56].

ADAM10 has α-secretase activity: ADAM10 cleaves β amyloid precursor protein (βAPP) in HEK293 cells and generates the soluble sAPPα. The cleavage between residues Lys^{683} and Leu^{684} happens both on the cell surface and along the secretory pathway [57]. APPs can also be processed by β-secretase and γ-secretase, generating the amyloid β (Aβ) peptide, which has been associated with Alzheimer's disease. However, cleavage by α-secretase in the middle of Aβ inhibits the formation of Aβ. Thus ADAM10 may be beneficial in alleviating Alzheimer's disease [57].

ADAM10 may also be involved in prion diseases [58]. The glycosylphosphatidylinositol (GPI)-anchored cellular prion protein (PrP^c) might possibly be cleaved by ADAM10 at two distinct sites. One is in the middle of the protein, generating N1 metabolite for neuron protection [59]. The other is at the C-terminal end, releasing the soluble PrP (sPrP) from the plasma membrane [60, 61]. So ADAM10 may be involved in protecting against the development of prion disorders by inhibiting the conversion of PrP^c to the insoluble infectious PrP^{sc} [58].

However, ADAM10 is not always beneficial. Excessive ADAM10 activity is related to Fragile X syndrome (FXS) [62]. The Fragile X mental retardation protein (FMRP) down-regulates the translation of ADAM10 and βAPP [62]. Mutations in FMRP lead to increased level of ADAM10 and βAPP, resulting in elevated production of sAPPα, and subsequent hyperactivation of the mGluR5/MAPK pathway. These misbalances would ultimately cause synaptic deficits and intellectual disabilities in children [62].

Huntingtin (htt) is a protein critical for neural tube formation during embryonic development. Htt functions through the inhibition of ADAM10-dependent cleavage of N-cadherin [63]. However, whether ADAM10 is involved in Huntington disease development remains to be investigated.

Although proteolysis by ADAMs takes place outside the plasma membrane, the cleavage is mostly controlled by signals inside the cell that result in intracellular modifications of the substrates [51]. In addition to intracellular modifications, homo-dimerization of substrates through cysteine disulfide bridges may also be required for cleavage by ADAMs, possibly by regulating the accessibility of the metalloprotease to the substrates in the extracellular space [64].

1.3.2 ADAM10 in C. elegans

Mammalian ADAM10 is the homolog of Drosophila KUZBANIAN and *C. elegans* SUP-17 [65]. KUZBANIAN functions in neurogenesis [66] and activates Notch signaling [67]. SUP-17 was first identified and characterized by the Horvitz and the Greenwald labs to facilitate LIN-12/Notch signaling [65, 68]. ADM-4, the *C. elegans* ortholog of ADAM17, shares functional redundancy with SUP-17 in Notch signaling pathway: double mutants are sterile [69].

1.4 Tetraspanins

Tetraspanins are members of a large family of proteins that have four transmembrane domains, three short intracellular regions (including the N- and C-

termini), and two extracellular loops of unequal sizes: the small extracellular loop (SEL/EC1) and the large extracellular loop (LEL/EC2). The unique features of the LEL are the highly conserved CCG motif, and four, six or eight cysteine residues forming disulfide bonds that stabilize this domain [70]. Tetraspanins can be post-translationally modified through N-linked glycosylations, palmitoylations and ubiquitinations. The N-linked glycosylations may occur at the asparagine residues in the LEL. Tetraspanins can also be palmitoylated on the intracellular cysteine residues that contribute to tetraspanin-protein interactions [71, 72]. Tetraspanins can also be ubiquitinated at cytoplasmic sites that function in down-regulation [73]. Tetraspanins arrange the plasma membrane by forming the tetraspanin enriched microdomains (TEMs) and interact with signaling molecules, such as adhesion molecules, signaling receptors and intracellular signaling molecules, to regulate cellular signaling [74]. There are 33 tetraspanins in human, and 21 in *C. elegans*.

In HEK293T cells, ADAM10 interacts directly with six different tetraspanins, including Tspan5, Tspan10, Tspan14, Tspan15, Tspan17 and Tspan33, in the cysteine-rich domain and the membrane-proximal stalk region of ADAM10 [50]. These tetraspanins constitute a subgroup of tetraspanins called TspanC8 that have eight cysteines in their large extracellular loop. All six TspanC8 tetraspanins assist ADAM10 maturation and its exits from endoplasmic reticulum (ER). TspanC8 tetraspanins co-immunoprecipitate with ADAM10 with different efficiency and differentially regulate ADAM10 subcellular localization and substrate specificity in U_2OS cells. The stalk region of ADAM10 is sufficient for Tspan15 interaction but not for the other five TspanC8 tetraspanins. Tspan10, Tspan14 and Tspan17 can only

weakly interact with the stalk region of ADAM10, whereas Tspan5 and Tspan33 cannot interact with the stalk region. And the interaction can be enhanced with the presence of the cysteine-rich domain. Tspan10 and Tspan17 target ADAM10 to late endosomes, and Tspan5, Tspan14, Tspan15 and Tspan33 facilitate ADAM10 localization to the plasma membrane [75, 76].

TspanC8 tetraspanins differentially regulate ADAM10 substrate specificity. Tspan5 and Tspan14, but not Tspan15, promote Notch activation; Tspan15 but not other TspanC8 tetraspanins promotes N-cadherin cleavage [77]. One of the explanations of how tetraspanins regulate ADAM10 substrate specificity is that tetraspanins differentially regulate ADAM10 membrane compartmentalization, thus regulating ADAM10 accessibility to the substrates. Indeed, Tspan5 and Tspan15 differentially regulate ADAM10 membrane compartmentalization: in the presence of Tspan15, ADAM10 diffuses faster whereas ADAM10 is less soluble with the expression of Tspan5; Tspan5 interacts better with the tetraspanin web, whereas Tspan15 expression reduces the interaction between ADAM10 and the tetraspanin web [77].

In addition to the TspanC8 tetraspanins, ADAM10 also interacts with non-TspanC8 tetraspanins. Tspan12 associates with ADAM10 and promotes its maturation and the proteolysis of APP (amyloid precursor protein) in a palmitoylation-dependent manner. A non-palmitoylatable Tspan12 mutant fails to associate with ADAM10 and has the opposite effects on ADAM10 maturation and APP proteolysis [78]. Tspan3 is also identified as an ADAM10 interaction partner. In mammalian cells, Tspan3 co-immunoprecipitates with ADAM10, APP and the γ-secretase protease presenilin.

Tspan3 is localized mainly in the early and late endosomes, and mutating the internalization motif of Tspan3 results in increased cell surface localization of ADAM10 and APP [79].

In *C. elegans*, the TspanC8 subfamily has two members, TSP-12 and TSP-14. They share functional redundancy in regulating Notch and BMP signaling pathway [80, 81].

1.5 UNC-40/Neogenin

Neogenin is a multifunctional type I transmembrane protein that belongs to the immunoglobulin superfamily. Neogenin shares about 50% amino acid sequence identity and identical secondary structure to its paralog Deleted in Colorectal Cancer (DCC). Neogenin and DCC are highly conserved in the extracellular domains that consist of four immunoglobulin (Ig) motifs and six fibronectin type III (FNIII) repeats. The intracellular domains contain P1, P2 and P3 motifs, but are less conserved. Unlike DCC where has restricted expression in the nervous system, Neogenin is widely expressed in heart, gut, lung, liver, pancreas and limb bud cartilage in addition to the nervous system in mouse [82, 83]. Both Neogenin and DCC are receptors for netrins, and Neogenin is also the receptor for repulsive guidance molecules (RGMs). RGMs are glycosylphosphatidylinositol (GPI)-anchored glycoproteins. In mice, there are three orthologs of RGM, RGMa, RGMb/DRAGON and RGMc.

In *C. elegans*, UNC-40 is the homolog of both Neogenin and DCC. *C. elegans* UNC-40 shares 33% amino acid identity with human Neogenin and 34% with human

DCC. In addition to its role in axon guidance, UNC-40 also functions to positively modulate BMP signaling by binding to the RGM protein DRAG-1 [38]. Interestingly, the extracellular domain of UNC-40 is sufficient to regulate BMP signaling, and this mechanism is conserved in mammals [38]. These findings suggest that UNC-40 may be processed to release the extracellular domain to function in BMP signaling. In accordance with this hypothesis, the UNC-40 homolog Neogenin is cleaved by ADAM17 in cultured rat cortical neurons for proper axon guidance [84]; DCC proteolytic processing is blocked by inhibitors of ADAMs [85].

1.6 Dissertation Outline

This dissertation describes the characterization of a newly discovered BMP modulator and ADAM protease SUP-17 in *C. elegans*.

Chapter 2 describes the involvement of SUP-17 in BMP-like Sma/Mab signaling, including SUP-17 localization, the cell types in which it functions in BMP signaling and its interaction with tetraspanins.

Chapter 3 describes the regulation of SUP-17 subcellular localization and prodomain cleavage by three tetraspanins: TSP-12, TSP-14 and TSP-21.

Chapter 4 focuses on the regulation of UNC-40 by SUP-17, tetraspanins and other BMP signaling components.

Chapter 5 summarizes my work and discusses future directions to follow up the research.

CHAPTER 2

TWO PARALOGOUS TETRASPANINS TSP-12 AND TSP-14 FUNCTION WITH THE ADAM10 METALLOPROTEASE SUP-17 TO PROMOTE BMP SIGNALING IN *C. ELEGANS*[1]

2.1 ABSTRACT

The highly conserved bone morphogenetic protein (BMP) signaling pathway regulates many developmental and homeostatic processes. While the core components of the BMP pathway have been well studied, much research is needed for understanding the mechanisms involved in the precise spatiotemporal control of BMP signaling *in vivo*. Here, we provide evidence that two paralogous and evolutionarily conserved tetraspanins, TSP-12 and TSP-14, function redundantly to promote BMP signaling in *C. elegans*. We further show that the ADAM10 (a disintegrin and metalloprotease 10) ortholog SUP-17 also functions to promote BMP signaling, and that TSP-12 can bind to and promote the cell surface localization of SUP-17. SUP-17/ADAM10 is known to be involved in the ligand-induced proteolytic processing of the Notch receptor. We have evidence that the function of SUP-17, and of TSP-12/TSP-14 in BMP signaling is independent of their roles in Notch signaling.

[1] This chapter was published in *PLOS Genetics* (Wang L, Liu Z, Shi H, Liu J. PLoS Genet. 2017 Jan;13(1): 10.1371) and is reprinted with permission. Tetraspanins work was performed by Z. Liu, SEL-12 and HOP-1 analysis, yeast two hybrid assay and molecular cloning were performed by J. Liu and H. Shi.

Furthermore, presenilins, core components of the γ-secretase complex involved in processing Notch, do not appear to play a role in BMP signaling. These studies established a new role of the TSP-12/TSP-14/SUP-17 axis in regulating BMP signaling, in addition to their known function in the Notch signaling pathway. We also provide genetic evidence showing that a known BMP signaling modulator, UNC 40/neogenin/DCC, is one of the substrates of SUP-17/ADAM10 in the BMP signaling pathway.

2.2 AUTHOR SUMMARY

Bone morphogenetic protein (BMP) signaling regulates multiple developmental and homeostatic processes. Misregulation of this pathway can cause various diseases, including cancers. Thus, it is essential to understand how BMP signaling is tightly regulated spatiotemporally *in vivo*. We have identified a highly conserved ADAM (a disintegrin and metalloprotease) protein, SUP-17/ADAM10, as an important factor in modulating BMP signaling in *C. elegans*. We showed that the proper localization and function of this ADAM protease require two conserved tetraspanin proteins, TSP-12 and TSP-14. We provided genetic evidence showing that one of the substrates of SUP-17/ADAM10 in the BMP signaling pathway is a known BMP signaling modulator, UNC 40/neogenin/DCC. Our studies established a new role of the TSP-12-TSP-14-SUP-17 axis in regulating BMP signaling, in addition to and independent of their known function in the Notch signaling pathway.

2.3 INTRODUCTION

The highly conserved bone morphogenetic protein (BMP) pathway is repeatedly used in metazoan development to regulate multiple distinct processes in different cellular contexts. In canonical BMP signaling, secreted BMP ligands bind to the heteromeric type I/type II receptor complexes and induce the phosphorylation of type I receptors by type II receptors, which in turn phosphorylate the R-Smads. The phosphorylated R-Smads then complex with Co-Smad and enter the nucleus to regulate gene transcription. Increasing evidence has shown that BMP signaling is tightly regulated spatiotemporally and that misregulation of this pathway can cause many different disorders in humans, such as cardiovascular diseases and cancers [86-90]. Recent studies have identified a number of factors that modulate BMP signaling at the level of the ligand-receptor complex [31, 33, 39, 91, 92]. In particular, we have previously shown that the small transmembrane tetraspanin proteins are important in promoting BMP signaling in *C. elegans* [39].

Tetraspanins are a large group of integral membrane proteins with a characteristic protein topology. They contain four transmembrane domains and a number of conserved residues, such as the featured CCG motif in the second extracellular loop [70]. Recent studies have shown that a subgroup of tetraspanins, the TspanC8 family of tetraspanins, functions to promote another highly conserved signaling pathway, the Notch pathway [75, 76, 81, 93]. In particular, the TspanC8 tetraspanins physically associate with ADAM10 and promotes its cell surface localization. ADAM10, in turn, cleaves the Notch receptor in a process called "ectodomain shedding", releasing the intracellular domain of Notch for subsequent

activation of downstream gene expression [75, 76, 93]. Previously, we have shown that in *C. elegans*, the TspanC8 tetraspanins TSP-12 and TSP-14 function in modulating BMP signaling [39]. However, whether they exert their functions in BMP regulation by acting through the *C. elegans* ADAM10 protein is not known. Similarly, because of their roles in both BMP signaling and Notch signaling, it is not clear whether TSP-12 and TSP 14 regulate these two pathways independently. In this study, we investigated how TSP-12 and TSP-14 regulate BMP signaling in *C. elegans.* The *C. elegans* BMP-like pathway is called the Sma/Mab pathway. This pathway is known to regulate body size, male tail patterning and mesoderm development [94]. Core members of this pathway include the ligand DBL-1/BMP, the type I and type II receptors, SMA 6/RI and DAF-4/RII, the R-Smads SMA-2 and SMA-3, as well as the Co-Smad SMA-4 [94]. Loss-of-function mutations in any of these core members will result in a small body size, male tail sensory ray formation defects [27], reduced expression of the RAD-SMAD reporter [38], and suppression of the *sma-9(cc604)* M lineage defect [28]. In particular, mutations in the *C. elegans* schnurri homolog *sma-9* cause a dorsal-to-ventral cell fate transformation in the postembryonic M lineage, thus the loss of two M-derived coelomocytes (CCs). Loss-of-function mutations in any core members of the Sma/Mab pathway can suppress this M lineage defect (Figure 1A, B), resulting in the reappearance of the two M-derived CCs. Thus, Sma/Mab pathway mutants exhibit a Susm (suppression of the *sma-9* M lineage) phenotype ([28]; Figure 1A-1E). We have previously shown that the Susm phenotype can be used as a specific and sensitive assay to screen efficiently for mutants with defects in Sma/Mab signaling [39]. Using the Susm assay, we have identified several highly conserved

factors that function to modulate BMP signaling at the level of the ligand-receptor complex. These include the RGM protein DRAG-1 [37], the neogenin/DCC homolog UNC-40 [38], the tetraspanin TSP-21 [39], as well as two redundant tetraspanins, TSP-12 and TSP-14.

Here, we show that TSP-12 and TSP-14 function redundantly in BMP signaling by regulating the cell surface localization of the ADAM10 (a disintegrin and metalloprotease 10) ortholog SUP-17. We demonstrate that the function of SUP-17 in BMP signaling is independent of its well-established role in Notch signaling. Finally, we provide genetic evidence indicating that a known BMP modulator, UNC 40/neogenin/DCC, is one of the substrates of SUP 17/ADAM10 in the BMP signaling pathway.

2.4 MATERIAL AND METHODS

C. elegans strains

All strains were maintained at 20°C using standard culture conditions [95] unless otherwise noted. The following mutations, transgenes and balancers were used: Linkage group I (LG I): *drag-1(jj4)*, *hop-1(ar179)*, *unc-40(n1430)*, *unc-40(ev495)*, *unc-40(tr115)*, *sup-17(n316)*, *sup-17(n1258)*, *sup-17::gfp(jj98)*, *arIs37(secreted CC::gfp)*; LG II: *sma-6(jj1); jjIs2437 (RAD-SMAD)*; LG III: *lon-1(jj67)*, *sma-3(jj3)*, *lin-12(n941)*, *lin-12(ok2215)*, *ccIs4438(intrinsic CC::gfp)*, *hT2[qIs48]*; LG IV: *tsp-12(ok239)*, *gfp::3×flag::tsp-12(jj181)*, *gfp::3×flag::tsp-12(jj182); nT1[qIs51]*; LG V: *dbl-1(wk70)*, *him-5(e1467)*; LG X: *sel-12(ar171)*, *sel-12(ok2078)*, *lon-2(e678)*, *tsp-14(jj95)*, *tsp-14(jj96)*, *tsp-14(jj97)*, *adm-4(ok265)*, *sma-9(cc604)*.

Body size measurement and RAD-SMAD reporter assay

Body size measurement and RAD-SMAD reporter assays were performed following the protocols described in Tian et al. [38]. Hermaphrodite worms at the L4 stage (identified based on vulva development) were used for body size measurement. Body sizes were measured using segmented lines in Fiji [96] after images were taken. Synchronized L3 hermaphrodites carrying the RAD-SMAD reporter *jjis2437* II [38] were used for imaging. The reporter fluorescence intensity was measured using Fiji.

Oligonucleotides, plasmid constructs and transgenic lines

Oligonucleotides used in this study are listed in SI Appendix, Table S2. Plasmids generated are listed in SI Appendix, Table S3. The *tsp-12* cDNA was amplified from the Vidal RNAi library [97], while *yk23h2* contains the full-length *sup-17* cDNA. Each clone contains a point mutation in the respective coding regions of *tsp-12* and *sup-17*, which were respectively fixed via site-directed mutagenesis, resulting in the generation of pJKL1079 (containing the *tsp-12* ORF), and pJKL1140 (containing the *sup-17* cDNA). pK3, a rescuing plasmid containing 7kb of the *sup-17* genomic region, is a kind gift from Iva Greenwald (Columbia University).

One of the following plasmids were used as co-injection markers to generate transgenic lines: pRF4 (*rol-6(su1006)*), LiuFD61 (*mec-7p::mRFP*), pJKL449 (*myo-2p::gfp::unc-54 3'UTR*), or pCFJ90 (*myo-2p::mCherry::unc-54 3'UTR*) [98]. Stable integrants carrying pZL51 were generated using γ-radiation, followed by outcrossing with N2 animals five times.

Generating *tsp-14* deletion alleles using the dual sgRNA-guided CRISPR/Cas9 system

To generate deletion alleles of *tsp-14*, we designed two sgRNAs targeting both the N-terminus (ACCACCGCGCGAGCTCGCGT) and the C-terminus (AAGCGGCTGAAGGCATCCG) of the *tsp-14* coding region (SI Appendix, S1 Figure). The sgRNA plasmids pZL8 and pZL9 (S3 Table) were generated by replacing the *unc-119* gRNA sequence in the *pU6::unc-119* sgRNA vector [99] with the *tsp-14* sgRNA sequence. The following plasmid mix was injected into young hermaphrodite N2 adults: (1) the Cas9 expression plasmid pDD162 (*peft-3-cas9+empty sgRNA*) [100], (2) two *tsp-14*-specific sgRNA plasmids pZL8 and pZL9, and (3) the co-injection marker pRF4 (*rol-6d*). Positive Rol F1 worms were picked and placed onto fresh NGM plates (3 worms/plate). After they have laid eggs, the F1 worms were pooled for PCR screening using primers ZL4 and ZL5 (S2 Table). After screening 282 F1s, we obtained three *tsp-14* deletion alleles, *jj95*, *jj96* and *jj97*, which were confirmed by Sanger sequencing (SI Appendix, S1 Figure).

Generating endogenously tagged TSP-12::GFP or SUP-17::GFP strains using CRISPR/Cas9-mediated homologous recombination

We tagged the endogenous TSP-12 at either the N-terminus or the C-terminus using CRISPR/Cas9. To generate these TSP-12 knock-ins, we followed the strategy described in Arribere et al. [101] to generate two sgRNA expression plasmids for each tagging strategy (see S2 Table and S3 Table for oligo and plasmid information). We

then used the method described in Dickinson et al. [102] to generate the homologous repair templates, and to subsequently obtain stable knock-in strains that carry either GFP::3×FLAG::TSP-12 (*jj181* and *jj182*) or TSP 12::GFP::3×FLAG (*jj194* and *jj196*). We first confirmed the success of knock-ins by genotyping, and then tested *jj181* and *jj194* for functionality by crossing each of them into the *tsp-14(0)* background and examined the strains for viability and fertility.

The *sup-17::gfp* knock-in strain was generated by injecting the following mix of plasmid DNAs into N2 worms: (1) a Cas9 expression plasmid pDD162 [100], (2) two sgRNA plasmids (pLW4 and pLW5, generated using the *pU6::unc-119* sgRNA plasmid described in Friedland et al. [99], (3) the homologous repair template pJKL1034 (SUP-17::GFP translational fusion, with GFP inserted between amino acid 876 and 877, see S3 Table), and (4) a co-injection marker pRF4 (*rol-6d*). GFP knock-in events were screened via PCR using primers LW27, LW30 and JKL269 (see S2 Table). Single worm PCR of 33 F1 rollers failed to detect any germline integration event. However, we screened the F3 worms from six high transmission efficiency (>30%) *rol* transgenic lines and found that five of the six lines examined had a *gfp* knock-in event. After genotyping and confirming homozygous *sup-17::gfp* knock-ins, we kept three of the lines, *jj98*, *jj99* and *jj100*, for further analysis.

Microscopy

To examine the male tail, the developing vulva or developing embryos, animals were visualized under a Leica DMRA2 compound microscope equipped with a Hamamatsu Orca-ER camera using the iVision software (Biovision technology, Inc.).

An inverted Zeiss LSM880 confocal microscope with Airyscan was used to examine the expression and subcellular localization patterns of GFP::3×FLAG::TSP-12 or SUP-17::GFP. Fluorescence was detected with an Airyscan detector using the 40× objective (NA 1.4, WD 0.13 mm) and in the super-resolution mode (pinhole is around 2.25 AU). The laser line for GFP excitation is at 488 nm, and for mCherry is at 561 nm. Collected images were subsequent processed by ZEN (Carl Zeiss), and further quantification of the fluorescence signals was performed using Fiji.

To quantify the fluorescence intensity and bright intracellular puncta of SUP 17::GFP, live embryos from worms of different genotypes that were grown under the same condition were collected on the same day and imaged using the same settings as described above. Images of stage-matched embryos were further processed in the same way using Fiji. Average SUP 17::GFP fluorescence intensity was calculated by drawing a straight line of fixed length (for cell surface signal) or by drawing an oval of fixed width and height (for intracellular signal). Only cells with focal plane going through the nucleus were used for this purpose. Bright puncta were defined as those signals that are above a threshold of brightness (3,500 pixels) and size (the area is above 0.07 μm^2). Signals on top of the cell membrane were excluded from the counting.

Split ubiquitin yeast two-hybrid assay

The split-ubiquitin yeast two-hybrid experiments were carried out by following the protocol described in Grefen et al. [103]. The bait CubPLV and prey NubG fusion constructs used are listed in SI Appendix, Table S2. After transforming into yeast,

interactions among each pair of bait and prey constructs were visualized by streaking diploid cells on SC-Trp, -Leu, -Ade, -His, -Ura, -Met plates that were supplemented with four different concentrations of methionine: 0mM, 0.075mM, 0.150mM, 0.300mM, respectively. Growth was monitored for 2-9 days at 30°C. The plasmids KAT-1-Cub-PLV, KAT-1-NubG (in XN21 vector), empty NubG vector, and the vector expressing soluble wild-type Nub (NubWT) were used as controls [39]. Confirmation of expression of each fusion protein was by western blot analysis using rabbit polyclonal anti-VP16 antibodies (ab4808, Abcam, for CubPLV fusions) and monoclonal anti-HA antibodies (Clone 12CA5, Sigma, for NubG fusions).

Statistical analyses

Statistical analyses were conducted with Prism 5 (GraphPad), and the test for significance for groups of two were analyzed using the unpaired Student's t-test. Two-tailed *p* values were calculated. Data was shown as mean ± 95% confidence interval (CI).

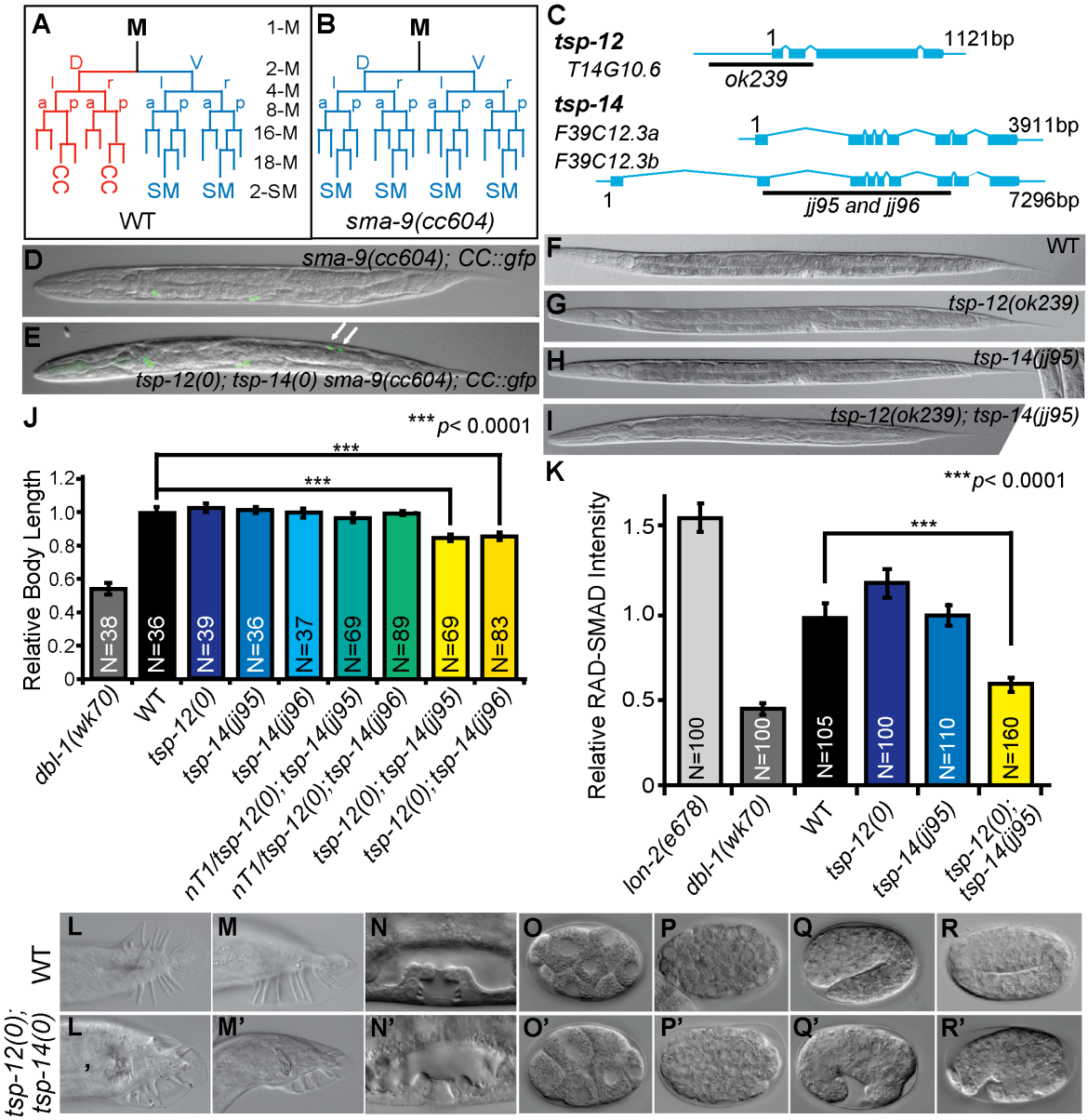
A
M
1-M
2-M
4-M
8-M
16-M
18-M
2-SM
D
V
SM
WT
B
sma-9(cc604)
C
tsp-12
T14G10.6
ok239
1121bp
tsp-14
F39C12.3a
F39C12.3b
3911bp
7296bp
jj95 and jj96
D
sma-9(cc604); CC::gfp
E
tsp-12(0); tsp-14(0) sma-9(cc604); CC::gfp
F
WT
G
tsp-12(ok239)
H
tsp-14(jj95)
I
tsp-12(ok239); tsp-14(jj95)
J
***p< 0.0001
Relative Body Length
N=38
N=36
N=39
N=36
N=37
N=69
N=89
N=69
N=83
dbl-1(wk70)
WT
tsp-12(0)
tsp-14(jj95)
tsp-14(jj96)
nT1/tsp-12(0);tsp-14(jj95)
nT1/tsp-12(0);tsp-14(jj96)
tsp-12(0);tsp-14(jj95)
tsp-12(0);tsp-14(jj96)
K
***p< 0.0001
Relative RAD-SMAD Intensity
N=100
N=100
N=105
N=100
N=110
N=160
lon-2(e678)
dbl-1(wk70)
WT
tsp-12(0)
tsp-14(jj95)
tsp-12(0); tsp-14(jj95)
WT
tsp-12(0); tsp-14(0)
L
M
N
O
P
Q
R
L'
M'
N'
O'
P'
Q'
R'

Figure 2.1 *tsp-12(0); tsp-14(0)* double mutants exhibit defects in Sma/Mab signaling.

(A, B) Schematic representation of the M lineage in wild type (WT) or *tsp-12(0); tsp-14(0) sma-9(0)* (A), and *sma-9(0)* animals (B). CC: coelomocyte, SM: sex myoblast, v: ventral, d: dorsal, l: left, r: right, a: anterior, p: posterior. (C) Diagrams depicting the tsp-12 and tsp-14 genomic regions and the locations of *tsp-12(ok239)* and *tsp-14(jj95, jj96)* deletions. See also S1 Fig. (D, E) Merged GFP and DIC images of late L4 stage *sma-9(cc604)* and *tsp-12(ok239); tsp-14(jj95) sma-9(cc604*) worms carrying the coelomocyte (CC) GFP marker CC::gfp. Arrows point to M-derived CCs. (F-I) Representative DIC images of developmental stage-matched WT (F), *tsp-12(ok239)* (G), *tsp-14(jj95)* (H) and *tsp-12(ok239); tsp-14(jj95)* (I) worms, showing the smaller body size of *tsp-12(ok239); tsp-14(jj95)* worms. (J) Relative body length of developmental stage-matched worms of various genotypes grown at 20°C. The mean body length of WT worms is normalized to 1.0. Error bars represent 95% confidence intervals (CI) for the normalized body length. (K) Quantification of the RAD-SMAD reporter GFP fluorescence intensity in various mutants compared with WT animals (set to 1.0). Error bars represent 95% confidence intervals (CI) for the normalized mean RAD-SMAD fluorescence intensity. (L-R') DIC images of WT (L, M, N, O, P, Q, R) and *tsp-12(ok239); tsp-14(jj95)* mutant (L', M', N', O', P', Q', R') male tails (L-M), hermaphrodite vulva at the Christmas tree stage (N), and embryos at different developmental stages (O-R). (L', M', N') Images of *tsp-12(ok239); tsp-14(jj95)* worms produced by heterozygous *tsp-12(ok239)/+; tsp-14(jj95)* mothers. (O'-R') Images of *tsp-12(ok239); tsp-14(jj95)* embryos produced by homozygous *tsp-12(ok239); tsp-14(jj95)* mothers, showing ventral enclosure defects.

2.5 RESULT

2.5.1 The paralogous TSP-12 and TSP-14 function redundantly to promote BMP signaling

The *C. elegans* genome encodes 21 tetraspanins. We have previously reported a weak Susm (suppression of the *sma-9* M lineage) phenotype in the *tsp-12(ok239)* null mutants, which is enhanced by *tsp-14*(RNAi), but not by RNAi of any of the remaining 19 *tsp* genes in *C. elegans* [39]. To further determine mechanistically how TSP-12 and TSP-14 function in Sma/Mab signaling, we generated three deletion alleles of *tsp-14* (*jj95*, *jj96* and *jj97*) using CRISPR/Cas9 system (Figure 1C; see Materials and Methods). We used both *jj95* and *jj96* in all our analyses described below, and found them to behave identically. We therefore refer to both alleles as *tsp-14(0)*. Similarly, we refer to the deletion allele *tsp-12(ok239)* as *tsp-12(0)*.

tsp-12(0) and *tsp-14(0)* single mutants are each fully viable and fertile. *tsp-12(0); tsp 14(0)* double mutants produced by *tsp-12(0)/+; tsp-14(0)* mothers are also viable, but exhibit vulva morphogenesis defect (Figure 1N') and are egg-laying defective (Egl). They also exhibit multiple Sma/Mab signaling defects: unlike the *tsp-12(0)* or *tsp-14(0)* single mutants, these *tsp-12(0); tsp-14(0)* double mutants have a smaller body size (Figure 1F-1J), exhibit reduced RAD-SMAD reporter activity (Figure 1K) and double mutant males have severe tail defects (Figure 1L' and 1M'), including crumpled spicules, fused and shortened sensory rays, and smaller fans. *tsp-12(0); tsp-14(0)* double mutants also suppress the *sma-9(cc604)* M lineage defect at high penetrance (Figure 1A, 1B, 1D, 1E and Table 1). These observations indicate that

TSP-12 and TSP-14 share redundant functions in promoting BMP signaling. In addition to these phenotypes, the *tsp 12(0); tsp-14(0)* double mutants also exhibit 100% maternal-effect embryonic lethality: all their eggs die in late embryogenesis, with defects in ventral enclosure (Figure 1O'-1R' and SI Appendix, Movies S1-S2). The ability of *tsp-12(0); tsp-14(0)* double mutants produced by tsp *12(0)/+; tsp-14(0)* mothers to survive through embryogenesis is likely due to the perdurance of maternally loaded *tsp-12* mRNA or TSP-12 protein by the *tsp-12(0)/+; tsp-14(0)* mothers. Thus, TSP-12 and TSP-14 share redundant functions that are essential for both embryonic and postembryonic development.

Table 1. TSP-12 and TSP-14 function redundantly to promote Sma/Mab signaling.

Genotype	Susm penetrance[a] (# of animals examined)
sma-9(cc604)	--
tsp-12(ok239); sma-9(cc604)	13% (N=343)
tsp-14(jj95) sma-9(cc604)	1% (N=725)
tsp-14(jj96) sma-9(cc604)	0% (N=829)
nT1[qIs51]/tsp-12(ok239); tsp-14(jj95) sma-9(cc604)	8% (N=913)
tsp-12(ok239); tsp-14(jj95) sma-9(cc604)	**73% (N=405)**[*** b]
nT1[qIs51]//tsp-12(ok239); tsp-14(jj96) sma-9(cc604)	6% (N=707)
tsp-12(ok239); tsp-14(jj96) sma-9(cc604)	**64% (N=591)**[*** b]

[a] The Susm penetrance refers to the percent of animals with 1-2 M-derived CCs as scored by the *CC::gfp* reporter.

[***]$p < 0.0001$ (unpaired two-tailed Student's *t*-test)

[b] Statistical analysis was conducted by comparing the *tsp-12(ok239); tsp-14(0) sma-9(cc604)* triple mutants with the *tsp-12(ok239); sma-9(cc604)* double mutants.

2.5.2 TSP-12 is widely expressed and is localized to both the cell surface and the cytoplasm in multiple cell types

To determine how TSP-12 functions to promote BMP signaling, we determined the expression and subcellular localization patterns of TSP-12. We tagged the endogenous TSP-12 with GFP at either the N-terminus or at the C-terminus using CRISPR/Cas9-triggered homologous recombination ([101, 102]; see Materials and Methods). Both tagged proteins are fully functional because when introduced into the *tsp-14(0)* background, neither GFP::TSP-12 nor TSP-12::GFP caused any defects observed for *tsp-12(0); tsp 14(0)* double mutants as described above. Additionally, both GFP::TSP-12 and TSP-12::GFP exhibited the same expression and localization pattern. As shown in Figure 2, GFP::TSP-12 is widely expressed from early embryos through larval development to adults in multiple cell types, which include the vulva precursor cells, the hypodermis, and the germline (Figure 2A-H). Within a cell, GFP::TSP-12 is both localized to the cell surface and in the cytoplasm in what appears to be small vesicles (Figure 2A, 2E and 2G). Because the fluorescence signal for the endogenously tagged GFP::TSP-12 in somatic cells is faint, we also generated integrated transgenic lines over-expressing a functional, C-terminally tagged TSP-12::GFP transgene (see Materials and Methods). In these animals, we detected TSP-12::GFP in the pharynx, intestine, neurons and M lineage cells (Figure 2I-2R). The cell surface TSP-12::GFP in the intestinal cells appears to be restricted to the basolateral membrane but absent in the apical membrane (Figure 2K and 2M).

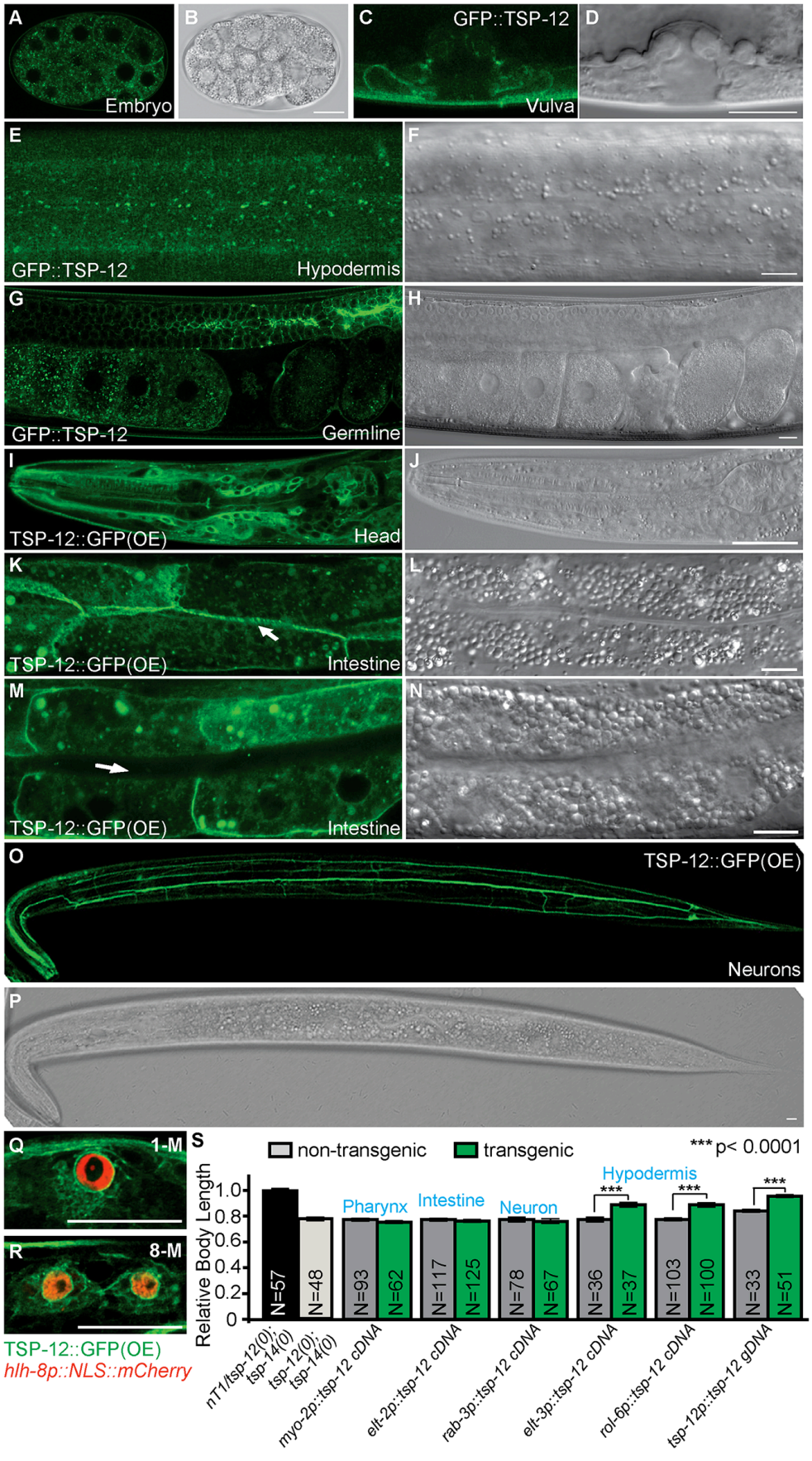
A
Embryo
B
C
GFP::TSP-12
Vulva
D
E
GFP::TSP-12
Hypodermis
F
G
GFP::TSP-12
Germline
H
I
TSP-12::GFP(OE)
Head
J
K
TSP-12::GFP(OE)
Intestine
L
M
TSP-12::GFP(OE)
Intestine
N
O
TSP-12::GFP(OE)
Neurons
P
Q
1-M
R
8-M
TSP-12::GFP(OE)
hlh-8p::NLS::mCherry
S
non-transgenic
transgenic
*** p< 0.0001
Relative Body Length
1.0
0.8
0.6
0.4
0.2
0
Pharynx
Intestine
Neuron
Hypodermis
***
***
***
N=57
N=48
N=93
N=62
N=117
N=125
N=78
N=67
N=36
N=37
N=103
N=100
N=33
N=51
nT1/tsp-12(0); tsp-14(0)
tsp-12(0); tsp-14(0)
myo-2p::tsp-12 cDNA
elt-2p::tsp-12 cDNA
rab-3p::tsp-12 cDNA
elt-3p::tsp-12 cDNA
rol-6p::tsp-12 cDNA
tsp-12p::tsp-12 gDNA

Figure 2.2 TSP-12 is localized both to the cell surface and in cytoplasmic vesicles in multiple cell types, including known Sma/Mab signal-receiving cells.

(A-P) Confocal fluorescent images (A, C, E, G, I, K, M, O) and corresponding DIC images (B, D, F, H, J, L, N, P) of transgenic worms expressing endogenous GFP::TSP-12 (A, C, E, G) or over-expressed (OE) TSP-12::GFP (I, K, M, O) in the early embryo (A), L4 developing vulva (C), late L3 hypodermis (E), young adult gonad (G), L3 larva head (I), L4 intestine (K: basolateral focal plane of the intestine and the arrow points to the lateral membrane, M: middle focal plane of the intestine and the arrow points to the apical lumen of the intestine), and L3 neurons (O). (Q and R) L1 transgenic animals carrying both over-expressed TSP-12::GFP and the M lineage specific reporter hlh-8p::NLS::mCherry. TSP-12::GFP is present in M lineage cells from 1-M (Q) to 8-M (R) stages. Some M lineage cells are out of the focal planes shown. Scale bars represent 10μm in A-R. (S) Rescue of the small body size of *tsp-12(ok239); tsp-14(jj95)* worms produced by *tsp-12(ok239)/+; tsp-14(jj95)* mothers using tissue-specific *tsp-12* cDNA expression. The mean body length of WT worms is normalized to 1.0. Error bars represent 95% confidence intervals for the normalized body length.

2.5.3 TSP-12 functions in the signal-receiving cells to promote BMP signaling in regulating body size and mesoderm development

It has been well established that the Sma/Mab pathway receptors and downstream Smad proteins function in the hypodermal and M lineage cells to regulate body size and mesoderm development, respectively [28, 104, 105]. Since *tsp-12* is expressed in the hypodermal and M lineage cells, we asked whether it functions in these cells to promote Sma/Mab signaling. We forced the expression of *tsp-12* cDNA in specific tissues of the *tsp-12(0); tsp-14(0)* double mutants using tissue specific promoters. Forced expression of the *tsp-12* cDNA in the hypodermis (*elt-3p::tsp-12* cDNA and *rol-6p::tsp-12* cDNA) rescued the small body size of *tsp 12(0); tsp-14(0)* double mutants, but forced expression in the pharynx (*myo-2p::tsp-12* cDNA), intestine (*elt-2p::tsp-12* cDNA) or neurons (*rab-3p::tsp-12* cDNA) had no effect (Figure 2S). Forced expression of *tsp-12* in the M lineage (*hlh-8p::tsp-12* cDNA) partially rescued the Susm phenotype of *tsp-12(0); tsp-14(0)* double mutants: transgenic *tsp-12(0); tsp-14(0)* mutants carrying the *hlh-8p::tsp-12* cDNA transgene exhibited 15% (n=108) of the Susm phenotype, while non-transgenic *tsp-12(0); tsp-14(0)* mutants exhibited 59% (n=230) of the Susm phenotype. Thus, TSP-12 functions in the signal-receiving cells to promote Sma/Mab signaling in regulating body size and M lineage development.

2.5.4 The C. elegans ADAM10 ortholog SUP-17 functions in the BMP signaling pathway

TSP-12 and TSP-14 orthologs are known to regulate the maturation and trafficking of ADAM10 (a disintegrin and metalloprotease 10) to promote Notch signaling in Drosophila and mammalian cells [76]. We therefore tested whether the *C. elegans* ADAM10 ortholog, SUP-17 [65], and its close homolog ADM-4 [69], play any role in Sma/Mab signaling using the *sma-9* M lineage suppression assay. A deletion allele of *adm-4*, *ok265*, failed to suppress the *sma-9* M lineage defect; instead, two strong loss-of-function alleles of *sup-17*, *n1258* and *n316*, both partially suppressed the *sma-9* M lineage defect (Figure 3A and Table 2A; *sup-17* null mutants are embryonic lethal [65] and cannot be used in this assay). Both *sup-17(n1258)* and *sup-17(n316)* mutants also exhibit smaller body sizes (Figures 3B, 3C and 3F). *sup-17(n1258)* males exhibit severe tail patterning defects, including shortened and fused rays, smaller fans (Figure 3D and 3E) and crumpled spicules. Thus, *sup-17* strong loss-of-function mutants exhibit Sma/Mab signaling defects.

We then performed double mutant analysis between *sup-17(n1258)* and null mutations in the Sma/Mab pathway by assaying for their body sizes. We found that *sup-17(n1258); dbl 1(wk70)*, *sup-17(n1258); sma-6(jj1)* and *sup-17(n1258); sma-3(jj3)* double mutants were as small as the corresponding *dbl-1(wk70)*, *sma-6(jj1)* or *sma-3(jj3)* single mutants, respectively (Figure 3F). This lack of enhancement of the small body size phenotype of Sma/Mab pathway mutants by *sup-17(n1258)* is not because Sma/Mab pathway mutants have reached the minimal body size of *C. elegans*, because previous studies have shown that mutations in genes regulating body size but not

functioning in the Sma/Mab pathway, such as *sma-5* (encoding a MAPK, [106]) or *wts-1* (encoding a serine/threonine kinase, [107]), can make Sma/Mab pathway mutants much smaller. We therefore concluded that SUP-17 functions in the Sma/Mab pathway to regulate body size.

Table 2. Suppression of the *sma-9* M lineage phenotype by *sup-17* and *unc-40* mutations.

A. Susm[a] phenotype of *sup-17* mutations.	
Genotype	**% Susm (N)[b]**
sma-9(cc604)	--
adm-4(ok265) sma-9(cc604)	0% (N=387)
sup-17(n316); sma-9(cc604)	31.4% (N=379)
sup-17(n1258); sma-9(cc604) [20°C]	78.6% (N=751)
sup-17(n1258); sma-9(cc604) [25°C]	86.1% (N=607)
sup-17(n1258); sma-9(cc604); jjEx[sup-17p::sup-17 genomic::gfp]	40.1% (N=379) *** c
sup-17(n1258); sma-9(cc604); jjEx[sup-17p::sup-17 cDNA]	40.9% (N=653) *** c
sup-17(n1258); sma-9(cc604); jjEx[hlh-8p::sup-17 cDNA]	63.6% (N=176) * c
sup-17(n1258); sma-9(cc604); jjEx[rab-3p::sup-17 cDNA]	75.7% (N=136) ND c
B. Susm[a] phenotype of *sel-12* and *hop-1* mutations.	
Genotype	**% Susm (N)**
sel-12(ok2078) sma-9(cc604)	0% (N=100)
sel-12(ar171) sma-9(cc604)	0% (N=100)
hop-1(ar179); sma-9(cc604)	0.3% (N=326)
hT2[qIs48]/hop-1(ar179); sel-12(ok2078) sma-9(cc604)	6.9% (N=261)
hop-1(ar179); sel-12(ok2078) sma-9(cc604)	3.3% (N=92)
C. Susm[a] phenotype of *sup-17* and *unc-40* mutations.	
Genotype	**% Susm (N)**

sup-17(n1258); sma-9(cc604)	71.1% (N=622)
unc-40(e1430); sma-9(cc604)	94.2% (N=345)
unc-40(e1430) sup-17(n1258); sma-9(cc604)	95.4% (N=382)
unc-40(ev495); sma-9(cc604)	0% (N=130)
unc-40(ev495) sup-17(n1258); sma-9(cc604)	46.2% (N=195)
unc-40(tr115); sma-9(cc604)	0.9% (N=109)
unc-40(tr115) sup-17(n1258); sma-9(cc604)	47.6% (N=341)

In the absence of the *sma-9(cc604)* mutation, none of the single or double mutants listed above has any defects affecting the number of M-derived CCs.

[a] Unless noted, the Susm phenotype of various mutants was examined at 20°C.

[b] The Susm penetrance refers to the percent of animals with 1-2 M-derived CCs as scored by the *CC::gfp* reporter. Up to 3% of *sma-9(cc604)* single mutants have 1-2 M-derived CCs, as reported in Foehr et al. [28]

[c] Statistical analysis was conducted by comparing the transgenic *vs*. non-transgenic animals using unpaired two-tailed Student's *t*-test. $^{***}p< 0.0001$, $^{*}p< 0.05$, ND: not different.

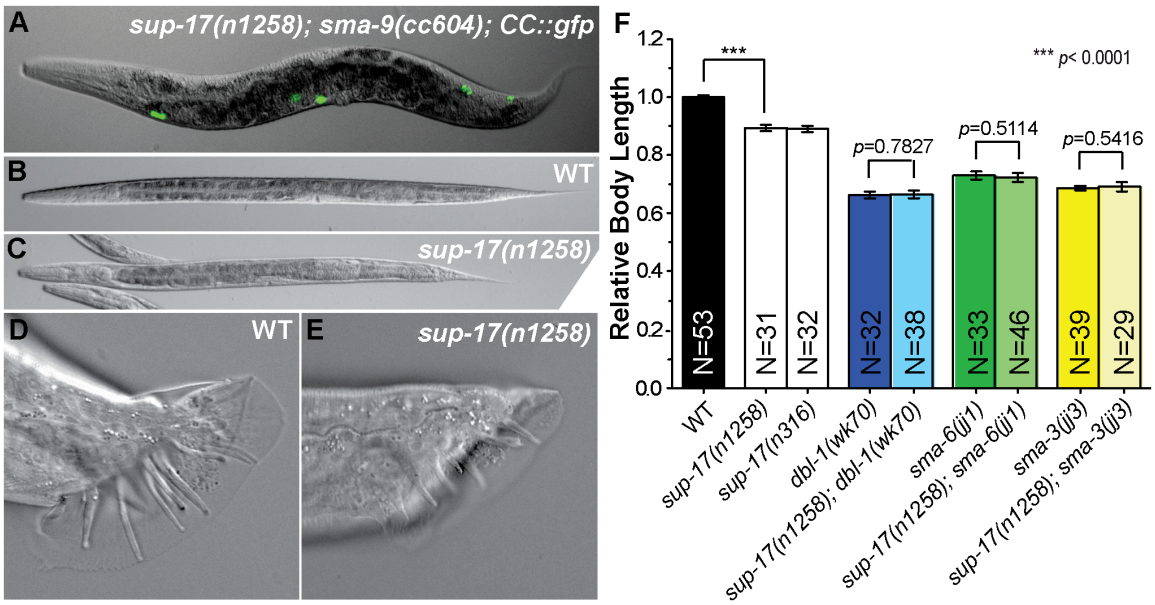

Figure 2.3 *sup-17* functions in Sma/Mab signaling.

(A) Merged GFP and DIC image of a *sup-17(n1258); sma-9(cc604)* animal carrying the *CC::gfp* reporter. (B-E) Representative DIC images of developmental stage-matched WT (B, D) and *sup-17(n1258)* (C, E) worms, showing the smaller body size (C) and abnormal male tail (E) of *sup-17(n1258)* worms. (F) Relative body length of stage-matched WT and various mutant worms measured at the L4 stage. Worms have developed to the L4 stage at 25°C from synchronized L1 stage. The mean body length of WT worms is normalized to 1.0. Error bars represent 95% confidence intervals (CI) for the normalized body length.

2.5.5 SUP-17 is expressed and functions in the signal-receiving cells to promote BMP signaling in in regulating body size and mesoderm development

To determine how SUP-17 functions in modulating Sma/Mab signaling, we tagged the endogenous SUP-17 by generating SUP-17::GFP knock-in strains using CRISPR/Cas9-triggered homologous recombination (see Materials and Methods). The SUP-17::GFP fusion is functional, because a transgene with the same SUP-17::GFP fusion rescued the small body size and Susm phenotypes of *sup-17(n1258)* mutants (Figure 4L). Like TSP-12, SUP-17::GFP is also widely expressed from the early embryo through larval development to adults. Cells expressing SUP-17::GFP include the germline, developing vulva, hypodermis, M lineage cells (Figure 4B-4K), and intestinal cells (Figure 4L-4M). Also like TSP-12, SUP-17::GFP is localized both at the cell surface and in the cytoplasm in small puncta (Figure 4B, 4D, 4F, 4H). In the early embryo, cell surface localized SUP-17::GFP is enriched in the basolateral, but not the apical, surfaces (Figure 4B). Forced expression of *sup-17* cDNA in the hypodermis (*rol-6p::sup-17* cDNA), but not in the intestine (*elt-2p::sup-17* cDNA), rescued the small body size of *sup-17(n1258)* mutants (Figure 4N). Similarly, forced expression of *sup-17* cDNA in the M lineage (*hlh-8p::sup-17* cDNA) partially rescued the Susm phenotype of *sup-17(n1258)* mutants (Table 2A). These findings indicate that SUP-17 also functions in the signal-receiving cells to modulate Sma/Mab signaling in regulating body size and mesoderm development.

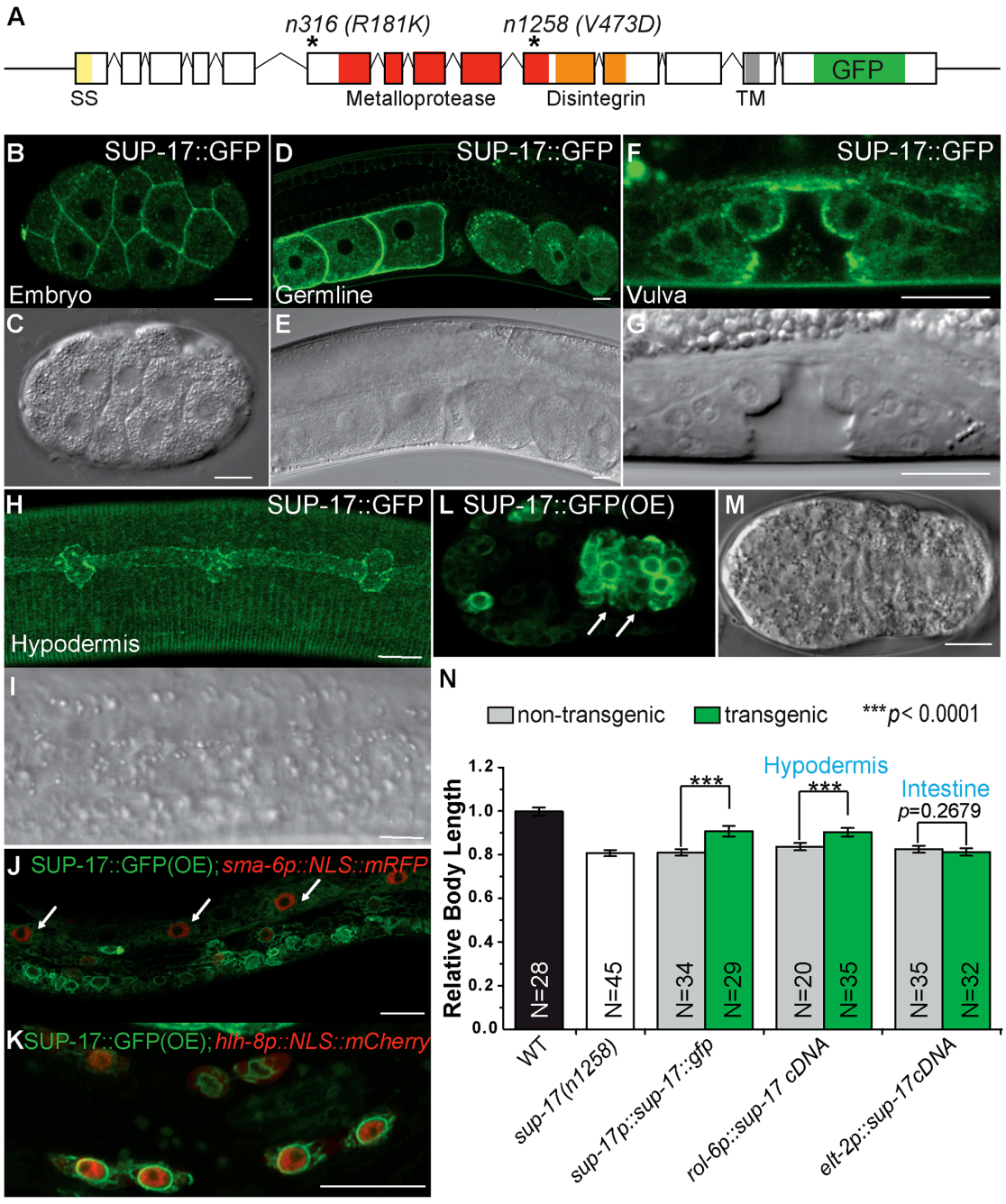
A
n316 (R181K)
n1258 (V473D)
SS
Metalloprotease
Disintegrin
TM
GFP
B SUP-17::GFP
Embryo
D SUP-17::GFP
Germline
F SUP-17::GFP
Vulva
C
E
G
H SUP-17::GFP
Hypodermis
L SUP-17::GFP(OE)
M
I
J SUP-17::GFP(OE); sma-6p::NLS::mRFP
K SUP-17::GFP(OE); hlh-8p::NLS::mCherry
N
non-transgenic
transgenic
***p< 0.0001
Relative Body Length
Hypodermis
Intestine
p=0.2679
***
***
N=28
N=45
N=34
N=29
N=20
N=35
N=35
N=32
WT
sup-17(n1258)
sup-17p::sup-17::gfp
rol-6p::sup-17 cDNA
elt-2p::sup-17cDNA

Figure 2.4 SUP-17 is localized both to the cell surface and in the cytoplasm in multiple cell types, including known Sma/Mab signal-receiving cells.

(A) A schematic of the *sup-17* genomic region (not to scale), depicting the location of various protein domains, the GFP insertion site and the location of the *n1258* and *n316* molecular lesions. (B-I) Confocal fluorescent images (B, D, F, H) and corresponding DIC images (C, E, G, I) of transgenic worms expressing endogenous SUP-17::GFP (B, D, F, H) in the early embryo (B), gravid adult gonad (D), L4 developing vulva (F) and L3 hypodermis (H). (J) An L3 transgenic animal carrying both over-expressed SUP-17::GFP and sma-6p::NLS::mRFP, showing expression of SUP-17::GFP in the hypodermal cells (arrows). (K) An L1 transgenic animal carrying both over-expressed SUP-17::GFP and the M lineage specific reporter *hlh-8p::nls::mCherry* at the 16-M stage. Some M lineage cells are out of the focal planes shown. (L-M) GFP (L) and DIC (M) images of a mid-stage transgenic embryo carrying over-expressed SUP-17::GFP, showing GFP expression in the intestinal precursor cells (marked by arrows). Anterior is to the left. Scale bars represent 10 μm in B-M. (N) Rescue of the small body size of *sup-17(n1258)* worms by tissue-specific sup-17 cDNA expression. The mean body length of WT worms is normalized to 1.0. Error bars represent 95% confidence intervals for the normalized body length.

2.5.6 TSP-12 can bind to SUP-17 and promote its cell surface localization

The shared expression/localization pattern and function of TSP-12, TSP-14 and SUP-17 in Sma/Mab signaling suggest that TSP-12 and TSP-14 may be functionally linked with SUP-17 in their roles in the Sma/Mab pathway. Using the mating-based split ubiquitin yeast-two-hybrid assay for membrane protein interactions (see Materials and Methods), we found that SUP-17 can bind to TSP-12 and TSP-14 (Figure 5A). We then examined the localization of SUP-17::GFP in *tsp-12(0)* and *tsp-14(0)* single mutants, and in *tsp-12(0); tsp-14(0)* double mutants. We focused on the early embryo for these localization studies because of the large cell sizes and the brighter GFP signals in these embryos. Wild-type embryos expressing the endogenously-tagged SUP-17::GFP showed GFP localization both at the cell surface and in the cytoplasm (Figure 5B and 5F). This localization pattern does not change in *tsp-14(0)* mutant embryos (Figure 5C and 5F). However, in *tsp-12(0)* or *tsp-12(0); tsp-14(0)* mutant embryos, there is a significant reduction of cell surface SUP-17::GFP accompanied by an increase of intracellular SUP-17::GFP (Figure 5B-5F) and an increase in the number of bright puncta in the cytoplasm (Figure 5G). These findings indicate that TSP-12 and TSP-14 can bind to SUP-17 and that TSP-12, but not TSP-14, promotes the cell surface localization of SUP-17 in embryos.

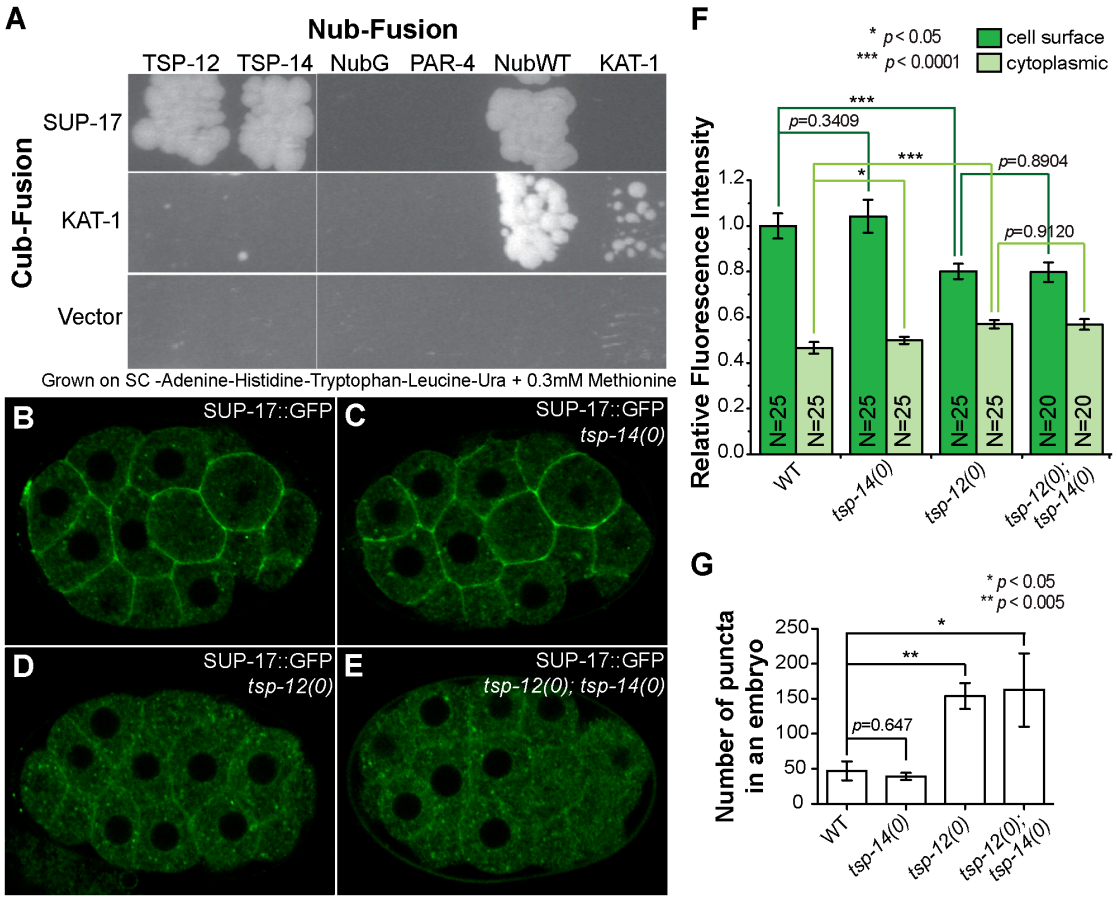

Figure 2.5 TSP-12 binds to and promotes the cell surface localization of SUP-17.

(A) Mating-based split ubiquitin yeast-two-hybrid assay showing that SUP-17 can bind to TSP-12 and TSP-14. (B-E) Confocal images showing the localization of endogenously-tagged SUP-17::GFP in WT (B), *tsp-14(0)* (C), *tsp-12(0)* (D) and *tsp-12(0); tsp-14(0)* (E) backgrounds. (F) Quantification of relative fluorescence intensity of cell surface and cytoplasmic SUP-17::GFP in WT and various mutants (see Materials and Methods). A total of 20 or 25 cells, five cells/30-cell stage embryo, was measured. The mean cell surface fluorescence intensity in WT embryos is normalized to 1.0. Error bars represent 95% confidence intervals (CI) for the normalized mean fluorescence intensity. (G) Quantification of the number of intra-cellular puncta in embryos of WT and various mutants (see Materials and Methods). Three to five 30-cell stage embryos were measured. Error bars represent standard error of the mean (SEM).

2.5.7 The two C. elegans presenilins SEL-12 and HOP-1 do not appear to be required for Sma/Mab signaling

The involvement of SUP-17/ADAM10 in Sma/Mab signaling prompted us to test whether the γ-secretase functions in Sma/Mab signaling, because Notch undergoes sequential cleavage by ADAM and γ-secretase [108]. *C. elegans* has three paralogous genes encoding presenilins, *sel-12*, *hop-1* and *spe-4* [109-111], and presenilins are major components of the γ-secretase complex. Because *spe-4* appears to be specifically expressed and functions in the germline during spermatogenesis, and because *sel-12* and *hop-1* share redundant functions, in particular in Notch signaling [109-111], we tested whether mutations in *sel-12* and *hop-1* exhibited any Susm phenotypes. Using null alleles for each gene, we found that *sel-12(ar171)*, *sel-12(ok2078)*, *hop-1(ar179)* single mutants or *hop-1(ar179); sel 12(ar171)* and *hop-1(ar179); sel-12(ok2087)* double mutants did not exhibit any Susm phenotype (Table 2B), suggesting that the γ-secretase is unlikely to be involved in Sma/Mab signaling in *C. elegans*.

2.5.8 The neogenin homolog UNC-40 is one of the substrates of SUP-17/ADAM10 in Sma/Mab signaling

ADAM10 is known to cleave transmembrane or membrane-associated proteins in a process called ectodomain shedding [41, 112]. We have previously shown that the extracellular domain of UNC-40 is sufficient to function in promoting Sma/Mab signaling, suggesting that UNC-40 may be cleaved for its function in Sma/Mab signaling [38]. We therefore tested genetically whether UNC-40 is a SUP-

17/ADAM10 substrate. We reasoned that if UNC-40 is a SUP-17 substrate in BMP signaling, then the extracellular domain of UNC-40, which is sufficient to function in promoting Sma/Mab signaling, should be able to, either completely or partially, rescue the Sma/Mab signaling defects of *sup-17* mutants. We, therefore, tested whether two unc-40 alleles that lead to the production of truncated UNC-40 proteins lacking the intracellular domain (ICD), *ev495* and *tr115* [38, 113], could rescue the Susm phenotype of *sup-17(n1258)* mutants. As shown in Table 2C, a null *unc-40* allele, *e1430*, did not rescue the Susm phenotype of *sup-17(n1258)* mutants, while both *unc-40(ev495)* and *unc-40(tr115)* partially suppressed the Susm phenotype of *sup-17(n1258)* mutants. The similar penetrance of the Susm phenotype shared by *unc-40(e1430)* and *unc-40(e1430) sup-17(n1258)* mutants, and the partial suppression of the *sup-17(n1258)* Susm phenotype by *unc-40(ev495)* and *unc-40(tr115)* suggest that: 1) UNC-40 and SUP-17 function in the same pathway to regulate Sma/Mab signaling, and 2) UNC-40 is a substrate of SUP-17 in the Sma/Mab pathway. The incomplete suppression of the Susm phenotype of *sup-17(n1258)* mutants by *unc-40(ev495* or *tr115)* suggests that additional SUP-17 substrates must exist in the Sma/Mab pathway.

2.6 DISCUSSION

2.6.1 The TspanC8 tetraspanins and ADAM10 positively promote BMP signaling independent of their roles in Notch signaling

In this study, we extended our previous work [39]and provided additional evidence that TSP-12 and TSP-14, two paralogous TspanC8 tetraspanins, function

redundantly to promote BMP signaling in *C. elegans*. We further showed the ADAM10 ortholog SUP-17 also functions in the BMP pathway. Both *tsp-12; tsp-14* double mutants and *sup-17* single mutants exhibited BMP signaling defects, including a smaller body size, male tail abnormalities, reduced RAD-SMAD reporter activity, and suppression of the *sma-9* mesoderm phenotype (Susm). Both TSP-12 and SUP-17 are expressed and function in the signaling-receiving cells to promote BMP signaling in regulating body size and M lineage development. TSP-12 and TSP-14 can bind to SUP-17. TSP-12 and SUP-17 share similar expression and subcellular localization patterns. Additionally, TSP-12 promotes the cell surface localization of SUP-17 in embryos.

TspanC8 tetraspanins and ADAM10 are known to promote Notch signaling in *C. elegans*, Drosophila, and mammalian tissue culture cells [65, 75, 81, 114, 115]. Three lines of evidence suggest that the function of these proteins in promoting BMP signaling is independent of their role in Notch signaling. First, unlike *lin-12(0)* mutants, which exhibit a ventral-to-dorsal fate transformation in the M lineage [116], *tsp-12(0)*, *tsp-14(0)*, *tsp-12(0); tsp-14(0)* or *sup-17(n1258)* mutants do not exhibit any M lineage defects. Second, two *lin-12* null mutants, *lin-12(n941)* and *lin-12(ok2215)*, do not exhibit any body size defects (Table S1). Third, we have previously reported that *lin-12(0)* mutants do not suppress the M lineage defects of *sma-9(0)* mutants [117]. Thus our findings uncover an additional function for TspanC8 tetraspanins and ADAM10 in promoting BMP signaling. Notably, TSP-12 and TSP-14 may have other functions in addition to modulating Notch and BMP signaling. In particular, *tsp-12(0); tsp-14(0)* double mutant embryos exhibited ventral enclosure defects, but Notch and

BMP signaling pathways have not been previously implicated in the regulation of ventral enclosure in *C. elegans* [118].

Over-expression and knockdown experiments in Drosophila and mammalian tissue culture cells have shown that TspanC8 tetraspanins promote the cell surface localization of ADAM10 [75, 76, 93]. Our work demonstrates that this function of the TspanC8 tetraspanins is evolutionarily conserved. How TspanC8 tetraspanins regulate the cell surface localization of ADAM10 requires further investigation. Tetraspanins are known to regulate intracellular trafficking of various cargo proteins via multiple distinct mechanisms [70, 119]. Previous work showing that TspanC8 tetraspanins function to promote the exit of ADAM10 from the endoplasmic reticulum (ER) relied on examining the localization of over-expressed ADAM10 proteins in tissue culture cells [75, 76, 93]. We noted in our work that SUP-17::GFP from transgenic lines overexpressing this transgene exhibited a strong perinuclear, ER-like localization pattern with very little cell surface localization (Figure 4J and 4K). However, endogenously-tagged SUP-17::GFP exhibited much more prominent cell surface localization (Figures 4B, 4D, 4F and 4H, Figure 5B). We showed that this cell surface localization is significantly reduced in *tsp-12(0)* and *tsp-12(0); tsp-14(0)* mutants; while there was a concomitant increase of bright SUP-17::GFP-positive puncta in these mutant embryos (Figure 5B-5G). Whether these signals represent SUP-17::GFP trapped in the ER or in other intracellular organelles will need further investigation.

The basolateral plasma membrane localization of TSP-12 in intestinal cells (Figure 2K-2N) resembles the localization patterns of both SMA-6/RI and DAF-4/RII of the BMP pathway [91]. We have previously shown that both TSP-12 and TSP-14

can bind to SMA-6 in yeast [39]. Whether TSP-12, TSP-14 or both of them are required for the proper localization of SMA-6 and DAF-4 will require further investigation.

Our phenotypic analysis clearly showed that TSP-12 and TSP-14 function redundantly to promote BMP signaling (Figure 1F-1K). Both proteins can also bind to SUP-17 in yeast (Figure 5A). However, only *tsp-12(0)* mutant embryos showed severe defect in SUP-17::GFP localization, and this defect is not enhanced in *tsp-12(0); tsp-14(0)* double mutant embryos (Figure 5B-5G). Due to technical challenges, our SUP-17::GFP localization study was carried out in embryos but not in tissues relevant to Sma/Mab signaling. It is possible that TSP-14 may function similarly as TSP-12 to promote the cell surface localization of SUP-17 in other cell types, but not in the early embryo. Alternatively, it is possible that while TSP-12 and TSP-14 exhibit functional redundancy in regulating BMP signaling and other developmental processes at the organismal level, they may differ in their functions at the sub-cellular and/or molecular level.

2.6.2 The role of SUP-17/ADAM10 in the BMP signaling pathway

In worms, flies and mammals, ADAM proteases are well known for their role in processing the Notch receptor upon ligand binding [120-122]. Notch undergoes sequential cleavage, first by the ADAM protease, followed by subsequent cleavage by the γ-secretase. Although ADAM10 has not been previously implicated in BMP signaling in any organisms, the ADAM10 paralog ADAM17 or TACE (tumor necrosis factor-alpha-converting enzyme) has been shown to play a role in TGFβ signaling in

mammals [123]. Earlier work by Liu and colleagues indicated that ADAM17/TACE-mediated cleavage of the type I TGFβ receptor (TβR1) causes downregulation of TGF β signaling in CHO cells [123]. Cleavage of TβR1 by ADAM17/TACE and Presenilin 1, a γ-secretase catalytic core component, has also been found in multiple cancer cell lines, which results in the translocation of the intracellular domain (ICD) of TβR1 into the nucleus and activation of genes involved in tumor invasion [124, 125]. More recently, polymorphic variants of the *Adam17* gene have been found to differentially regulate TGFβ signaling and influence the severity of *Tgfb1*-dependent vascular pathology in mice and humans [126]. Because ADAM10 and ADAM17 are known to share a number of common substrates [112], and in *C. elegans* SUP-17/ADAM10 and ADM-4/ADAM17 share redundant functions [69], our findings raise the possibility that ADAM10 or ADAM17 may also play a role in regulating BMP signaling in mammals. Consistent with this notion, Jackson and colleagues reported that ADAM17/TACE-null mice exhibit defects in valvulogenesis that are associated with aberrant BMP signaling [127].

How SUP-17/ADAM10 functions to modulate BMP signaling is an open question. Our genetic studies suggest that the neogenin/DCC ortholog UNC-40 is one of the substrates of SUP-17. UNC-40, like its vertebrate ortholog neogenin, functions through the RGM (repulsive guidance molecule) proteins to promote BMP signaling [38]. We have previously shown that the extracellular domains of UNC-40 and neogenin are sufficient to mediate BMP signaling in *C. elegans* and in mammalian tissue culture cells, respectively [38]. There are other reports showing that neogenin or

DCC can be cleaved by ADAM proteases. Earlier work using ADAM inhibitors and rat dorsal spinal cord explants showed that DCC undergoes ADAM-dependent proteolytic processing, which may affect its role in regulating axon migration [85]. Okamura and colleagues showed that ADAM17/TACE can bind to and cleave neogenin, regulating the behavior of rat cortical neurons in response to RGM [84]. Recently, van Erp and colleagues showed that ADAM17/TACE-mediated cleavage of neogenin is regulated by the leucine-rich repeats and immunoglobulin-like domains (Lrig) protein Lrig2, and that this regulation is required for RGM-mediated neurite growth inhibition in vitro and cortical neuron migration *in vivo [128]*. How SUP-17 cleaves UNC-40 and whether similar types of regulatory interactions also occur in the BMP signaling pathway will require further experimentation. Nevertheless, cleavage of UNC-40 by SUP-17 may not be followed by subsequent cleavage by the γ-secretase, because *hop-1(0); sel-12(0)* double mutants, which lack two of the redundant *C. elegans* presenilins, do not exhibit any BMP signaling defects (Table 2). We are aware that we assayed the Susm phenotype in *hop-1(0); sel-12(0)* animals produced by *hop-1(0)/+; sel-12(0)* mothers due to the sterility of the *hop-1(0); sel-12(0)* double mutants. Thus, although unlikely, we cannot rule out the possibility that residual γ-secretase activity is still present in *hop-1(0); sel-12(0)* double mutants due to maternally loaded HOP-1 and that this residual activity is sufficient for proper Sma/Mab signaling.

Our genetic studies suggested that UNC-40/neogenin is not the only substrate of SUP-17/ADAM10 in the BMP pathway. Identifying the additional substrate(s) and determining the functional consequences of ADAM processing of these substrates *in*

vivo will provide insight into the intricate levels of modulation of BMP signaling. Notably, ADAM10 and ADAM17 mutations are associated with many diseases in humans, including a variety of cancers [112, 129, 130]. We speculate that some of these incidences could be due to abnormal processing of factors involved in BMP signaling caused by altered activities of ADAM10 and/or ADAM17.

2.7 ACKNOWLEDGEMENTS

We thank Josh Arribere, John Calarco, Dan Dickinson, Andy Fire, Barth Grant, Bob Goldstein, Iva Greenwald, Oliver Hobert, Shohei Mitani and Rick Padgett for strains or plasmids, and Melisa DeGroot and Erich Schwarz for critical comments on the manuscript. Some strains were obtained from the *C. elegans* Genetics Center, which is funded by NIH Office of 27 Research Infrastructure Programs (P40 OD010440). The confocal imaging data was acquired through the Cornell University Biotechnology Resource Center, with NYSTEM (CO29155) and NIH (S10OD018516) funding for the shared Zeiss LSM880 confocal/multiphoton microscope. This work was supported by NIH R01 GM066953 and R01 GM103869 to J.L.

CHAPTER 3

TETRASPANIN PROTEINS REGULATE THE PROPER SUBCELLULAR LOCALIZATION OF SUP-17/ADAM10

3.1 Introduction

ADAM10 belongs to the "a disintegrin and metalloprotease" (ADAM) family of type I transmembrane proteins. ADAM10 is known to cleave many cell surface proteins through 'ectodomain shedding', thus regulating the localization and functions of its substrates. Owing to the versatility and importance of its substrates, ADAM10 is a potential target for many human diseases including cancer. However, targeting ADAM10 for therapeutic goals is challenging because of the potential side effects due to its wide-spread substrates [131]. Therefore it is important to gain a better understanding of ADAM10 and its regulation. Some trafficking proteins, such as mouse SAP-97 [132] and mammalian Tetraspanins [75, 76, 93], are reported to control ADAM10 cell biology. Tetraspanins are a large family of integral membrane proteins with four conserved transmembrane domains, intracellular N and C termini, resulting in 2 extracellular loops and one intracellular region. There is a CCG motif in the second extracellular loop. Tetraspanins can interact with each other using their second extracellular loop and organize membrane to form tetraspanin-enriched microdomains [133, 134]. Tetraspanins promote highly conserved signaling pathways, such as the Notch and BMP pathway [75, 81]. Furthermore, the C8 subfamily of tetraspanins are

reported to accelerate ADAM10 exit from the ER, thereby promoting maturation and cell surface localization of the protease [75, 76, 93]. Transmembrane proteins can be transported to the cell surface after synthesis from the ER. and the cell surface protein can also be endocytosed into the cell. The internalized protein can be then sorted in in early endosomes to either degradation or traffic back to the cell surface. The reduction of the cell surface SUP-17 in *tsp-12* mutants may be due to regulation of either one or a combination of the pathways. In this chapter, I will use various markers to determine where is SUP-17 normally localized and where does SUP-17 localize in *tsp-12* mutants.

In *C. elegans*, the ADAM10 ortholog SUP-17 is predicted to have a prodomain between the signal peptide and the metalloprotease domain [65] (Figure 3.5 A). The prodomain is predicted to be cleaved off by proprotease convertase (PC) to release the mature protease domain. SUP-17 can interact with tetraspanins including TSP-12, TSP-14 and TSP-21 ([80] and Jun Liu, personal communication). Mutations in *tsp-12* cause decreased SUP-17 cell surface localization accompanied by an increase of intracellular SUP-17 as well as increased number of intracellular puncta [80]. However, it is not known precisely where SUP-17 accumulates in *tsp-12(ok239)* mutants. Like other transmembrane proteins, SUP-17 can go through the secretory pathway and be transported to the cell surface after synthesis, and can presumably be recycled back into the cell through endocytosis [135]. TSP-12 could be involved in regulating the cell surface localization of SUP-17 through either pathway. One way to address this question is to identify the puncta in which SUP-17 accumulates in *tsp-12(ok239)* mutants. For this purpose, I used various intracellular organelle markers to

determine where SUP-17::GFP is localized in wild-type and *tsp-12(ok239)* mutant background. Endogenous SUP-17 showed increased accumulation in early and late endosomes in the absence of TSP-12.

3.2 Material and methods

C. elegans strains

All strains were maintained at 20°C using standard cultre conditions [95]. The following mutations and markers were used: Linkage group I (LG I): *sup-17::gfp(jj98), sup-17::mKate2::3×flag(jj175)*. LG IV: *tsp-12(ok239)*, *gfp::3×flag::tsp-12(jj181)*, *gfp::3×flag::tsp-12(jj182)*. LG X: *tsp-14(jj95)*, *tsp-21(jj168)*, *tsp-21(tm6269)*. ER marker *OCF15: unc-119(ed3); ocfIs2[pie-1 prom::mCherry::sp12::pie-1 3'UTR + unc-119(+)]*. Early endosome marker RT1043: *pie-1p::mCherry::rab-5(pwIs403)*. Late endosome marker RT1331: *pie-1p::mCherry::rab-7 (pwIs508)*. Recycling endosome marker RT1196: *pie-1p::mCherry::rab-11 (pwIs476)*. Strains generated for research in this Chapter are summarized in Table 3.1.

Reagents

Mouse anti-FLAG M2 (Sigma F3165, for western blotting), Goat anti-mouse IgG (for western blotting), Goat anti-mouse IgM (for western blotting), Goat anti-GFP (Rockland Immunochemicals, for immunofluorescence), Rabbit anti-RET-1 (a gift from Karen Oegema). 5xSDS sample buffer (10% SDS, 10 mM β-Mercaptoethanol, 20% Glycerol, 0.2 M Tris-HCl pH 6.8, 0.05% Bromophenol blue, 3 M Urea). Transfer

buffer (Trizma base 12 g, Glycine 57.6 g, 20% SDS 20 mL, MeOH 700 mL, H_2O to 4 L).

Immunofluorescence staining

Animal fixation and immunostaining were performed as described previously [136]. Microscopy and image analysis were performed following previously published protocols [80]. Goat anti-GFP (Rockland Immunochemicals, 1:500), Rabbit anti-RET-1 (from Karen Oegema's lab, 1:4000 [137]) were used. Secondary antibodies were from Jackson ImmunoResearch Laboratories and used at a dilution of Alexa fluor@488 donkey anti-goat 1:400 and Cy3 donkey anti-rabbit 1:100, respectively.

Western blotting

Worms were grown to adulthood before synchronization through bleaching, and the released embryos were collected in M9 buffer, followed by snap freezing in liquid nitrogen. The frozen worm pellets were then mixed with 5×SDS sample buffer without bromophenol blue, a small aliquot was taken from the sample to measure protein concentration using nanodrop (Thermo scientific) after diluting in ddH_2O for 10 times. Bromophenol blue was then added to the original sample and the sample heated at 95℃ for 10 min. The samples were centrifuged at top speed for 1 min before being loaded on 8% SDS-PAGE gels. Proteins were then transferred to Millipore Immobilon-P membrane and blocked with 10% milk in PBST (1×PBS with 0.05% Tween) for 1 hour at room temperature. The resultant membranes were incubated with Sigma-Aldrich F3165 (mouse anti-FLAG M2, 1:10000) in 5% milk in PBST (1×PBS

with 0.05% Tween) at 4℃ overnight, and then incubated with Goat anti-mouse IgG (1:10000) in 5% milk in PBST (1×PBS with 0.05% Tween) at room temperature for 2 hours. Membranes were washed in 1×PBS with 0.05% Tween for 10 min, repeated twice, before detection using 250 μL Advansta WesternBright^{TM} ECL for each membrane. The membrane was then stripped using Thermo restore^{TM} western blot stripping buffer, blocked with 10% milk and blotted with Hybridoma Bank JLA20 (mouse anti-actin, 1:500) and then Goat anti-mouse IgM (1:10000). Quantification were performed using Fiji (ImageJ).

Microscopy

To study the co-localization pattern between SUP-17::GFP and various intracellular organelles, live embryos of similar developmental stages were collected from different tetraspanin mutant worms. Imaging were done using either an inverted Zeiss LSM880 confocal microscope with Airyscan or Zeiss LSM710 confocal microscope. A 40× objective (NA 1.4, WD 0.13 mm) and the super-resolution mode (pinhole is around 2.25 AU) were used for fluorescence detection. The excitation laser line is at 488 nm for GFP, and at 561 nm for mCherry. Collected images were then processed by ZEN (Carl Zeiss), followed by analysis and quantification with Fiji.

To quantify the co-localization of SUP-17 with endosome markers, stage-matched live embryos of different genotypes were used for imaging under the same condition as described above, followed by processing using the same settings. In both green and red channels, bright puncta were selected as signals that are above a

threshold of brightness (3,500 pixels) and size (the area above 0.07 μm^2). Thereafter, bright puncta of both channels of the same image were subjected to an overlay (Figure 3.4 A), and the numbers of yellow, green and red puncta were counted for quantification (puncta on the cell surface were excluded from the counting).

Table 3.1 Strains generated for this Chapter

Strain	Genotype
TSP-12 may regulate SUP-17 localization in early endosomes	
LW3705	SUP-17::GFP*(jj98)*
LW3706	SUP-17::GFP *(jj99)*
LW3707	SUP-17::GFP *(jj100)*
LW4467	SUP-17::GFP*(jj98)*; RT1043 *(pie-1p::mCherry::rab-5)* isolate 4
LW4468	SUP-17::GFP*(jj98)*; RT1043 *(pie-1p::mCherry::rab-5)* isolate 6
LW4469	SUP-17::GFP*(jj98)*; RT1043 *(pie-1p::mCherry::rab-5)* isolate 8
LW4470	SUP-17::GFP*(jj98)*; RT1043 *(pie-1p::mCherry::rab-5)* isolate 16
LW4510	RT1043 *(pie-1p::mCherry::rab-5)*; *3×FLAG::GFP::TSP-12(jj181)* isolate 8
LW4511	RT1043 *(pie-1p::mCherry::rab-5)*; *3×FLAG::GFP::TSP-12(jj181) isolate 37*
LW4517	RT1043 *(pie-1p::mCherry::rab-5)*; 3×FLAG::GFP::TSP-12*(jj181) isolate 7*
LW4508	RT1043 *(pie-1p::mCherry::rab-5)*; 3×FLAG::GFP::TSP-14a*(jj183)* isolate 3
LW4509	RT1043 *(pie-1p::mCherry::rab-5)*; 3×FLAG::GFP::TSP-14a*(jj183)* isolate 27
LW4560	RT1043 *(pie-1p::mCherry::rab-5)*; 3×FLAG::GFP::TSP-14a*(jj183)* isolate 4
LW4561	RT1043 *(pie-1p::mCherry::rab-5)*; 3×FLAG::GFP::TSP-14a*(jj183)* isolate 5
LW4551	SUP-17::GFP*(jj98)*; RT1043 *(pie-1p::mCherry::rab-5)*; *tsp-12(ok239)* isolate 24.2
LW4552	SUP-17::GFP*(jj98)*; RT1043 *(pie-1p::mCherry::rab-5)*; *tsp-12(ok239)* isolate 6.11
TSP-12 may regulate SUP-17 localization in late endosomes	
LW4525	SUP-17::GFP*(jj98)*; RT1331 *(pie-1p::mCherry::rab-7)* isolate 5
LW4584	RT1331 *(pie-1p::mCherry::rab-7)*; GFP::3×FLAG::TSP-12*(jj181)* isolate5
LW4585	RT1331 *(pie-1p::mCherry::rab-7)*; GFP::3×FLAG::TSP-12*(jj181)* isolate1
LW4562	RT1331 *(pie-1p::mCherry::rab-7)*; GFP::3×FLAG::TSP-14*(jj183)* isolate6
LW4563	RT1331 *(pie-1p::mCherry::rab-7)*; GFP::3×FLAG::TSP-14*(jj183)* isolate11
LW4553	SUP-17::GFP*(jj98)*; RT1331 *(pie-1p::mCherry::rab-7)*; *tsp-12(ok239)* isolate 2.6
LW4554	SUP-17::GFP*(jj98)*; RT1331 *(pie-1p::mCherry::rab-7)*; *tsp-12(ok239)* isolate 20.7
LW4748	SUP-17::GFP*(jj98)*; RT1331 *(pie-1p::mCherry::rab-7)*; *tsp-14(jj95)* isolate 26
LW4772	SUP-17::GFP*(jj98)*; *RT1331 (pie-1p::mCherry::rab-7)*; *tsp-21(jj168) isolate 9*
LW4773	SUP-17::GFP*(jj98)*; RT1331 *(pie-1p::mCherry::rab-7)*; *tsp-21(jj168) isolate 36*
LW4778	SUP-17::GFP*(jj98)*; RT1331 *(pie-1p::mCherry::rab-7)*; *tsp-21(jj168) isolate 41*
TSP-12 may regulate SUP-17 localization in recycling endosomes	
LW4540	SUP-17::GFP*(jj98)*; RT1196 *(pie-1p::mCherry::rab-11)* isolate 3
LW4596	RT1196 *(pie-1p::mCherry::rab-11)*; GFP::3×FLAG::TSP-12*(jj181)* isolate 8
LW4597	RT1196 *(pie-1p::mCherry::rab-11)*; GFP::3×FLAG::TSP-12*(jj181)* isolate 5
LW4565	RT1196 *(pie-1p::mCherry::rab-11)*; GFP::3×FLAG::TSP-14a*(jj183)*
LW4591	SUP-17::GFP*(jj98)*; RT1196 *(pie-1p::mCherry::rab-11)*; *tsp-12(ok239)* isolate 4.1
LW4592	SUP-17::GFP*(jj98)*; RT1196 *(pie-1p::mCherry::rab-11)*; *tsp-12(ok239)* isolate 5.11

LW4593	SUP-17::GFP*(jj98)*; RT1196 *(pie-1p::mCherry::rab-11)*; *tsp-12(ok239)* isolate 7.6
LW4749	SUP-17::GFP*(jj98)*; RT1196 *(pie-1p::mCherry::rab-11)*; *tsp-14(jj95) isolate 46*
LW4775	SUP-17::GFP*(jj98)*; RT1196 *(pie-1p::mCherry::rab-11)*; *tsp-14(jj95) isolate 13*
LW4779	SUP-17::GFP*(jj98)*; RT1196 *(pie-1p::mCherry::rab-11)*; *tsp-21(jj168) isolate 27*
LW4780	SUP-17::GFP*(jj98)*; RT1196 *(pie-1p::mCherry::rab-11)*; *tsp-21(jj168) isolate 14*
Tetraspanins may not dramatically alter SUP-17 localization in the ER	
LW4750	SUP-17::GFP*(jj98)*; OCF15 (*pie-1p::mCherry::sp-12*) isolate 1
LW4751	SUP-17::GFP*(jj98)*; OCF15 (*pie-1p::mCherry::sp-12*) isolate 2
LW4760	SUP-17::GFP*(jj98)*; OCF15 (*pie-1p::mCherry::sp-12*) isolate 9
LW4753	OCF15 *(pie-1p::mCherry::sp-12)*; 3×FLAG::GFP::TSP-12*(jj181)* isolate 1
LW4754	OCF15 *(pie-1p::mCherry::sp-12)*; 3×FLAG::GFP::TSP-12*(jj181)* isolate 2
LW4755	OCF15 *(pie-1p::mCherry::sp-12)*; 3×FLAG::GFP::TSP-12*(jj181)* isolate 24
LW4756	OCF15 *(pie-1p::mCherry::sp-12)*; 3×FLAG::GFP::TSP-14a*(jj184)* isolate 39
LW4770	OCF15 *(pie-1p::mCherry::sp-12)*; 3×FLAG::GFP::TSP-14a*(jj184)* isolate 19
LW4761	SUP-17::GFP*(jj98)*; OCF15 *(pie-1p::mCherry::sp-12)*; *tsp-12(ok239) isolate 12*
LW4762	SUP-17::GFP*(jj98)*; OCF15 *(pie-1p::mCherry::sp-12)*; *tsp-12(ok239) isolate 19*
LW4771	SUP-17::GFP*(jj98)*; OCF15 *(pie-1p::mCherry::sp-12)*; *tsp-14(jj95) isolate 28*
LW4752	SUP-17::GFP*(jj98)*; OCF15 *(pie-1p::mCherry::sp-12)*; *tsp-21(jj168) isolate 1*
LW4763	SUP-17::GFP*(jj98)*; OCF15 *(pie-1p::mCherry::sp-12)*; *tsp-21(jj168) isolate 38*
Tetraspanins do not seem to regulate SUP-17 total protein level	
LW4225	SUP-17::mKate2::3FLAG *(jj175)* （generated by Zhiyu Liu）
LW4721	SUP-17::mKate2::3FLAG *(jj175)*; *tsp-12(ok239)* isolate 1
LW4722	SUP-17::mKate2::3FLAG *(jj175)*; *tsp-12(ok239)* isolate 3
LW4723	SUP-17::mKate2::3FLAG *(jj175)*; *tsp-12(ok239)* isolate 11
LW4711	SUP-17::mKate2::3FLAG *(jj175)*; *tsp-14(jj95)* isolate 38
LW4731	SUP-17::mKate2::3FLAG *(jj175)*; *tsp-14(jj95)* isolate 22
LW4712	SUP-17::mKate2::3FLAG *(jj175)*; *tsp-21(jj168)* isolate 4
LW4713	SUP-17::mKate2::3FLAG *(jj175)*; *tsp-21(jj168)* isolate 7
Study the co-localization between SUP-17 and Tetraspanins	
LW4512	SUP-17::mKate2::3FLAG*(jj175)*; GFP::3FLAG::TSP-12*(jj181)* isolate 25
LW4513	SUP-17::mKate2::3FLAG(*jj175*); GFP::3FLAG::TSP-12*(jj181)* isolate 38
LW4514	SUP-17::mKate2::3FLAG(*jj175*); GFP::3FLAG::TSP-14a*(jj183)* isolate 21
LW4515	SUP-17::mKate2::3FLAG(*jj175*); GFP::3FLAG::TSP-14a*(jj183)* isolate 22
LW4516	SUP-17::mKate2::3FLAG(*jj175*); GFP::3FLAG::TSP-14a*(jj183)* isolate 38
Mutations in *sup-17* may not alter the expression level of BMP receptors	
LW4002	*sup-17(n1258ts); [DAF-4::GFP]* isolate2.13
LW4003	*sup-17(n1258ts); [DAF-4::GFP]* isolate11.9
LW4291	*sup-17(n1258)*; SMA-6::GFP*(jj166)* isolate 13
LW4292	*sup-17(n1258)*; SMA-6::GFP*(jj166)* isolate 14

BMP signaling may not be able to regulate SUP-17 expression in embryos	
LW4691	SUP-17::GFP*(jj98); dbl-1(wk70)* isolate 2
LW4692	SUP-17::GFP*(jj98); dbl-1(wk70)* isolate 4
LW4693	SUP-17::GFP*(jj98); dbl-1(wk70)* isolate 5
LW4697	SUP-17::GFP *(jj98); sma-6(jj1)* isolate 5
LW4698	SUP-17::GFP *(jj98); sma-6(jj1)* isolate 21
LW4699	SUP-17::GFP *(jj98); sma-6(jj1)* isolate 25
LW4700	SUP-17::GFP *(jj98); sma-3(jj3)* isolate 7
LW4710	SUP-17::GFP *(jj98); sma-3(jj3)* isolate 17

3.3 Results

3.3.1 SUP-17 localization in the ER is not dramatically altered in tsp-12(0) and tsp-14(0) mutants.

My goal was to utilize the ER marker mCherry::SP-12 and compare the endogenous SUP-17::GFP localization pattern in embryos of the following genotypes: wild-type, *tsp-12(ok239), tsp-14(jj95)* single mutants and *tsp-12(ok239);tsp-14(jj95)* double mutants. My preliminary data suggested that SUP-17 is localized in the ER using both live imaging (Figure 3.1 A-C, A'-C') and immunofluorescence staining (Figure 3.1 D-F, D'-F'). However, SUP-17::GFP localization pattern in the ER is not dramatically changed in *tsp-12(ok239);tsp-14(jj95)* double mutants (Figure 3.1 G-I, G'-I'). Additional images of the same developmental stage and same focal plane still needs to be collected. Where SUP-17 mislocalizes in the ER of *tsp-12(ok239)* and *tsp-14(jj95)* single mutants is not clear.

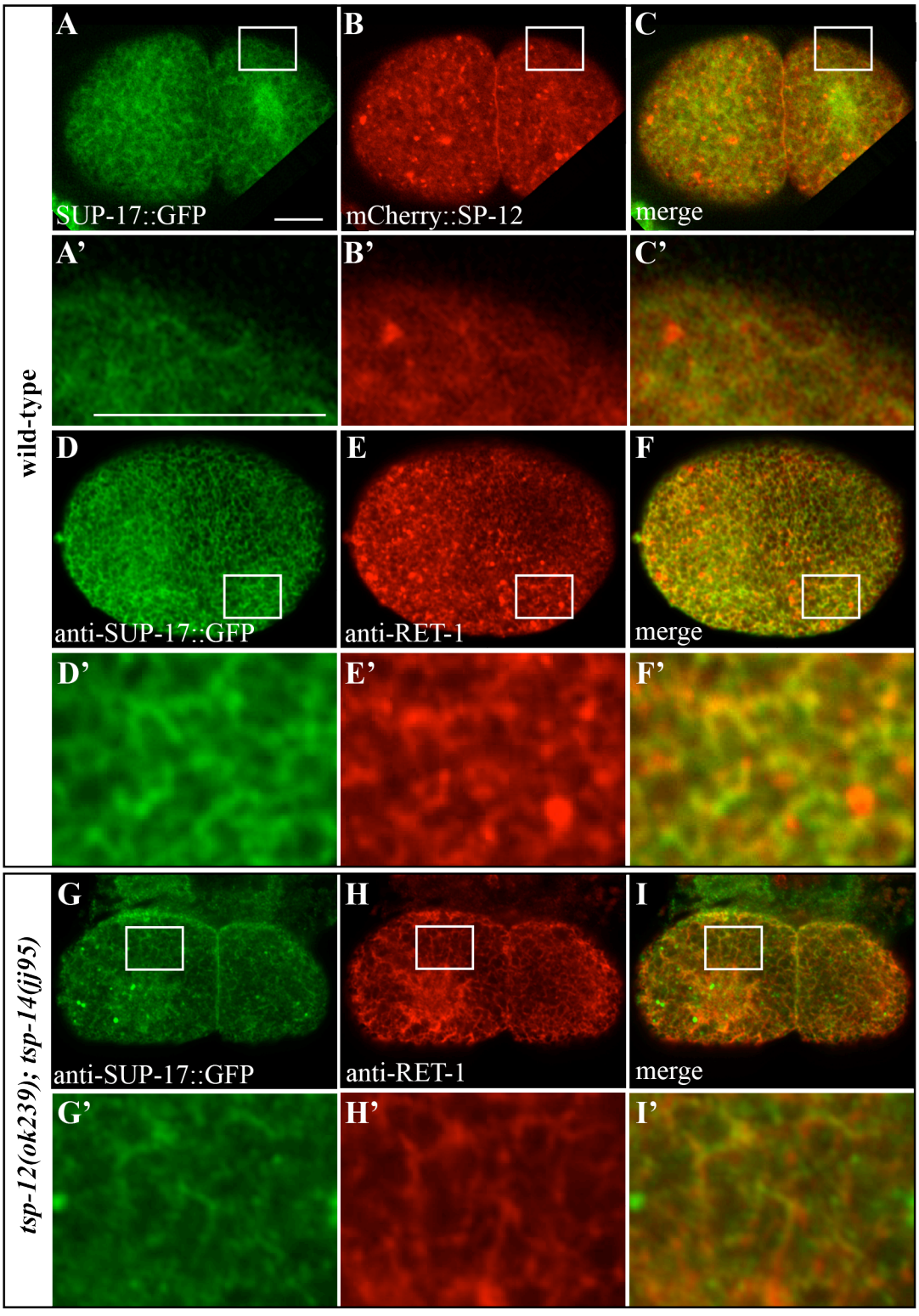
wild-type
A
SUP-17::GFP
B
mCherry::SP-12
C
merge
A'
B'
C'
D
anti-SUP-17::GFP
E
anti-RET-1
F
merge
D'
E'
F'
tsp-12(ok239); tsp-14(jj95)
G
anti-SUP-17::GFP
H
anti-RET-1
I
merge
G'
H'
I'

Figure 3.1 SUP-17 localization in the ER using 1-2 cell stage embryos of wild-type and tetraspanin mutants.

(A-C) Live imaging of SUP-17::GFP localization with ER marker mCherry::SP-12 in wild-type. (D-F) Antibody staining against SUP-17::GFP and RET-1 in a wild-type embryo. (G-H) Antibody staining against SUP-17::GFP and RET-1 in a *tsp-12(ok239);tsp-14(jj95)* double mutant embryo. (A'-I') Enlarged view of the corresponding white rectangle regions in (A-I). Scale bars represent 10 μM. Images were collected using the same magnification.

3.3.2 SUP-17::GFP shows increased accumulation in early and late endosomes in tsp-12(0) mutants

Because the bright puncta in SUP-17::GFP embryos resembles endosome structures, I then examined the localization of SUP-17::GFP in various endosomes, including the early, late and recycling endosomes. Using an early endosome marker RAB-5 and a late endosome marker RAB-7, I found that SUP-17::GFP is localized in both early and late endosomes in wild-type embryos (Figure 3.2 A-C, G-I). In *tsp-12(ok239)* mutant embryos, there is a moderate increase in SUP-17::GFP in both early and late endosomes (Figure 3.2 A-L, Figure 3.4 B). I did not detect any SUP-17::GFP in the recycling endosome using RAB-11 as a marker in either wild-type (Figure 3.3 A-C) or *tsp-12(ok239)* mutant embryos (Figure 3.3 D-F, Figure 3.4 B). In summary, my data suggests that SUP-17::GFP is mis-localized in early and late endosomes in *tsp-12(ok239)* mutants. TSP-12 regulates SUP-17 subcellular localization in early endosomes, late endosomes and to the cell surface.

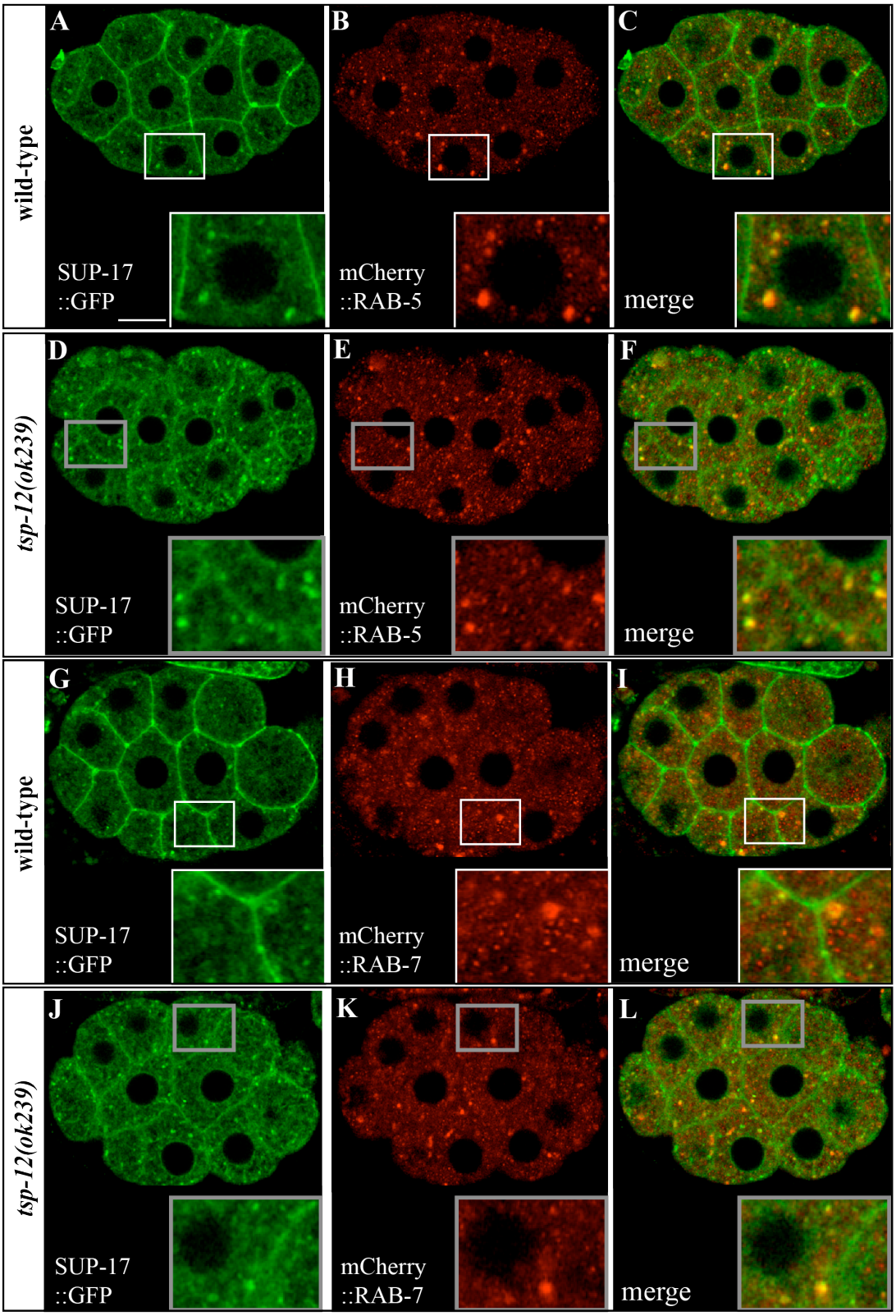
wild-type
A
SUP-17
::GFP
B
mCherry
::RAB-5
C
merge
tsp-12(ok239)
D
SUP-17
::GFP
E
mCherry
::RAB-5
F
merge
wild-type
G
SUP-17
::GFP
H
mCherry
::RAB-7
I
merge
tsp-12(ok239)
J
SUP-17
::GFP
K
mCherry
::RAB-7
L
merge

Figure 3.2 SUP-17 localization in early and late endosomes using embryos of wild-type and *tsp-12(ok239)* mutants.

(A-F) Live imaging of wild-type (A-C) and *tsp-12(ok239)* (D-F) embryos expressing the early endosome marker mCherry::RAB-5 and the endogenous SUP-17::GFP. (G-L) Live imaging of wild-type (G-I) and *tsp-12(ok239)* (J-L) embryos expressing the late endosome marker mCherry::RAB-7 and the endogenous SUP-17::GFP. Rectangles show enlarged views of selected areas in wild-type background and *tsp-12(ok239)* backgrounds. Scale bar represents 10 μM.

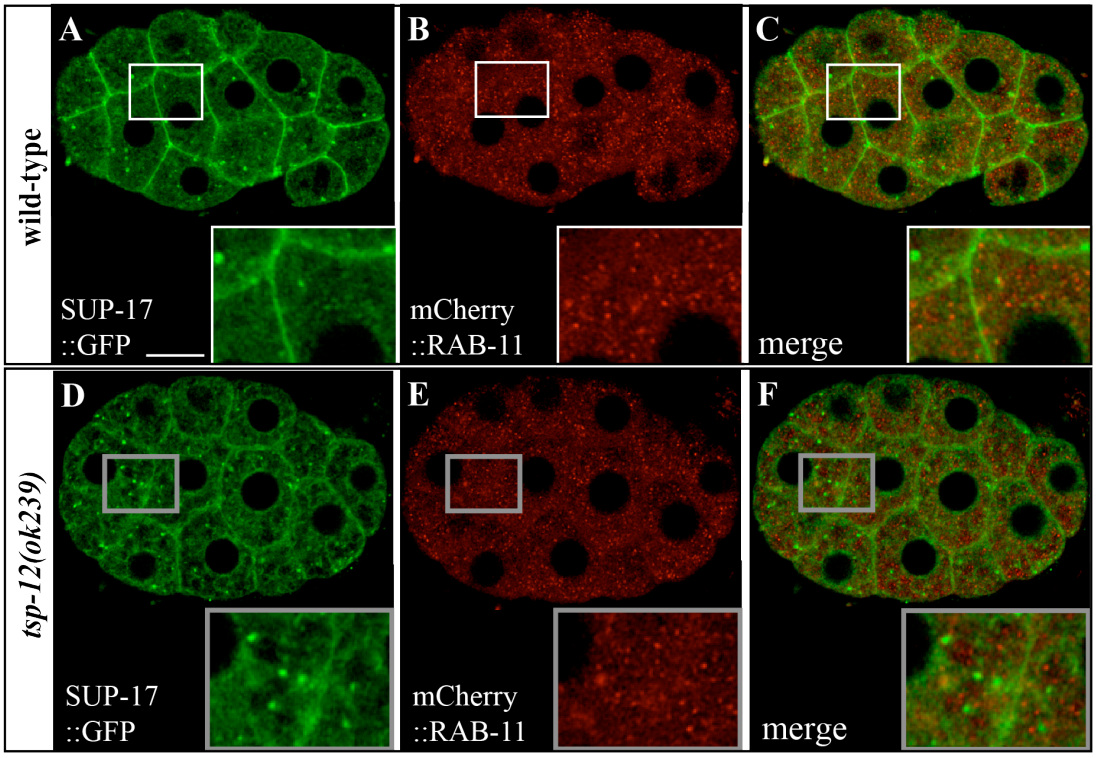

Figure 3.3 SUP-17 localization in recycling endosomes using stage-matched embryos of wild-type and *tsp-12(ok239)* mutants.

Live imaging of wild-type (A-C) and *tsp-12(ok239)* (D-F) embryos expressing the recycling endosome marker mCherry::RAB-11 and the endogenous SUP-17::GFP. Rectangles show enlarged views of the selected regions. Scale bar represents 10 μM.

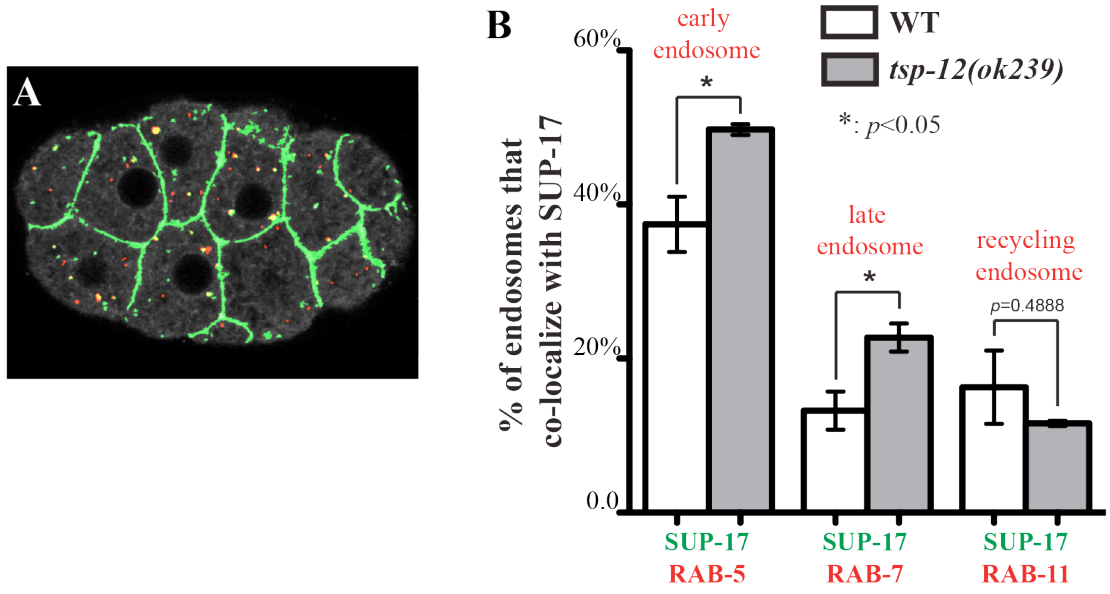

Figure 3.4 Quantification of SUP-17 co-localization with different endosome markers in wild-type and *tsp-12(ok239)* mutant embryos.

(A) A schematic illustrating the method used for quantifying GFP and mCherry colocalization using Fiji (see Materials and methods). Shown in the example is a wild-type embryo expressing SUP-17::GFP and early endosome marker. (B) Quantified percentage of endosome puncta that co-localize with SUP-17::GFP puncta in wild-type (white bars) and *tsp-12(ok239)* (grey bars) mutants.

3.3.3 Total SUP-17 protein level do not appear to change in tetraspanin mutants

My results described above and my previous observation that there is reduced cell surface SUP-17::GFP in *tsp-12(ok239)* embryos suggest that in *tsp-12(ok239)* mutants, SUP-17::GFP may be trapped in early and late endosomes, possibly leading to further degradation in the lysosomes. So I tested if SUP-17 protein level is altered in the absence of tetraspanins. For this purpose, I used a strain generated by Zhiyu Liu in the lab, who tagged the endogenous SUP-17 through CRISPR-Cas9 mediated homologous recombination: SUP-17::mKate2::3xFLAG(*jj175*) [100, 102]. The tag does not appear to affect the function of *sup-17* because Kelly Liu showed that the *jj175* worms did not exhibit any overt phenotypic defect nor showed any suppression of the *sma-9(cc604)* M lineage phenotype. I introduced SUP-17::mKate2::3xFLAG(*jj175*) into individual tetraspanin null mutant backgrounds, including *tsp-12(ok239)*, *tsp-14(jj95)* and *tsp-21(jj168)*. Using Western Blotting of embryos probed with antibodies against FLAG, I detected two bands in *jj175*, but not in the untagged N2 background. There are presumably SUP-17 bands (Figure 3.5 B). Although the observed protein bands ran slower than expected, the two bands likely represent the immature, unprocessed SUP-17 with its prodomain attached (predicted to be 128 kDa), and the mature protease domain (predicted to be 105 kDa). The total protein level of SUP-17::mKate2::3xFLAG does not seem to change in *tsp-12(ok239), tsp-14(jj95)* or *tsp-21(jj168)* mutants. However, the ratio of the top to bottom bands appears to be slightly increased in *tsp-12(ok239)* mutants, suggesting that TSP-12 may play a role in promoting the maturation of SUP-17. In accordance with that, quantification using a short exposure film implicated that TSP-12 may indeed promote

SUP-17 prodomain cleavage (Table 3.2). However, repeats of western blotting and statistics is still required.

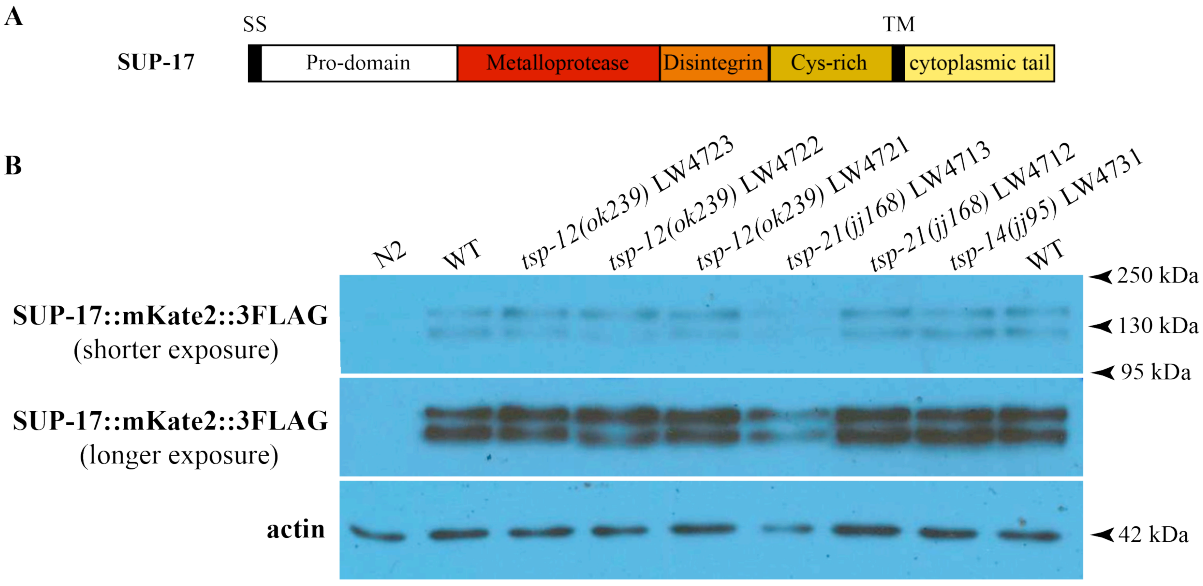

Figure 3.5. SUP-17 protein level in wild-type and tetraspanin mutants.

(A) Predicted domains of SUP-17, modified from Wen et al [65].

(B) Western blotting of embryos of different genotypes probed with anti-FLAG and anti-actin antibodies. Three independent isolates of *tsp-12(ok239)* mutants, 1 isolate of *tsp-14(jj95)* and 2 isolates of *tsp-21(jj168)* mutants were included on the same gel.

Table 3.2 Quantification of SUP-17 protein level in putative mature and immature forms of wild-type and various tetraspanin mutated adults.

Lane#	Strain		Total SUP-17	Mature/ immature SUP-17
Lane 1	N2		N.A.	N.A.
Lane 2	LW4425	SUP-17::mKate2::3xFLAG*(jj175)*	1.67	1.74
Lane 3	LW4723	SUP-17::mKate2::3xFLAG*(jj175); tsp-12(ok239)*	2.05	0.70
Lane 4	LW4722	SUP-17::mKate2::3xFLAG*(jj175); tsp-12(ok239)*	2.33	0.46
Lane 5	LW4721	SUP-17::mKate2::3xFLAG*(jj175); tsp-12(ok239)*	2.15	0.71
Lane 6	LW4713	SUP-17::mKate2::3xFLAG*(jj175); tsp-21(jj168)*	1.23	1.10
Lane 7	LW4712	SUP-17::mKate2::3xFLAG*(jj175); tsp-21(jj168)*	1.94	0.95
Lane 8	LW4731	SUP-17::mKate2::3xFLAG*(jj175); tsp-14(jj95)*	2.64	1.54
Lane 9	LW4425	SUP-17::mKate2::3xFLAG(*jj175*)	2.13	1.08

Quantifications of western blotting protein levels of putative mature, immature SUP-17 and actin were done using the "plot lanes" and "wand" functions in ImageJ. Total protein level of SUP-17 in each strain was the sum of mature protein level normalized to actin and immature protein level normalized to actin. N.A. not applicable.

3.3.4 TSP-21 may slightly promote SUP-17 localization to the cell surface as well as inside the cell

To determine if TSP-21 regulates SUP-17 localization, endogenous SUP-17::GFP was introduced into *tsp-21(jj168)* and *tsp-21(tm6269)* single mutants. Live imaging and the subsequent quantifications were done following the protocol described in Wang et al [80]. It seems that mutations in *tsp-21* cause an increase in the intracellular signal of SUP-17::GFP and decrease in the ratio of cell surface *v.s*. intracellular fluorescence intensity (Figure 3.6 A and B). Quantification using ImageJ suggested that there is indeed a decrease of cell surface *v.s.* intracellular signal (Table 3.3 a and b). However, both the signals on the cell surface and inside the cell increased about 15% (Table 3.3 c). Similar to *tsp-12* mutants, mutations in *tsp-21* also caused an increased number of bright punctate structures inside the cell (Table 3.3 d). These results suggested that TSP-21 may slightly promote SUP-17::GFP level in embryos. However, western blotting in adults did not suggest a clear increase of SUP-17 protein level in *tsp-21(jj168)* (Table 3.2). This may be because the possible increase of the protein level may be too subtle to be detected by western blotting and not enough repeats of western blotting have been done.

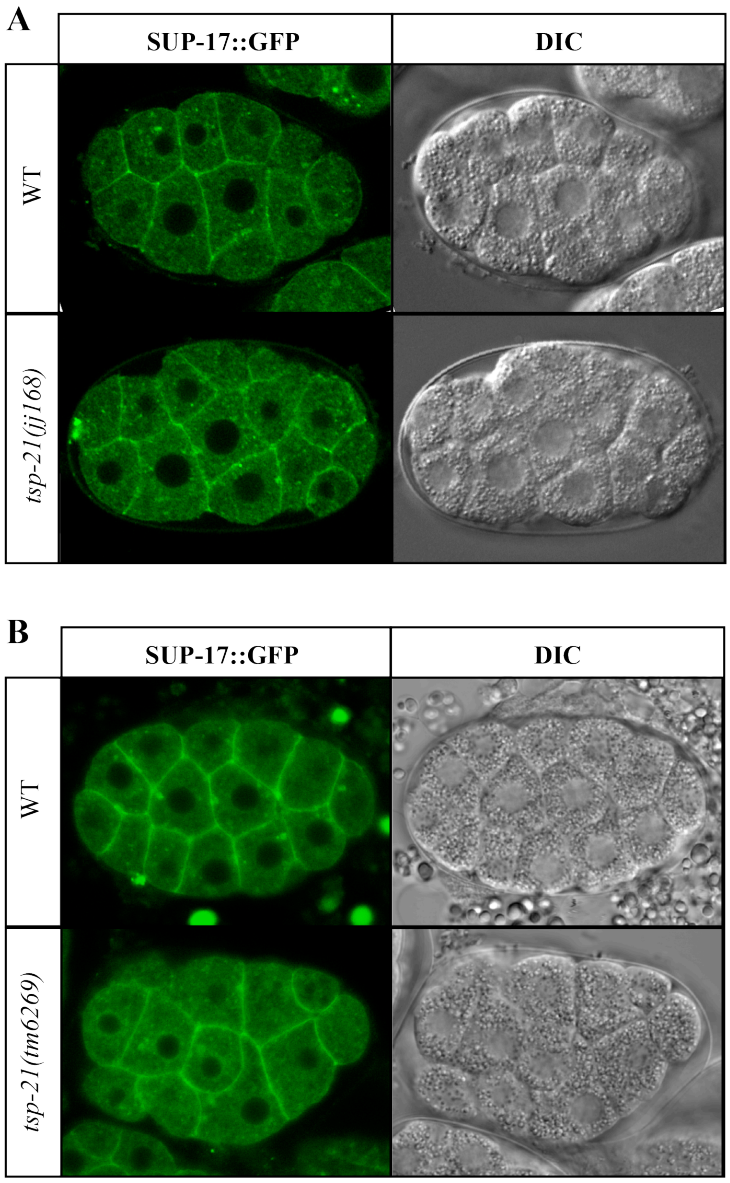

Figure 3.6 SUP-17 localization in wild-type and in *tsp-21* mutants.

(A) Endogenous SUP-17 localization in wild-type and *tsp-21(jj168)* embryos. Images were collected using Zeiss LSM880 confocal microscope with Airyscan. (B) Endogenous SUP-17 localization in wild-type and *tsp-21(tm6269)* embryos. Images were collected using Zeiss LSM710 confocal microscope.

Table 3.3 SUP-17::GFP localization pattern in various tetraspanin mutants.

a. Ratio of cell surface *v.s.* intracellular fluorescence signal in wild-type, *tsp-12(ok239), tsp-14(jj95), tsp-12(ok239); tsp-14(jj95) and tsp-21(jj168)* mutants

Genotypes	mean±SD
SUP-17::GFP*(jj98)*	2.14±0.29
SUP-17::GFP*(jj98); tsp-12(ok239)*	1.41±0.14***
SUP-17::GFP(*jj98); tsp-14(jj95)*	2.09±0.35^{ns}
SUP-17::GFP*(jj98); tsp-12(ok239); tsp-14(jj95)*	1.40±0.16***
SUP-17::GFP*(jj98); tsp-21(jj168)*	1.94±0.22**

Images taken using Zeiss LSM880 confocal microscope with Airyscan were used for quantification in ImageJ. Results were described with mean and standard deviation. Statistics were done by comparing with SUP-17::GFP(*jj98*). $^{***}p<0.0001$, $^{**}p<0.01$

b. Ratio of cell surface *v.s.* intracellular fluorescence signal in wild-type, *tsp-12(ok239), tsp-14(jj95), tsp-12(ok239); tsp-14(jj95) and tsp-21(tm6269)* mutants

Genotypes	mean±SD
SUP-17::GFP*(jj98)*	1.81±0.25
SUP-17::GFP*(jj98); tsp-12(ok239)*	1.20±0.15***
SUP-17::GFP(*jj98); tsp-14(jj95)*	1.87±0.27^{ns}
SUP-17::GFP*(jj98); tsp-12(ok239); tsp-14(jj95)*	1.25±0.17***
SUP-17::GFP*(jj98); tsp-21(tm6269)*	1.53±0.30***

Images taken using Zeiss LSM710 confocal microscope were used for quantification in ImageJ. Results were described with mean and standard deviation. Statistics were done by comparing with SUP-17::GFP(*jj98*). $^{***}p<0.0001$

c. SUP-17::GFP fluorescence intensity on the cell surface and inside the cell in wild-type and *tsp-21(jj168)* mutants.

Genotypes	mean±SD
cell surface SUP-17::GFP(*jj98*)	1±0.13 [a]
intracellular SUP-17::GFP(*jj98*)	0.47±0.06 [a]
cell surface SUP-17::GFP(*jj98*); *tsp-21(jj168)*	1.17±0.12***
intracellular SUP-17::GFP(*jj98*); *tsp-21(jj168)*	0.60±0.06***

Images taken using Zeiss LSM880 confocal microscope with Airyscan were used for quantification in ImageJ. Results were described with mean and standard deviation. The mean of SUP-17::GFP*(jj98)* cell surface fluorescence intensity was normalized to 1. Statistics were done by comparing with the corresponding cell surface or intracellular fluorescence intensity of SUP-17::GFP*(jj98)* respectively. ***$p<0.0001$, [a]published data in Wang et al [80].

d. SUP-17::GFP localization in intracellular bright punctate structures of wild-type and *tsp-21(jj168)* embryos.

Genotypes	mean±SD
SUP-17::GFP*(jj98)*	47±30[a]
SUP-17::GFP*(jj98); tsp-12(ok239)*	154±41**,[a]
SUP-17::GFP(*jj98); tsp-14(jj95)*	39±10[ns,a]
SUP-17::GFP*(jj98); tsp-12(ok239); tsp-14(jj95)*	165±107*,[a]
SUP-17::GFP*(jj98); tsp-21(jj168)*	159±64**

Images taken using Zeiss LSM880 confocal microscope with Airyscan were used for quantification in ImageJ. Puncta with size above 0.07 μm^2 and brightness above 3,500 pixels were selected for counting. Results were described with mean and standard deviation. Statistics were done by comparing with SUP-17::GFP(*jj98*). **$p<0.01$, *$p<0.05$, [a]published data in Wang et al [80].

3.4 Discussion

Previous studies in mammalian cell lines showed that the TspanC8 subfamily of tetraspanins regulate the endoplasmic reticulum (ER)-exit of overexpressed ADAM10 in cultured cell lines [75, 76, 93]. However in my preliminary work, endogenous SUP-17 is not enriched in the SP-12 positive ER structures in the absence of both TSP-12 and TSP-14 in *C. elegans*. This inconsistency is possibly due to the difference between endogenous expression and overexpression, or due to different cell types or organisms. evidence thus far supports the explanation of overexpression *v.s.* endogenous expression: In hypodermal cells, endogenous SUP-17::GFP*(jj98)* generated through CRISPR showed predominant localization to the cell surface with no obvious enrichment in intracellular ER-like structures [80]. However, transgenicly overexpressed SUP-17::GFP dramatically accumulates in the intracellular ER-like structures, though ER markers were not used to confirm that these are indeed ER structures.

I provided *in vivo* evidence that TSP-12 plays a major role in regulating SUP-17: TSP-12 is required for SUP-17 cell surface localization, may regulate SUP-17 localization in endosomes, and seems to promote SUP-17 prodomain cleavage ([80] and this Chapter). Whether TSP-14 and TSP-21 could affect SUP-17 localization in endosomes remains to be determined. Since TSP-12 and TSP-14 have redundant roles [80], it is worth investigating whether *tsp-12(ok239)*; *tsp-14(jj95)* double mutants can cause more severe mislocalization of SUP-17 in endosomes as well as altered protein levels on western blotting.

In summary, there are multiple modulators of BMP signaling in *C. elegans* and these modulators can interact with each other. For example, SUP-17 modulates the BMP signaling pathway in *C. elegans*, possibly through cleaving the extracellular domain of UNC-40 [80]. On the other hand, the subcellular localization of SUP-17 is regulated by TSP-12, which is also a modulator for BMP signaling [39, 80]. In *tsp-12* mutants, embryonic SUP-17::GFP localization on the cell surface is reduced accompanied by an accumulation in early and late endosomes, without an obvious change in total protein level of SUP-17. TSP-21 may also play a role in regulating SUP-17 localization.

CHAPTER 4

ATTEMPTS TOWARDS AN UNDERSTANDING OF THE REGULATION OF UNC-40/NEOGENIN FUNCTION IN THE BMP SIGNALING PATHWAY

4.1 Introduction

The BMP signaling pathway is strictly regulated spatiotemporally, and mis-regulation of the pathway can cause many disorders in humans, such as skeleton disorders, heart diseases and cancers [86-90]. Therefore, studying the modulators of the pathway and understanding their regulation are crucial for our understanding of the BMP signaling pathway and can shed light on BMP-related diseases. UNC-40/Neogenin is a positive modulator that is expressed and functions in signal receiving cells of the BMP signaling pathway [38]. Moreover, the extracellular domain of UNC-40/Neogenin is sufficient for its role in BMP signaling, suggesting UNC-40/Neogenin may be cleaved to mediate BMP signaling. Consistent with this, Neogenin is cleaved by ADAM17 in rat cultured cortical neurons for proper axon guidance [84].

SUP-17/ADAM10 belongs to the ADAM (a disintegrin and metalloprotease) family, and I have previously shown that SUP-17/ADAM10 functions in the BMP signaling pathway [80]. ADAM10 is known to cleave many membrane or membrane-associated proteins, such as Notch [115], TNFα precursor [138] and amyloid precursor protein (APP) [57]. I have genetic evidence suggesting that UNC-40/Neogenin is one of the substrates of SUP-17/ADAM10 in BMP signaling [80]. However, whether SUP-17/ADAM10 biochemically cleaves UNC-40/Neogenin

is not known. Here, I used a combination of molecular genetic methods and western blotting to study the possible cleavage of UNC-40 and its regulation by other BMP pathway components.

4.2 Material and methods

Generating endogenously tagged UNC-40::mKate2::3xFLAG *sup-17(n1258ts)*, UNC-40::GFP::3xFLAG *sup-17(n1258ts)* or UNC-40(L1072A, V1073A)::mKate2::3xFLAG strains using CRISPR/Cas9-mediated homologous recombination

Zhiyu Liu in our lab has previously used CRISPR to tag the endogenous UNC-40 with GFP or mKate2 and generated the following strains: UNC-40::GFP::3xFLAG and UNC-40::mKate2::3xFLAG, respectively. I then used the same strategy to tag UNC-40 in the *sup-17(n1258ts)* background by using the sgRNA plasmid pZL71 and the repair template pZL72 (for mKate2 insertion) or pZL105 (for GFP insertion), and followed the protocol described in Dickinson et al [102]. I obtained the following knock-in strains: LW4735: *unc-40(jj217)[UNC-40::mKate2::3xFLAG] sup-17(n1258ts)*, LW5101: *unc-40(jj245)[UNC-40::GFP::3xFLAG] sup-17(n1258ts)*, and LW5102: *unc-40(jj246)[UNC-40::GFP::3xFLAG] sup-17(n1258ts)*. The success of knock-in was confirmed by genotyping using primers listed in Table 4.2 b. *UNC-40::GFP::3xFLAG* knock-in was further confirmed by imaging.

Mutated UNC-40 that replaced both amino acid 1072 Leu and amino acid 1073 Val with Ala were also generated using CRISPR-Cas9 mediated homologous recombination. Oligo LW-59 was used as repair template and pLW-7 was used as sgRNA. I obtained three independent isolates *unc-40: [unc-40(L1072A, V1073A)::mKate2::3xFLAG]*, named *jj239, jj240* and *jj241*. Mutations were confirmed by PCR (see Table 4.2 b for primers) and sequencing.

Generating truncated UNC-40 without the intracellular domain through CRISPR-mediated non-homologous end joining

I used sgRNA pLW-2 targeting the transmembrane domain of UNC-40 to generate truncated UNC-40 without the intracellular domain. pD162(*Peft-3::Cas9 + empty sgRNA*) was used and following the protocol described in Friedland et al [99]. The resultant *unc-40* alleles are summarized in Table 4.5 a and b.

Generating transgenic lines expressing UNC-40 with FLAG tag inserted in the extracellular domain

Kelly Liu and Herong Shi generated two plasmids that have a single copy of FLAG inserted in two different locations in the extracellular domain of UNC-40: one with the FLAG tag inserted immediately after the signal peptide (pJKL1032[N-FLAG::UNC-40::GFP]) and the other with the FLAG tag inserted between the immunoglobin (Ig) domains and fibronectin type III (FNIII) domains (pJKL1033[M-FLAG::UNC-40::GFP]). I then generated transgenic lines carrying each of these two plasmids by injecting 150 ng/µL of pJKL1032 or pJKL1033 with 3 ng/µL of the co-injection marker LiuFD188 (*myo-2p::mCherry*) into *unc-40(e1430)* worms. The transgenes were then integrated into the genome through gamma irradiation (1500 rads). I obtained 4 integrants of N-FLAG::UNC-40::GFP (*jjIs4802, jjIs4815*) and 3 integrants of M-FLAG::UNC-40::GFP (*jjIs4805, jjIs4806 and jjIs4814*). I then outcrossed each line 4 times with wildtype worms before crossing them into *unc-40(e1430) sup-17(n1258ts)/hT2[qIs48]*, *drag-1(jj4) unc-40(e1430)* and *unc-40(e1430); sma-9(cc604); cc::gfp* mutants respectively. The *drag-*

1(jj4), unc-40(e1430), sup-17(n1258ts) or *sma-9(cc604)* mutations were confirmed by PCR followed by sequencing using primers listed in Table 4.2.

Scoring of the uncoordinated movement phenotype and the egg-laying defective phenotype

Adult worms were bleached and allowed to hatch in M9 for 2 days, synchronized L1s were then grown on NGM/OP50 plates at 20℃ for different lengths of time. At 72 hours post-plating, the uncoordinated movement (Unc) phenotype was determined by visualizing the movement of animals. Score 1 was given to wild type-like moving animals and score 4 was given to the animals that rarely moved or moved in an extremely uncoordinated manner upon stimulation. At 100 hours post-plating, the egg-laying defective (Egl) phenotype was determined by counting the number of animals that died as 'bag of worms' due to defective egg laying.

Body size measurement was done in the same way as described in Chapter 2 [80].

Western blotting

Adult worms were bleached, and the released embryos were allowed to hatch in M9 at 16℃ for 2 days. The synchronized L1s were plated on NGM/OP50 plates and grown to desired stages at either 25℃ (for assays including *sup-17* mutants) or 20℃ (for all other assays). The same number of worms (unless other noted) of identical developmental stages were picked into 20 μL M9 buffer, followed by snap freezing in liquid nitrogen. The frozen worm pellets were then mixed with 5 μL 5×SDS sample buffer with 3M Urea, and heated at 95℃ for 10 min. The samples were centrifuged to top speed for 1 min before being loaded on 8% SDS-PAGE gels. Proteins were then transferred to Millipore Immobilon-P membrane and blocked with 10% milk in PBST (1×PBS with 0.05% Tween) for 1 hour at room temperature. Thereafter, the

membranes were incubated with Sigma-Aldrich F3165 (mouse anti-FLAG M2, 1:10000) in 5% milk in PBST (1×PBS with 0.05% Tween) at 4℃ overnight, and then incubated with Goat anti-mouse IgG(1:10000) in 5% milk in PBST (1×PBS with 0.05% Tween) at room temperature for 2 hours. Membranes were washed in 1×PBS with 0.05% Tween for 10 min, repeated twice, before detection using 250 μL Advansta WesternBright™ ECL for each membrane. The membrane was then stripped using Thermo restore™ western blot stripping buffer, blocked with 10% milk and blotted with Hybridoma Bank JLA20 (mouse anti-actin, 1:5000) and then Goat anti-mouse IgM (1:10000).

Plasmids and strains

The plasmids used for this analysis are shown in Table 4.2 a.

Strains I generated or used for this analysis are summarized in Table 4.1.

Table 4.1 Strains used for experiments described in this chapter

a. Strains I generated.

Strains of *unc-40* alleles without the intracellular domain (generated via CRISPR)	
LW3627	*Ex[LiuFD241(Cas9+empty sgRNA) + pJKL815(myo-2::rfp) + pLW2.3]; sup-17(n1258ts)* isolate 1
LW3628	*Ex[LiuFD241(Cas9+empty sgRNA) + pJKL815(myo-2::rfp) + pLW2.3]; sup-17(n1258ts)* isolate 2
LW3509	*unc-40(jj86)*
LW3510	*unc-40(jj87)*
LW3511	*unc-40(jj88)*
LW3531	*unc-40 (jj89)*
LW3703	*unc-40(jj90) sup-17(n1258ts) / hT2[qIs48]*
LW3698	*unc-40(jj91) sup-17(n1258ts) / hT2[qIs48]*
LW3699	*unc-40(jj92) sup-17(n1258ts) / hT2[qIs48]*
LW3787	*unc-40(jj86); sma-9 unc-9; ccx* isolate1
LW3792	*unc-40(jj86); sma-9 unc-9; ccx* isolate2
LW3825	*unc-40(jj87); sma-9 unc-9; ccx*
LW3790	*unc-40(jj88); sma-9 unc-9; ccx* isolate1
LW3791	*unc-40(jj88); sma-9 unc-9; ccx* isolate2
LW3788	*unc-40(jj89); sma-9 unc-9; ccx* isolate1
LW3789	*unc-40(jj89); sma-9 unc-9; ccx* isolate2
LW3679	*unc-40(jj90) sup-17(n1258ts) /* hT2[qIs48]*; sma-9 unc-9; ccx* isolate2
LW3780	*unc-40(jj90) sup-17(n1258ts) / hT2[qIs48]; sma-9 unc-9; ccx* isolate3
LW3781	*unc-40(jj90) sup-17(n1258ts) / hT2[qIs48]; sma-9 unc-9; ccx* isolate4
Strains generated to test for genetic interactions between *unc-40* and *sup-17* in BMP signaling	
LW4060	*unc-40(ev495) sup-17(n1258ts)/hT2[qIs48]* isolate9.28.3
LW4061	*unc-40(ev495) sup-17(n1258ts)/hT2[qIs48]* isolate44.4.16
LW4124	*unc-40(ev495) sup-17(n1258ts)/hT2[qIs48]; sma-9; ccx; cup-5* isolate9.28.1-24.1
LW4141	*unc-40(ev495) sup-17(n1258ts)/hT2[qIs48]; sma-9; ccx; cup-5* isolate9.28.1-3.1
LW4144	*unc-40(ev495) sup-17(n1258ts)/hT2[qIs48]; sma-9; ccx; cup-5* isolate44.4.16-4.1
LW4139	*unc-40(ev495) sup-17(n1258ts)/hT2[qIs48]; sma-9; ccx; cup-5* isolate44.4.16-8.1
LW4062	*unc-40(tr115) sup-17(n1258ts)/hT2[qIs48]* isolate9.17.2
LW4063	*unc-40(tr115) sup-17(n1258ts)/hT2[qIs48]* isolate28.16.5
LW4142	*unc-40(tr115) sup-17(n1258ts)/hT2[qIs48]; sma-9; ccx; cup-5* isolate9.17.2-4.1
LW4145	*unc-40(tr115) sup-17(n1258ts)/hT2[qIs48]; sma-9; ccx; cup-5* isolate9.17.2-23.1
LW4138	*unc-40(tr115) sup-17(n1258ts)/hT2[qIs48]; sma-9; ccx; cup-5* isolate28.16.5-5.1
LW4143	*unc-40(tr115) sup-17(n1258ts)/hT2[qIs48]; sma-9; ccx; cup-5* isolate9.28.1-2.1
LW4064	*unc-40(e1430) sup-17(n1258ts)/hT2[qIs48]* isolate2.17.5

LW4065	*unc-40(e1430) sup-17(n1258ts)/hT2[qIs48]* isolate6.21.5
LW4140	*unc-40(e1430) sup-17(n1258ts)/hT2[qIs48]; sma-9; ccx; cup-5* isolate2.17.5-1.1
LW4146	*unc-40(e1430) sup-17(n1258ts)/hT2[qIs48]; sma-9; ccx; cup-5* isolate2.17.5-2.1
LW4123	*unc-40(e1430) sup-17(n1258ts)/hT2[qIs48]; sma-9; ccx; cup-5* isolate6.21.5-7.1
LW4125	*unc-40(e1430) sup-17(n1258ts)/hT2[qIs48]; sma-9; ccx; cup-5* isolate6.21.5-8.1
LW5057	*unc-40(e1430); sma-9(cc604); ccx; Ex[pJKL1145(unc-40p::un-40EXD cDNA with 1/2GFP tail) + LiuFD188(myo-2::mCherry)]* isolate 1.4
LW5058	*unc-40(e1430); sma-9(cc604); ccx; Ex[pJKL1145(unc-40p::un-40EXD cDNA with 1/2GFP tail) + LiuFD188(myo-2::mCherry)]* isolate 6.5
LW5068	*unc-40(e1430); sma-9(cc604); ccx; Ex[pJKL1145(unc-40p::un-40EXD cDNA with 1/2GFP tail) + LiuFD188(myo-2::mCherry)]* isolate17.2
LW5069	*unc-40(e1430); sma-9(cc604); ccx; Ex[pJKL1145(unc-40p::un-40EXD cDNA with 1/2GFP tail) + LiuFD188(myo-2::mCherry)]* isolate 21.2
LW5007	*sup-17(n1258ts); sma-9(cc604); ccx; Ex[pJKL1145(unc-40p::un-40EXD cDNA with 1/2GFP tail) + LiuFD188(myo-2::mCherry)]* isolate 1.3
LW5011	*sup-17(n1258ts); sma-9(cc604); ccx; Ex[pJKL1145(unc-40p::un-40EXD cDNA with 1/2GFP tail)+ LiuFD188(myo-2::mCherry)]* isolate 6.2
LW5168	*unc-40(e1430); sma-9(cc604); ccx; Ex[pJKL1155(unc-40p::unc-40EXD::GFP cDNA) + pJKL724 (myo-3::rfp)]* isolate 3.4
LW5166	*unc-40(e1430); sma-9(cc604); ccx; Ex[pJKL1155(unc-40p::unc-40EXD::GFP cDNA) + pJKL724 (myo-3::rfp)]* isolate 6.6
LW5167	*unc-40(e1430); sma-9(cc604); ccx; Ex[pJKL1155(unc-40p::unc-40EXD::GFP cDNA) + pJKL724 (myo-3::rfp)]* isolate 7.1
LW5174	*sup-17(n1258ts); sma-9(cc604); ccx; Ex[pJKL1155(unc-40p::unc-40EXD::GFP cDNA) + pJKL724 (myo-3::rfp)]* isolate 10.3
LW5175	*sup-17(n1258ts); sma-9(cc604); ccx; Ex[pJKL1155(unc-40p::unc-40EXD::GFP cDNA) + pJKL724 (myo-3::rfp)]* isolate 12.3
LW5174	*sup-17(n1258ts); sma-9(cc604); ccx; Ex[pCXT-260(unc-40p::unc-40EXD::GFP cDNA-genomic hybrid) + pJKL724 (myo-3::rfp)]* isolate 5.3
LW5178	*sup-17(n1258ts); sma-9(cc604); ccx; Ex[pCXT-260(unc-40p::unc-40EXD::GFP cDNA-genomic hybrid) + pJKL724 (myo-3::rfp)]* isolate 7.2
LW5179	*sup-17(n1258ts); sma-9(cc604); ccx; Ex[pCXT-260(unc-40p::unc-40EXD::GFP cDNA-genomic hybrid) + pJKL724 (myo-3::rfp)]* isolate 11.4
Strains used for imaging the localization of UNC-40 and/or SUP-17	
LW4492	*unc-40(jj189)[UNC-40::mKate2::3FLAG] sup-17(jj98)[SUP-17::GFP]*
LW4493	*unc-40(jj190)[UNC-40::mKate2::3FLAG] sup-17(jj98)[SUP-17::GFP]*
LW3861	*sup-17(n1258ts); evIs103[UNC-40::GFP; rol-6(d)]* isolate 1
LW3862	*sup-17(n1258ts); evIs103[UNC-40::GFP; rol-6(d)]* isolate 2
LW5101	*unc-40(jj245)[UNC-40::GFP::3FLAG] sup-17(n1258ts)*
LW5102	*unc-40(jj246)[UNC-40::GFP::3FLAG] sup-17(n1258ts)*
Strains to monitor via western blotting possible cleavage of UNC-40 *in vivo*	
LW4735	*unc-40(jj217)[UNC-40::mKate2::3FLAG] sup-17(n1258ts) isolate 10.9.1*
LW4736	*unc-40(jj217)[UNC-40::mKate2::3FLAG] sup-17(n1258ts) isolate 10.9.3*
LW4871	*unc-40(jj217)[UNC-40::mKate2::3FLAG] sup-17 (n1258ts); Ex[pJKL1140(sup-17p::sup-17cDNA + myo-2::mCherry]* isolate2.6
LW4872	*unc-40(jj217)[UNC-40::mKate2::3FLAG] sup-17 (n1258ts); Ex[pJKL1140(sup-17p::sup-17cDNA + myo-2::mCherry]* isolate3.2

LW4873	*unc-40(jj217)[UNC-40::mKate2::3FLAG]) sup-17 (n1258ts); Ex[pJKL1140(sup-17p::sup-17cDNA + myo-2::mCherry]* isolate10.2
LW4867	*unc-40(jj239)[UNC-40(LV->AA)::mKate2::3FLAG]* isolate 3.84.8
LW4876	*unc-40(jj240)[UNC-40(LV->AA)::mKate2::3FLAG]* isolate 1.57
LW4877	*unc-40(jj241)[UNC-40(LV->AA)::mKate2::3FLAG]* isolate 2.13
LW5261	*drag-1(jj4) unc-40(jj221)[UNC-40::GFP::3FLAG]* isolate 9.17.8
LW5266	*drag-1(jj4) unc-40(jj221)[UNC-40::GFP::3FLAG]* isolate 10.8.3
LW5262	*drag-1(jj4) unc-40(jj221)[UNC-40::GFP::3FLAG]* isolate 20.18.2
Strains used to examine the expression pattern of UNC-40 EXD	
LW5232	*Ex[pJKL1155(unc-40p::unc-40EXD::GFP cDNA) + LiuFD188(myo-2::mCherry)]* isolate 11.12
LW5233	*Ex[pJKL1155(unc-40p::unc-40EXD::GFP cDNA) + LiuFD188(myo-2::mCherry)]* isolate 13.2
LW5234	*Ex[pJKL1155(unc-40p::unc-40EXD::GFP cDNA) + LiuFD188(myo-2::mCherry)]* isolate 14.1
LW5240	*drag-1(tm3773); Ex[pJKL1155(unc-40p::unc-40EXD::GFP cDNA) + LiuFD188(myo-2::mCherry)]* isolate 2.9
LW5235	*drag-1(tm3773); Ex[pJKL1155(unc-40p::unc-40EXD::GFP cDNA) + LiuFD188(myo-2::mCherry)]* isolate 6.1
LW5236	*drag-1(tm3773); Ex[pJKL1155(unc-40p::unc-40EXD::GFP cDNA) + LiuFD188(myo-2::mCherry)]* isolate 10.8
LW5237	*unc-40(e1430); Ex[pJKL1155(unc-40p::unc-40EXD::GFP cDNA) + LiuFD188(myo-2::mCherry)]* isolate 1.1
LW5238	*unc-40(e1430); Ex[pJKL1155(unc-40p::unc-40EXD::GFP cDNA) + LiuFD188(myo-2::mCherry)]* isolate 5.18
LW5239	*unc-40(e1430); Ex[pJKL1155(unc-40p::unc-40EXD::GFP cDNA) + LiuFD188(myo-2::mCherry)]* isolate 8.10
Strains with the extracellular domain of UNC-40 tagged with FLAG	
LW4705	*unc-40(e1430); Ex[LWIM22: pJKL1033.1(M-FLAG::UNC-40::GFP) + LiuFD188(myo-2::mCherry)]* isolate 7.4
LW4706	*unc-40(e1430); Ex[LWIM21: pJKL1032.8(N-FLAG::UNC-40::GFP) + LiuFD188(myo-2::mCherry)]* isolate4.2
LW4707	*unc-40(e1430); Ex[LWIM21: pJKL1032.8(N-FLAG::UNC-40::GFP) + LiuFD188(myo-2::mCherry)]* isolate 1.3
LW4708	*unc-40(e1430); Ex[LWIM22: pJKL1033.1(M-FLAG::UNC-40::GFP) + LiuFD188(myo-2::mCherry)]* isolate 1.7
LW4709	*unc-40(e1430); Ex[LWIM22: pJKL1033.1(M-FLAG::UNC-40::GFP) + LiuFD188(myo-2::mCherry)]* isolate 3.5
LW4802	*jjIs4802[N-FLAG::UNC-40::GFP + LiuFD188(myo-2::mCherry)]; unc-40(e1430)* #9
LW4803	*jjIs4803[N-FLAG::UNC-40::GFP + LiuFD188(myo-2::mCherry)]*; *unc-40(e1430)* #14
LW4815	*jjIs4815[N-FLAG::UNC-40::GFP + LiuFD188(myo-2::mCherry)]*; *unc-40(e1430)* #21
LW4804	*jjIs4804[N-FLAG::UNC-40::GFP + LiuFD188(myo-2::mCherry)]*; *unc-40(e1430)* #23
LW4805	*jjIs4805[M-FLAG::UNC-40::GFP + LiuFD188(myo-2::mCherry)]*; *unc-40(e1430)* #3
LW4814	*jjIs4814[M-FLAG::UNC-40::GFP + LiuFD188(myo-2::mCherry)]*; *unc-40(e1430)* #9
LW4806	*jjIs4806[M-FLAG::UNC-40::GFP + LiuFD188(myo-2::mCherry)]*; *unc-40(e1430)* #20
LW4863	*jjIs4802[N-FLAG::UNC-40::GFP + LiuFD188(myo-2::mCherry)]*#9 + 4x outcrossed

LW4862	*jjIs4803[N-FLAG::UNC-40::GFP + LiuFD188(myo-2::mCherry)]*#14 + 4x outcrossed
LW4864	*jjIs4815[N-FLAG::UNC-40::GFP + LiuFD188(myo-2::mCherry)]*#21 + 4x outcrossed
LW4865	*jjIs4804[N-FLAG::UNC-40::GFP + LiuFD188(myo-2::mCherry)]*#23 + 4x outcrossed
LW4859	*jjIs4805[M-FLAG::UNC-40::GFP + LiuFD188(myo-2::mCherry)]*#3 + 4x outcrossed
LW4860	*jjIs4814[M-FLAG::UNC-40::GFP + LiuFD188(myo-2::mCherry)]*#9 + 4x outcrossed
LW4861	*jjIs4806[M-FLAG::UNC-40::GFP + LiuFD188(myo-2::mCherry)]*#20 + 4x outcrossed
LW5270	*jjIs4802*[*N-FLAG::UNC-40::GFP + LiuFD188(myo-2::mCherry)*]#9; *unc-40(e1430)* + 4x outcrossed isolate3
LW5271	*jjIs4802*[*N-FLAG::UNC-40::GFP + LiuFD188(myo-2::mCherry)*]#9; *unc-40(e1430)* + 4x outcrossed isolate4
LW5272	*jjIs4802*[*N-FLAG::UNC-40::GFP + LiuFD188(myo-2::mCherry)*]#9; *unc-40(e1430)* + 4x outcrossed, isolate 5
LW5273	*jjIs4815*[*N-FLAG::UNC-40::GFP + LiuFD188(myo-2::mCherry)*]#21; *unc-40(e1430)* + 4x outcrossed isolate 12
LW5274	*jjIs4815*[*N-FLAG::UNC-40::GFP + LiuFD188(myo-2::mCherry)*]#21; *unc-40(e1430)* + 4x outcrossed isolate 14
LW5275	*jjIs4815*[*N-FLAG::UNC-40::GFP + LiuFD188(myo-2::mCherry)*]#21; *unc-40(e1430)* + 4x outcrossed isolate 19
LW5276	*jjIs4805*[*M-FLAG::UNC-40::GFP + LiuFD188(myo-2::mCherry)*]#3; *unc-40(e1430)* + 4x outcrossed isolate 2
LW5277	*jjIs4805*[*M-FLAG::UNC-40::GFP + LiuFD188(myo-2::mCherry)*]#3; *unc-40(e1430)* + 4x outcrossed isolate 6
LW5278	*jjIs4806*[*M-FLAG::UNC-40::GFP + LiuFD188(myo-2::mCherry)*]#20; *unc-40(e1430)* + 4x outcrossed isolate 6
LW5279	*jjIs4806*[*M-FLAG::UNC-40::GFP + LiuFD188(myo-2::mCherry)*]#20; *unc-40(e1430)* + 4x outcrossed isolate 10
LW5280	*jjIs4806[M-FLAG::UNC-40::GFP + LiuFD188(myo-2::mCherry)]*#20; *unc-40(e1430)* + 4x outcrossed isolate 13
LW5326	*jjIs4802*[*N-FLAG::UNC-40::GFP + LiuFD188(myo-2::mCherry)*]#9; *drag-1(jj4) unc-40(e1430)* isolate 2.1
LW5321	*jjIs4802*[*N-FLAG::UNC-40::GFP + LiuFD188(myo-2::mCherry)*]#9; *drag-1(jj4) unc-40(e1430)* isolate 7.1
LW5322	*jjIs4815*[*N-FLAG::UNC-40::GFP + LiuFD188(myo-2::mCherry)*]#21; *drag-1(jj4) unc-40(e1430)* isolate 7.3
LW5323	*jjIs4815*[*N-FLAG::UNC-40::GFP + LiuFD188(myo-2::mCherry)*]#21; *drag-1(jj4) unc-40(e1430)* isolate 11.2
LW5318	*jjIs4806[M-FLAG::UNC-40::GFP + LiuFD188(myo-2::mCherry)]*#20; *drag-1(jj4) unc-40(e1430)* isolate 5.5
LW5319	*jjIs4806[M-FLAG::UNC-40::GFP + LiuFD188(myo-2::mCherry)]*#20; *drag-1(jj4) unc-40(e1430)* isolate 6.2
LW5251	*jjIs4815[N-FLAG::UNC-40::GFP + LiuFD188(myo-2::mCherry)]*#21; *sup-17(n1258ts)* isolate 2
LW5256	*jjIs4815*[*N-FLAG::UNC-40::GFP + LiuFD188(myo-2::mCherry)*]#21; *sup-17(n1258ts)* isolate 4
LW5257	*jjIs4815[N-FLAG::UNC-40::GFP + LiuFD188(myo-2::mCherry)]*#21; *sup-17(n1258ts)* outcross isolate 8
LW5259	*jjIs4805[M-FLAG::UNC-40::GFP + LiuFD188(myo-2::mCherry)*]#3; *sup-17(n1258ts)* isolate 3
LW5260	*jjIs4805*[*M-FLAG::UNC-40::GFP + LiuFD188(myo-2::mCherry)*]#3; *sup-17(n1258ts)*

	isolate 4
LW5254	*jjIs4806*[*M-FLAG::UNC-40::GFP* + *LiuFD188(myo-2::mCherry)*]#20; *sup-17(n1258ts)* isolate 1
LW5258	*jjIs4806*[*M-FLAG::UNC-40::GFP* + *LiuFD188(myo-2::mCherry)*]#20; *sup-17(n1258ts)* isolate 4
LW5282	*jjIs4802*[*N-FLAG::UNC-40::GFP* + *LiuFD188(myo-2::mCherry)*]#9; *unc-40(e1430) sup-17(n1258ts)/hT2[qIs48]* isolate 4.6
LW5283	*jjIs4802*[*N-FLAG::UNC-40::GFP* + *LiuFD188(myo-2::mCherry)*]#9; *unc-40(e1430) sup-17(n1258ts)/hT2[qIs48]* isolate 6.4
LW5284	*jjIs4802*[*N-FLAG::UNC-40::GFP* + *LiuFD188(myo-2::mCherry)*]#9; *unc-40(e1430) sup-17(n1258ts)/hT2[qIs48]* isolate 7.2
LW5281	*jjIs4815*[*N-FLAG::UNC-40::GFP* + *LiuFD188(myo-2::mCherry)*]#21; *unc-40(e1430) sup-17(n1258ts)/hT2[qIs48]* isolate 6.1
LW5305	*jjIs4815*[*N-FLAG::UNC-40::GFP* + *LiuFD188(myo-2::mCherry)*]#21; *unc-40(e1430) sup-17(n1258ts)/hT2[qIs48]* isolate 11.5
LW5324	*jjIs4805*[*M-FLAG::UNC-40::GFP* + *LiuFD188(myo-2::mCherry)*]#3; *unc-40(e1430) sup-17(n1258ts)/hT2[qIs48]* isolate 2.1
LW5325	*jjIs4805*[*M-FLAG::UNC-40::GFP* + *LiuFD188(myo-2::mCherry)*]#3; *unc-40(e1430) sup-17(n1258ts)/hT2[qIs48]* isolate 7.1
LW5303	*jjIs4806*[*M-FLAG::UNC-40::GFP* + *LiuFD188(myo-2::mCherry)*]#20; *unc-40(e1430) sup-17(n1258ts)/hT2[qIs48]* isolate 2.1
LW5304	*jjIs4806*[*M-FLAG::UNC-40::GFP* + *LiuFD188(myo-2::mCherry)*]#20; *unc-40(e1430) sup-17(n1258ts)/hT2[qIs48]* isolate 3.1
LW4935	*jjIs4802*[*N-FLAG::UNC-40::GFP* + *LiuFD188(myo-2::mCherry)*]#9; *unc-40(e1430); sma-9(cc604); ccx* isolate2.2
LW4936	*jjIs4802*[*N-FLAG::UNC-40::GFP* + *LiuFD188(myo-2::mCherry)*]#9; *unc-40(e1430); sma-9(cc604); ccx* isolate4.3
LW4937	*jjIs4802*[*N-FLAG::UNC-40::GFP* + *LiuFD188(myo-2::mCherry)*]#9; *unc-40(e1430); sma-9(cc604); ccx* isolate11.4
LW4938	*jjIs4815*[*N-FLAG::UNC-40::GFP* + *LiuFD188(myo-2::mCherry)*]#21; *unc-40(e1430); sma-9(cc604); ccx* isolate5.1
LW4939	*jjIs4815*[*N-FLAG::UNC-40::GFP* + *LiuFD188(myo-2::mCherry)*]#21; *unc-40(e1430); sma-9(cc604); ccx* isolate8.2
LW4940	*jjIs4805*[*M-FLAG::UNC-40::GFP* + *LiuFD188(myo-2::mCherry)*]#3; *unc-40(e1430); sma-9(cc604); ccx* isolate1.1
LW4941	*jjIs4805*[*M-FLAG::UNC-40::GFP* + *LiuFD188(myo-2::mCherry)*]#3; *unc-40(e1430); sma-9(cc604); ccx* isolate4.1
LW4942	*jjIs4814*[*M-FLAG::UNC-40::GFP* + *LiuFD188(myo-2::mCherry)*]#9; *unc-40(e1430); sma-9(cc604); ccx* isolate2.2
LW4943	*jjIs4814*[*M-FLAG::UNC-40::GFP* + *LiuFD188(myo-2::mCherry)*]#9; *unc-40(e1430); sma-9(cc604); ccx* isolate5.4
LW4944	*jjIs4806*[*M-FLAG::UNC-40::GFP* + *LiuFD188(myo-2::mCherry)*]#20; *unc-40(e1430); sma-9(cc604); ccx* isolate1.4
LW4945	*jjIs4806*[*M-FLAG::UNC-40::GFP* + *LiuFD188(myo-2::mCherry)*]#20; *unc-40(e1430); sma-9(cc604); ccx* isolate2.1
Strains to examine the relationship between UNC-40 and tetraspanins	
LW3566	*unc-40(ev457); evIs103[UNC-40::GFP; rol-6(d)]*
LW4293	*evIs103[UNC-40::GFP; rol-6(d)] tsp-12(ok239)* isolate 35.3
LW4294	*evIs103[UNC-40::GFP; rol-6(d)]tsp-12(ok239)* isolate 52.6

LW4289	*evIs103[UNC-40::GFP; rol-6(d)]; tsp-14(jj95)* isolate 29
LW4290	*evIs103[UNC-40::GFP; rol-6(d)]; tsp-14(jj95)* isolate 51
LW4328	*evIs103[UNC-40::GFP; rol-6(d)] tsp-12(ok239)/nT1[qIs51]; tsp-14(jj95)* isolate 35.27.1
LW4329	*evIs103[UNC-40::GFP; rol-6(d)] tsp-12(ok239)/nT1[qIs51]; tsp-14(jj95)* isolate 35.27.2
LW4330	*evIs103[UNC-40::GFP; rol-6(d)] tsp-12(ok239)/nT1[qIs51]; tsp-14(jj95)* isolate 35.27.3
LW4331	*evIs103[UNC-40::GFP; rol-6(d)] tsp-12(ok239)/nT1[qIs51]; tsp-14(jj95)* isolate 52.6.1
LW4332	*evIs103[UNC-40::GFP; rol-6(d)] tsp-12(ok239)/nT1[qIs51]; tsp-14(jj95)* isolate 52.6.2
LW4333	*evIs103[UNC-40::GFP; rol-6(d)] tsp-12(ok239)/nT1[qIs51]; tsp-14(jj95)* isolate 52.6.3
LW4223	*unc-40(jj173)[UNC-40::mKate2::3FLAG]*
LW4716	*unc-40(jj173)[UNC-40::mKate2::3FLAG]; tsp-12(ok239)* isolate 1
LW4717	*unc-40(jj173)[UNC-40::mKate2::3FLAG]; tsp-12(ok239)* isolate 13
LW4718	*unc-40(jj173)[UNC-40::mKate2::3FLAG]; tsp-12(ok239)* isolate 17
LW4719	*unc-40(jj173)[UNC-40::mKate2::3FLAG]; tsp-12(ok239)* isolate 25
LW4720	*unc-40(jj173)[UNC-40::mKate2::3FLAG]; tsp-14(jj95)* isolate 27
LW4732	*unc-40(jj173)[UNC-40::mKate2::3FLAG]; tsp-14(jj95)* isolate 26
Strains used to test whether UNC-40 or SUP-17 can function in the nervous system	
LW4132	*unc-40(e1430); Ex[LWIM14.: pJKL1039(rab-3p::unc-40 cDNA gfp)+ pJKL449(myo-2p::gfp::unc-54 3' UTR)]*
LW4133	*unc-40(e1430); Ex[LWIM14.5: pJKL1039(rab-3p::unc-40 cDNA gfp)+ pJKL449(myo-2p::gfp::unc-54 3' UTR)]*
LW4175	*unc-40(e1430); Ex[LWIM14.5.1: pJKL1039(rab-3p::unc-40 cDNA gfp)+ pJKL449(myo-2p::gfp::unc-54 3' UTR)]; sma-9; ccx*
LW4176	*unc-40(e1430); Ex[LWIM14.1.3: pJKL1039(rab-3p::unc-40 cDNA gfp)+ pJKL449(myo-2p::gfp::unc-54 3' UTR)]; sma-9; ccx*
LW4186	*unc-40(e1430); Ex[LWIM14.2.1: pJKL1039(rab-3p::unc-40 cDNA gfp)+ pJKL449(myo-2p::gfp::unc-54 3' UTR)]; sma-9; ccx*
LW4404	*sup-17(n1258ts); Ex[LWIM16.1: pLW-6(rab-3p::sup-17 cDNA)+ LiuFD188(myo-2p::mCherry)]*
LW4405	*sup-17(n1258ts); Ex[LWIM16.5: pLW-6(rab-3p::sup-17 cDNA)+ LiuFD188(myo-2p::mCherry)]*
LW4411	*sup-17(n1258ts); Ex[LWIM16.4: pLW-6(rab-3p::sup-17 cDNA)+ LiuFD188(myo-2p::mCherry)]; sma-9; ccx*
LW4410	*sup-17(n1258ts); Ex[LWIM16.5: pLW-6(rab-3p::sup-17 cDNA)+ LiuFD188(myo-2p::mCherry)]; sma-9; ccx*

b. Strains generated by others.

strain name	genotype	generated by
LW4783	*jj221[UNC-40::GFP::3FLAG]*	Zhiyu Liu
LW5055	*jj221[UNC-40::GFP::3FLAG]; sma-6 (jj1)* isolate 1.11	Kelly Liu
LW5031	*jj221[UNC-40::GFP::3FLAG]; sma-6 (jj1)* isolate 3.2	Kelly Liu
LW5075	*jj221[UNC-40::GFP::3FLAG]; sma-3 (jj3)* isolate 1.2	Kelly Liu
LW5042	*jj221[UNC-40::GFP::3FLAG]; sma-3 (jj3)* isolate 1.8	Kelly Liu
LW5043	*drag-1 (tm3773) jj221[UNC-40::GFP::3FLAG]* isolate 122.17	Kelly Liu
LW5037	*drag-1 (tm3773) jj221[UNC-40::GFP::3FLAG]* isolate 153.3	Kelly Liu
LW5038	*drag-1 (tm3773) jj221[UNC-40::GFP::3FLAG]* isolate 197.13	Kelly Liu
LW5026	*jj221[UNC-40::GFP::3FLAG]; lon-1 (jj67)* isolate 1.2	Kelly Liu
LW5033	*jj221[UNC-40::GFP::3FLAG]; lon-1 (jj67)* isolate 1.9	Kelly Liu
LW5015	*jj221[UNC-40::GFP::3FLAG]; lon-2 (e678)* isolate 1.1	Kelly Liu
LW5010	*jj221[UNC-40::GFP::3FLAG]; lon-2 (e678)* isolate 2.6	Kelly Liu
LW5064	*jj221[UNC-40::GFP::3FLAG]; sma-10 (jj235)* isolate u3.4.17A	Riasat Zaman
LW5065	*jj221[UNC-40::GFP::3FLAG]; sma-10 (jj235)* isolate u3.4.17C	Riasat Zaman
LW4423	*jj173[UNC-40::mKate2::3FLAG]*	Zhiyu Liu
LW3275	*unc-40(e1430); CXTim132.1Ex[pCXT289(myo-3p::unc-40 cDNA)+ pJKL449(myo-2p::gfp::unc-54 3' UTR)*	Chenxi Tian
LW3276	*unc-40(e1430); CXTim132.4Ex[pCXT289(myo-3p::unc-40 cDNA)+ pJKL449(myo-2p::gfp::unc-54 3' UTR)*	Chenxi Tian
LW3349	*unc-40(e1430); CXTim119.2Ex[pCXT261(unc-40p::unc-40 cDNA)+ pJKL449(myo-2p::gfp::unc-54 3' UTR)*	Chenxi Tian
LW3347	*unc-40(e1430); CXTim119.3Ex[pCXT261(unc-40p::unc-40 cDNA)+ pJKL449(myo-2p::gfp::unc-54 3' UTR)*	Chenxi Tian

Table 4.2 Plasmids and genotyping primers used in this chapter.

a. plasmids

generating CRISPR-mediated HR/NHEJ	
LiuFD241	*Cas9+empty sgRNA*
pLW-2	sgRNA for making truncated UNC-40 without ICD
pZL-71	sgRNA for UNC-40::mKate2::3xFLAG knock-in
pLW-7	sgRNA for UNC-40(LV->AA)::mKate2::3xFLAG mutation
pZL-72	repair template for UNC-40::mKate2::3xFLAG knock-in
pZL-105	repair template for UNC-40::GFP::3xFLAG knock-in
functional study of UNC-40 and SUP-17	
pJKL-1155	*unc-40p::unc-40EXD cDNA::GFP*
pJKL-1145	*unc-40p::un-40EXD cDNA with 1/2GFP tail*
pCXT260	*unc-40p::unc-40EXD cDNA-genomic hybrid::GFP*
pJKL-1039	*rab-3p::unc-40 cDNA::GFP*
pLW-6	*rab-3p::sup-17 cDNA*
pJKL-1140	*sup-17p::sup-17cDNA*
pJKL-1032	*N-FLAG-UNC-40::GFP*
pJKL-1033	*M-FLAG-UNC-40::GFP*
co-injection markers	
pJKL-449	*myo-2p::gfp::unc-54 3' UTR*
pJKL-815	*myo-2p::rfp*
LiuFD188	*myo-2p::mCherry*
pJKL-724	*myo-3p::rfp*

b. Genotyping primers

Gene (allele)	**Primers for PCR**	**Expected size(s)**	**Primer for sequencing**
drag-1(jj4)	DS-157/DS-158	500 bp	DS-157
unc-40(e1430)	LW-36/LW-38	362 bp	LW-39
unc-40(jj86, jj87, jj88, jj89, jj90, jj91, jj92)	CXT-396/ JKL-1153	3.1 kb	LW-11
UNC-40::GFP ::3xFLAG(*jj221*)	ZL-349/ZL-350/ ZL-523	knock-in: 314 bp; wild-type: 230 bp	NA
UNC-40::mKate2 ::3xFLAG*(jj175)*	LW-44/LW-45/LW-46	knock-in: 687 bp; wild-type: 455 bp	NA
UNC-40(L1072A, V1073A)::mKate2:: 3xFLAG (*jj239, jj240, jj241*)	LW-60/LW-61	mutation: 242 bp; wild-type: no band	NA
	LW-11/LW-60	mutation: 347 bp, After AlwNI digestion: 120 + 227 bp; wild-type: 347 bp, resistant of AlwNI	JKL-1154
sup-17(n1258ts)	LW-23/LW-25	384 bp	LW-23
tsp-12(ok239)	JKL-1223/JKL-1224/ ZL-210	mutation: 241 bp; wild-type: 408 bp	NA
tsp-14(jj95)	ZL-178/ZL-179/ ZL-180	mutation: 205 bp; wild-type: 340 bp	NA
sma-9(cc604)	MLF-69/MLF-70	500 bp	LW-40

NA, not applicable

4.3 Results

4.3.1 Transgenic evidence supporting UNC-40 being one substrate of SUP-17 in BMP signaling

I previously showed that two different *unc-40* mutant alleles (*tr115* and *ev495*) that truncate the intracellular domain of UNC-40 can partially rescue the *sma-9* suppression (Susm) phenotype of partial loss-of-function *sup-17(n1258ts)* mutants, suggesting that UNC-40 is one substrate of SUP-17 in BMP signaling (Chapter 2; [80]). To rule out the possibility that functional UNC-40 proteins could be produced in these mutants due to cryptic alternative splicing, I used a transgenic approach to test directly whether expressing the extracellular domain of UNC-40 in *sup-17(n1258ts)* mutants is sufficient to rescue the Susm phenotype of *sup-17(n1258ts)* mutants. Kelly Liu and Herong Shi have generated a plasmid pJKL1155 (*unc-40p::unc-40 exd cDNA-gfp*) that has the *unc-40* promoter driving the expression of a cDNA encoding the extracellular domain (EXD) of *unc-40* fused to GFP. I injected this plasmid into both *unc-40 (e1430); sma-9(cc604)* and *sup-17(n1258ts); sma-9(cc604)* worms, respectively. As shown in Table 4.3, the transgene can partially rescue the Susm phenotype of the null *unc-40(e1430)* mutants and the Susm phenotype of *sup-17(n1258ts)* mutants. These results rule out the possibility that rescue by alternative splicing could explain results with *tr115* and *ev495* and further supported the notion that UNC-40 is one substrate of SUP-17 in BMP signaling.

Table 4.3. Partial rescue of the Susm phenotype of *unc-40* and *sup-17* mutants by a transgene expressing UNC-40EXD.

Mutant	Transgene	Susm (N)
unc-40(e1430)	none	96.6% (N=174)
unc-40(e1430)	*unc-40p::unc-40exd cDNA gfp*	45.4% (N=291)**
sup-17(n1258ts)	none	81.6% (N=163)
sup-17(n1258ts)	*unc-40p::unc-40exd cDNA gfp*	58.0% (N=264)**

Worms were grown at 20℃. The Susm phenotype was scored when worms were adults. Two independent transgenic lines for each injection mix were analyzed, and both transgenic lines showed similar phenotypes and data from both lines were combined for each genotype. Student's *t* test was performed between the penetrance of transgenic animals and un-injected non-transgenic animals. $^{**}p < 0.01$.

4.3.2 Neuronal-specific expression of unc-40 is sufficient to rescue the BMP defects of unc-40(0) mutants

The ligand of the BMP pathway is expressed in the nerve cord [139, 140], while the receptor is expressed and functions in the hypodermis to regulate body size, and in the M lineage to regulate M lineage patterning [94]. Chenxi Tian, a former graduate student in the lab, reported that *unc-40* expression in the hypodermis is sufficient to rescue the body size defects of *unc-40(0)* mutants, while *unc-40* expression in the M lineage is sufficient to rescue the Susm phenotype of *unc-40(0)* mutants [38]. She also noticed that ectopic expression of *unc-40* in the entire nervous system (driven by the pan-neuron *unc-119* promoter) can partially rescue the body size defect of *unc-40(0)* mutants [38]. To rule out the possibility of non-specificity of the *unc-119* promoter used, I tested whether forced expression of *unc-40* under the control of another well-studied pan-neuron-specific promoter *rab-3* [141] can also rescue the BMP defect of *unc-40(0)* mutants. I injected the plasmid *pJKL1039*(*rab-3p::unc-40 cDNA*), which was generated by Kelly Liu and Herong Shi, into *unc-40(e1430)* and *unc-40(e1430); sma-9(cc604); cc::gfp* strains respectively, and examined the respective transgenic worms for body size and M lineage phenotypes. Neuronally expressed *unc-40* (driven by the *rab-3* promoter) partially rescued the small body size of *unc-40(e1430)* mutants (Figure 4.1A) and fully rescued the Susm phenotype of *unc-40(e1430)* mutants (Table 4.4). However, expressing *unc-40* in body wall muscles (driven by the *myo-3* promoter) failed to rescue the small body size of *unc-40(e1430)* mutants (Figure 4.1A). As a control, expressing *sup-17* under the *rab-3* promoter failed to rescue both the body size (Figure 4.1B) and the Susm phenotype (Table 4.4) of *sup-17(n1258ts)* mutants. In conclusion, UNC-40 can also function in neurons to regulate body size and M lineage development in addition to BMP signal receiving cells. The lack of rescue of *unc-40(0)* BMP defects when *unc-*

40 is ectopic expressed in muscles (with the *myo-3* promoter, Figure 4.1), intestine or pharynx [38] suggests that UNC-40 does not simply function cell-non-autonomously. Instead, it functions in both the signal-producing cells (the nerve cord) and the signal receiving cells (the hypodermal cells for body size and the M lineage cells for M lineage development) to regulate BMP signaling.

Table 4.4. Expression of *unc-40* in neuronal cells can rescue the Susm phenotype of *unc-40(0)* mutants.

Mutant	Transgene	Susm (N)
unc-40(e1430)	none	96.6% (N=174)
unc-40(e1430)	*rab-3p::unc-40 cDNA*	2.01% (N=597) ***
sup-17(n1258ts)	none	81.6% (N=163)
sup-17(n1258ts)	*rab-3p::sup-17 cDNA*	75.74% (N=136) ns

Worms were grown at 20℃. The Susm phenotype was scored when worms were adults. Two independent transgenic lines for each injection mix were analyzed, and both transgenic lines showed similar phenotypes and data from both lines were combined for each genotype. Student's *t* test was performed between the penetrance of transgenic animals and un-injected non-transgenic animals. *** $p < 0.0001$, ns not significant.

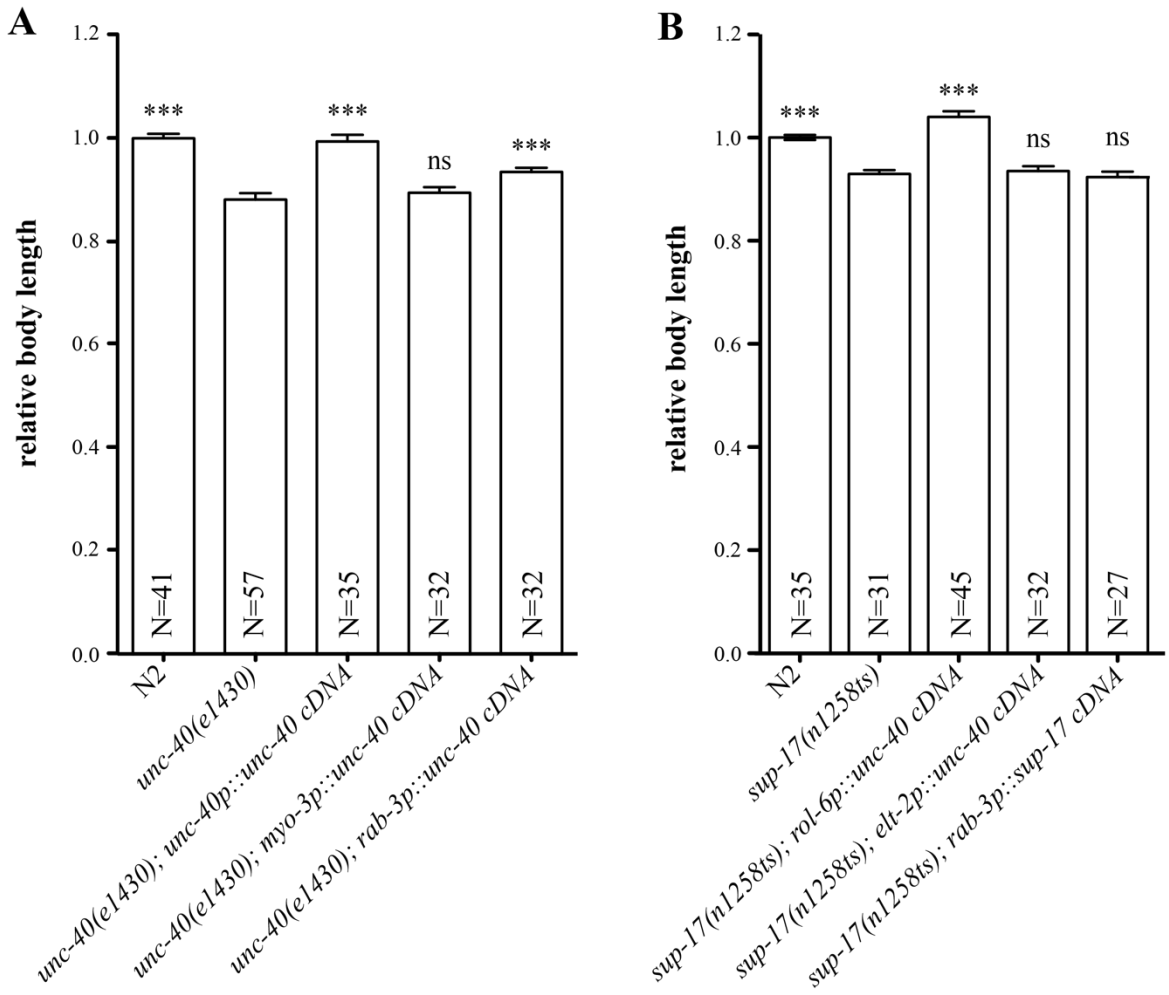

Figure 4.1 Expression of *unc-40* in neuronal cells can rescue the body size phenotype of *unc-40(0)* mutants.

Bar graphs showing the average body size of various mutants. Error bars represent the 95% confidence intervals. Body size of wild-type worms was set as 1 for normalization. Worms were grown at either 20℃(A) or 25℃(B) for measurements. Bar graphs are drawn using GraphPad Prism 6 software. Statistics was performed using Student's *t* test by comparing transgenic worms with mutant uninjected worms. $^{***}p < 0.0001$, ^{ns} not significant.

4.3.3 Initial attempts to generate unc-40EXD mutants via CRISPR identified potentially important sequences near the transmembrane domain of UNC-40 in BMP signaling

Two pre-existing alleles of *unc-40* have premature stop codons either right before the transmembrane (TM) domain (*ev495*) or immediately after the TM domain (*tr115*). In an attempt to generate additional *unc-40* alleles that truncate the UNC-40 protein before the intracellular domain (ICD), I tried to use CRISPR to target the juxta-membrane region of UNC-40EXD with a guide RNA, hoping to recover deletion or frameshift mutations through CRISPR-mediated non-homologous end joining (NHEJ). As described in Materials and methods, I used *pLW-2.3* as the sgRNA containing plasmid and performed injection into either the wild-type or the *sup-17(n1258ts)* backgrounds following the strategy described in Friedland et al. [99]. I obtained a total of 7 *unc-40* alleles and sequenced each of them (Table 4.5). Surprisingly, not all the 7 *unc-40* alleles exhibit functionality in the BMP pathway, and may suggest interesting structure-function relationships regarding the UNC-40 protein.

As shown in Table 4.5, *unc-40(jj88),* which changes amino acid 1084 to a stop codon, did not affect UNC-40 function in BMP signaling, consistent with previous results obtained for *ev495* and *tr115*. Similarly, *unc-40(jj86)* has an in-frame-deletion of amino acids 1082 to 1084 (PLY), but did not cause any noticeable phenotype, suggesting that these three amino acids are not important for UNC-40 function. On the other hand, *unc-40(jj89)* has a large deletion of over 0.5 kb sequences, and is predicted to produce a truncated UNC-40 without part of the FNIII6, TM and ICD motifs. *unc-40(jj89)* mutants exhibited phenotypes resembling those of the *unc-40(e1430)* null mutants. Considering that *unc-40(ev495),* which truncates the UNC-40 protein after the FNIII6 motif, is fully functional in BMP signaling, it is likely that the FNIII6 motif is critical for UNC-40 function in BMP signaling, as previously observed [38]. Other alleles of

unc-40, including *jj87, jj90, jj91* and *jj92,* all contain extra random amino acid sequences not present in the endogenous UNC-40 protein. Although some of them have UNC-40 protein sequences extending beyond amino acid 1074 (the C-terminal end of the predicted UNC-40 protein in *ev495*), they all appeared to either partially (*jj87*) or completely (*jj90, jj91* and *jj92*) disrupt the function of UNC-40 in BMP signaling. It is likely that the additional amino acids encoded by these mutant alleles (ISYFW LRLL in *unc-40(jj87)*, SHTFG CVCSD SDPYT DSYHN VLLET I in *unc-40(jj90)*, HTFGC VCSDS DPYTD SYHNV LLETI in *unc-40(jj91)*, or FYFWL RLL in *unc-40(jj92)* all affected the proper folding of the UNC-40EXD, thus compromising UNC-40 function.

Table 4.5 The *unc-40* truncation alleles generated by CRISPR-mediated NHEJ.

a. DNA sequences and phenotypes of the various *unc-40* alleles (only the mutated regions are shown).

***unc-40* allele**	**DNA sequences of the mutated region**	**Phenotype**
	8836 CTCTT CTTCA CTCTA ACCCA TTGTA TCTCA TACTT 8870	
wild-type	CTCTT CTTCA CTCTA ACCCA TTGTA TCTCA TACTT	wild-type
unc-40(jj86) △8854-8862, -9bp	CTCTT CTTCA CTCTA ACC-- ----- --TCA TACTT	wild-type
unc-40(jj87) △8856-8859, -4bp	CTCTT CTTCA CTCTA ACCCA ----A TCTCA TACTT	Unc, Egl
unc-40(jj88) +2bp	CTCTT CTTCA CTCTA ACCCA TTGTAATCTCTATACTT	Unc, Egl
unc-40(jj89) △8309-8865, -557bp	----- ----- ----- ----- ----- ----- TACTT	Unc, Egl, Sma
unc-40(jj90) △8857-8861, -5bp	CTCTT CTTCA CTCTA ACCCA T---- -CTCA TACTT	Unc, Egl
unc-40(jj91) △8839-8864, -26bp	CTC-- ----- ----- ----- ----- ----A TACTT	Unc, Egl
unc-40(jj92) △8822-8865, -44bp +4bp	----- ----- ----- ----- ----- -----TTTTTACTT	Unc, Egl

Deletions are marked as dashes (with the deleted region marked on the right after each allele); insertions are marked in red. The numbering system is based on the start codon being #1. Unc: uncoordinated, Egl: egg-laying defective, Sma: small.

b. Schematics of the predicted UNC-40 proteins encoded by the different *unc-40* alleles and their Susm phenotypes.

***unc-40* allele**	**Predicted UNC-40 protein**		***sup-17* allele**	**Susm penetrance**
	immunoglobin domains; fibronectin type III domains; TM P1 P2 P3			
+	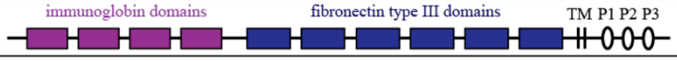		+	NA
e1430	 null		+	96.8% (N=410)
tr115		W1107STOP	+	2.6% (N=549) ***
ev495		Q1075STOP	+	0.3% (N=291) ***
jj86		△1082PLY1084	+	0.1% (N=851) ***
jj87	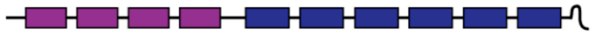	P1083+9aa+STOP	+	32.2% (N=357) ***
jj88		L1084STOP	+	0% (N=583) ***
jj89		D916+24aa+STOP	+	91.0% (N=704) *
+			*n1258ts*	78.4% (N=583)
tr115		W1107STOP	*n1258ts*	47.6% (N=341) [a]
ev495		Q1075STOP	*n1258ts*	46.2% (N=195) [a]
jj90		P1083+26aa+STOP	*n1258ts*	78.9% (N=336) ns
jj91		S1076+25aa+STOP	*n1258ts*	74.8% (N=412) ns
jj92		V1071+8aa+STOP	*n1258ts*	83.8% (N=437) ns

[a] data from Wang et al (2017).

Statistic analysis was done using Student's t test. ns not significant, compared to *unc-40(+) sup-17(n1258ts)*; *** $p<0.0001$, * $p<0.05$, compared to *unc-40(e1430)*.

Susm analysis were done using worms grown at 25℃

4.4.4 Reagents generated to examine the endogenous UNC-40 protein via western blotting

The different pieces of genetic evidence that I had obtained suggested that UNC-40 is a substrate of SUP-17 in BMP signaling. I attempted to obtain biochemical evidence by performing western blots using extracts of worms expressing tagged UNC-40. Multiple strains were generated for this purpose. Zhiyu Liu in our lab has previously used CRISPR to tag the endogenous UNC-40 with GFP or mKate2 and generated the following strains: UNC-40::GFP::3xFLAG and UNC-40::mKate2::3xFLAG, respectively. Kelly Liu and Herong Shi performed the *sma-9* suppression essay and showed that these tagged proteins are fully functional (Table 4.6a).

Zhiyu failed to obtain any tagged versions of UNC-40 via CRISPR by inserting GFP in the extracellular domain of UNC-40 (personal communication). I therefore generated integrated transgenic lines carrying a single FLAG either inserted at the N-terminus right after the signal peptide (N-FLAG::UNC-40::GFP) or in between the Ig domains and the FNIII domains (M-FLAG::UNC-40::GFP) (see Materials and methods). The FLAG insertion at either location rendered the UNC-40 protein partially functional. As shown in Table 4.6, the transgenes partially rescued the uncoordinated movement (Unc) phenotype of *unc-40(e1430)* mutants. The N-terminal tagged UNC-40 also rescued the egg-laying defective (Egl) phenotype of *unc-40(e1430)* mutants. Nevertheless, both transgenes appeared to rescue the body size of *unc-40(e1430)* mutants by eye scanning, suggesting that they are partially functional in BMP signaling.

I therefore used both the knock-ins and the integrated transgenic lines and crossed them to *sup-17(n1258ts)* mutants in order to determine whether UNC-40 might be processed *in vivo*, and if yes, whether SUP-17 plays role in UNC-40 processing.

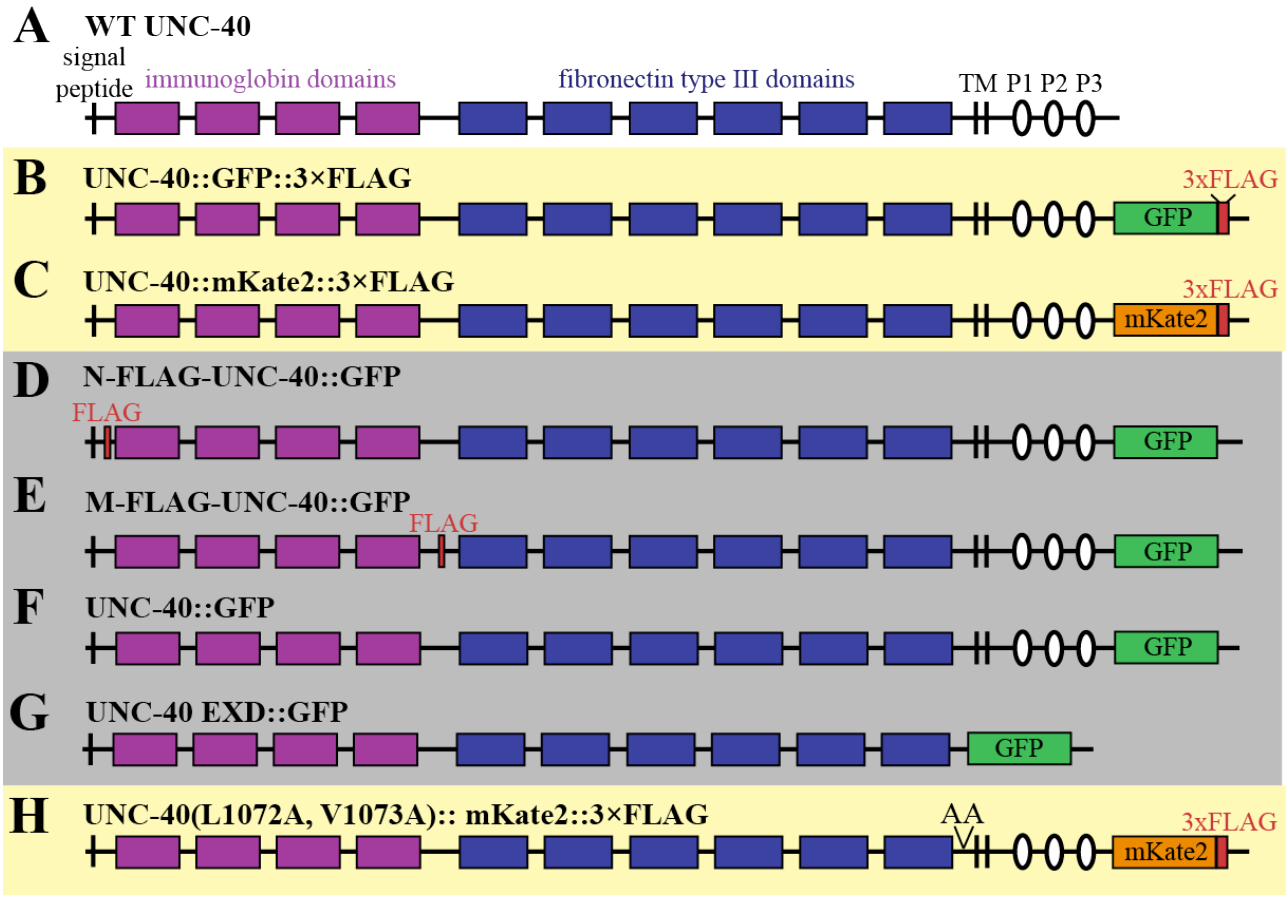

Figure 4.2 Schematics of UNC-40 protein with various tags.

Black bar on the left, signal peptide; purple rectangles, Immunoglobin (Ig) domains; blue squares, fibronectin type III (FNIII) domains; double black lines, transmembrane domain; white ovals, P1, P2, P3 motifs; green squares, GFP; orange squares, mKate2; thick red squares, 3×FLAG; thin red squares, FLAG; yellow background, endogenous tagging; grey background, transgene. Plasmids B and C made by Zhiyu Liu, plasmids D, E, G, H made by Herong Shi. Strain F was a gift from Joe Culotti.

Table 4.6 Summary of the functionality of various tagged forms of *unc-40* or *sup-17* generated via CRISPR knock-in or integration of transgenes.

a. Functionality of different CRISPR-mediated knock-in alleles.

Knock-in alleles	Susm penetrance	Conclusion
unc-40(jj221)[UNC-40::GFP::3xFLAG]	1.40% (N=290)	fully functional
unc-40(jj173)[UNC-40::mKate::3xFLAG]	0.35% (N=828)	fully functional
unc-40(jj239)[UNC-40(L1072A, V1073A)::mKate::3xFLAG]	0% (N=400)	fully functional
sup-17(jj98)[SUP-17::GFP]	3.04% (N=659)	fully functional
sup-17(jj175)[SUP-17::mKate::3xFLAG]	1.20% (N=675)	fully functional

The knock-in alleles were crossed into *sma-9(cc604); cc::gfp (ccX)* strains to examine the Susm (suppression of the *sma-9* mesoderm defect) phenotype. Strains were generated and data were collected by Kelly Liu and Herong Shi.

b. Functionality of integrated *unc-40* transgenes that have the FLAG insertion in the extracellular domain of UNC-40.

mutant alleles	Transgene	Unc	Egl (%)	Body size[a]
wild-type	none	1 (N>100)	0 (N>100)	wide-type
unc-40(e1430)	none	3.89 (N=124)	29.75% (N=242)	small
unc-40(e1430)	N-FLAG::UNC-40::GFP	2.91 (N=122)***	16.66%(N=154)**	wide-type
unc-40(e1430)	M-FLAG::UNC-40::GFP	2.93 (N=122)***	27.01%(N=119)^{ns}	wide-type

Statistical analysis was performed using Student's *t* test by comparing the transgenic lines with non-injected *unc-40(e1430)* mutants. $^{***}p<0.0001$; $^{**}p<0.01$; ns, not significant. [a] body size was determined by visualization under the dissecting microscope without measurement. The Unc and Egl phenotypes were scored according to Materials and methods.

4.4.5 Examining possible cleavage of UNC-40 by SUP-17 via western blotting

I first performed western blotting using extracts from stage-matched wild-type and *sup-17(n1258ts)* mutant worms that express endogenously tagged UNC-40: UNC-40::GFP::3xFLAG and UNC-40::mKate2::3xFLAG. I probed the blots using anti-FLAG antibodies. The predicted size for the full length, GFP- or mKate- tagged UNC-40 is ~180 kDa, and the predicted intracellular domain of UNC-40 with the GFP- or mKate- tag is ~60 kDa. Indeed, a band around 180 kDa can be detected in UNC-40::GFP::3xFLAG strains whereas no such band exists in N2 (Figure 4.3A). So the 180 kDa band is likely to be full length UNC-40::GFP::3xFLAG. Above the putative full length UNC-40 band, there is another band around 250 kDa, even stronger than the band around 180 kDa, in all the stages tested. This band may be full length UNC-40::GFP::3xFLAG that has gone through post-translational modifications, and the types of modifications remain to be determined.

Both UNC-40::GFP::3xFLAG and UNC-40::mKate2::3xFLAG strains showed bands around 250 kDa and 180 kDa (Figure 4.3B). However, UNC-40::GFP::3xFLAG seems to be expressed at a higher level than UNC-40::mKate2::3xFLAG, because with similar loading, the bands from UNC-40::GFP::3xFLAG strains are stronger than those from UNC-40::mKate2::3xFLAG strains (Figure 4.3B). This is possibly due to the mKate2::3xFLAG tag makes the protein less functional and leads to degradation. I therefore chose to use the UNC-40::GFP::3xFLAG strains for subsequent analysis.

If sufficient amount of UNC-40 is cleaved by SUP-17 in worms at the L3, L4 or adult stage, I would expect to see an accumulation of full length UNC-40 in *sup-17(n1258ts)* mutants. I would also expect to see bands around 60 kDa, which is the predicted size for the intracellular domain of UNC-40 (ICD) with the GFP and 3xFLAG tag. However, I did not obtain consistent

results across independent experiments regarding both the accumulation of full length UNC-40 and the existence of UNC-40 ICD (Figure 4.3A, B).

The GFP::3xFLAG tag is at the C-terminus of UNC-40. It is possible that the intracellular domain of UNC-40 is unstable after cleavage. To overcome this limitation, I also performed western blotting using integrated transgenic worms carrying the partially functional N- or M- FLAG-tagged UNC-40 transgenes described above (Figure 4.2D and E). I only carried out these experiments once each with L4, adult or mixed staged animals in the *sup-17(+)* background. As shown in Figure 4.3C, the abundance of both N-FLAG-UNC-40 and M-FLAG-UNC-40 appears to be less compared to the endogenously tagged UNC-40. And there appeared to be multiple bands around the 120 kDa region. Future experiments are needed to determine if any one of them corresponds to the UNC-40 EXD and if there is any change of abundance of any of these bands in *sup-17(n1258ts)* mutants.

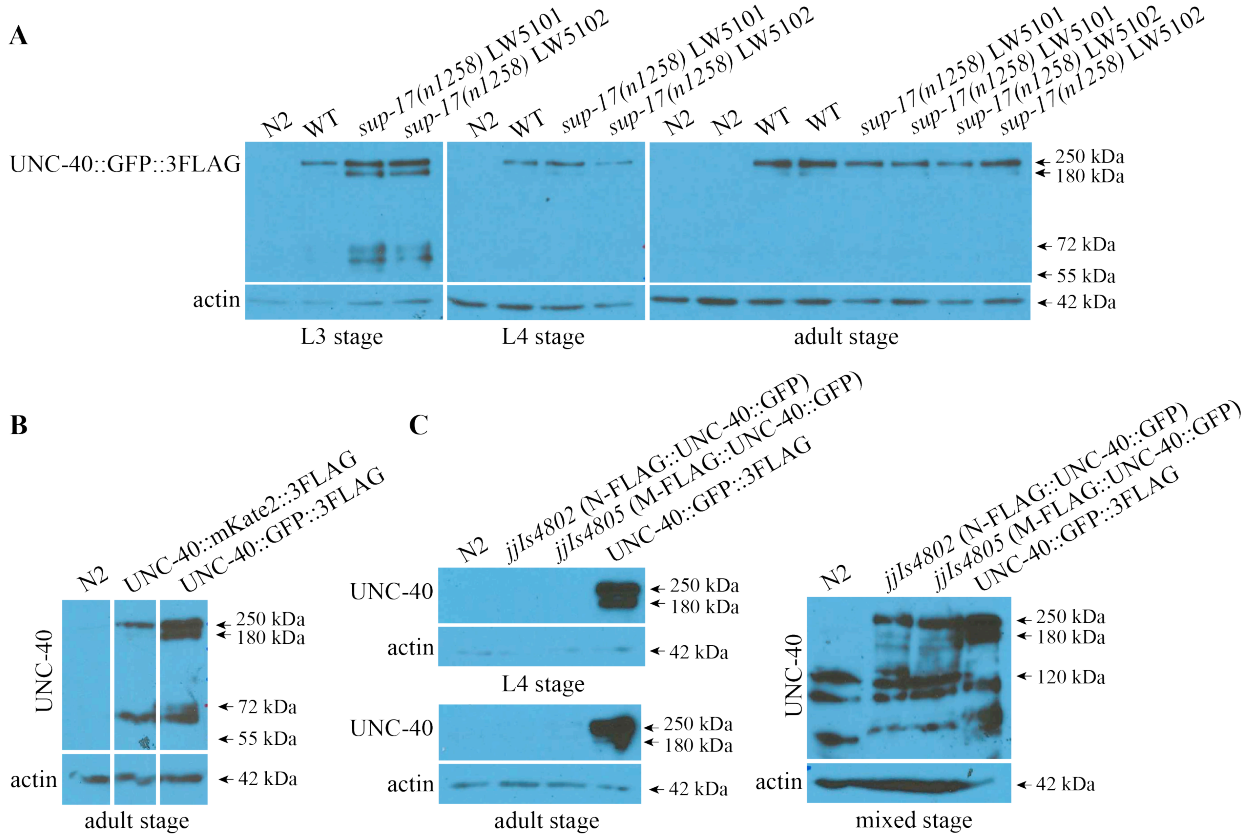

Figure 4.3 Western Blotting of UNC-40 in wild-type and *sup-17(n1258ts)* backgrounds. All worms were cultured at 25℃ under the same condition, because 25℃ is the restrictive temperature of *sup-17(n1258ts)*. Each sample contains fifty worms unless otherwise noted. (A) Endogenous UNC-40::GFP::3xFLAG protein in L3, L4 or adult stage wild type and *sup-17(n1258ts)* mutants probed with anti-FLAG antibody. Duplicate samples from adult stage worms were loaded on the gel. (B) Adult worms carrying either UNC-40::mKate2::3×FLAG or UNC-40::GFP::3×FLAG were run on the same gel for comparison of the abundance of UNC-40 protein with different tags. (C) L4, adult or mixed stage worms carrying integrated N- or M-FLAG::UNC-40::GFP probed with anti-FLAG antibody. For mixed stage worm samples carrying N- or M-FLAG::UNC-40::GFP, 20 µL sample was used in each well with the volume ratio of worm pellet to 5xSDS sample buffer around 4:1.

4.4.6 Amino Acids 1072L and 1073V are not essential for unc-40 function in BMP signaling

My genetic data showing that UNC-40 is a substrate of SUP-17 motivated me to identify the cleavage site of SUP-17/ADAM10 in the juxtamembrane region of UNC-40 EXD. The cleavage sites of several known ADAM10 substrates have been previously identified. One of the well studied substrates of ADAM10 is Notch, which is cleaved at $Ala^{1710}Val^{1711}$, 13 amino acids upstream of the transmembrane domain [115, 142]. In addition, the precursor of TNFα is cleaved by ADAM10 between residues Ala^{76} and Val^{77}, 19 amino acids outside the transmembrane domain [138]. Similarly, the amyloid precursor protein (APP) is cleaved by ADAM10 between Lys^{16} and Leu^{17}, 12 amino acids upstream of its transmembrane domain [57]. Alignment of the amino acid sequences between the 6^{th} FNIII motif and the transmembrane domain of UNC-40 from various nematode species showed that the juxtamembrane region is conserved in nematode, but not in vertebrate neogenin or DCC proteins (Figure 4.4). Nevertheless, we decided to test the importance of residues $Leucine^{1072}Valine^{1073}$ because they are located 12 amino acids upstream of the UNC-40 transmembrane domain and are conserved in multiple nematode species.

I used CRISPR-Cas9 mediated homologous recombination and mutated both L^{1072} and V^{1073} to Alanines in the *unc-40::mKate2::3XFLAG* background (Figure 4.2 H). The resulting strains, *jj239, jj240* and *jj241*, did not exhibit any visible defects in body size, movement or egg-laying behavior. Moreover, the mutation did not suppress the *sma-9* M lineage phenotype (Table 4.6 a). When I performed western blotting analysis, I did not detect any obvious difference between the wildtype UNC-40::mKate2::3XFLAG protein and the UNC-40(LV to AA)::mKate2::3XFLAG protein (Figure 4.5). Collectively, these observations suggest that $L^{1072}V^{1073}$ are not important for UNC-40 function in BMP signaling.

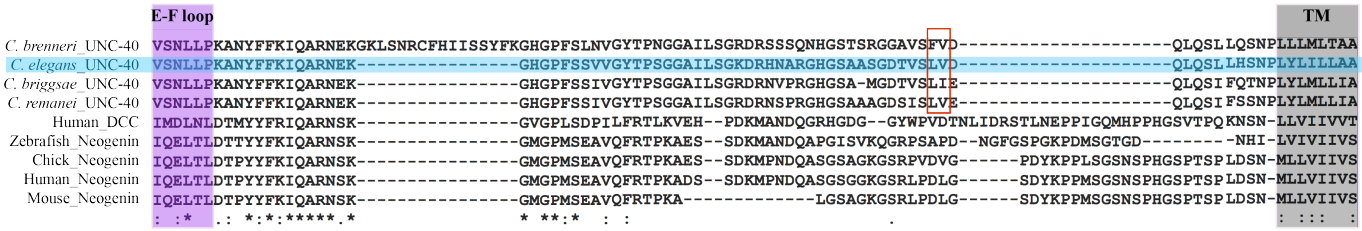

Figure 4.4 Alignment of UNC-40 protein sequences upstream of the transmembrane domain.

The E-F loop is in the FNIII6 motif of UNC-40, which is critical for its function in BMP signaling [38]. The end of E-F loop in the FN6 motif is shaded in purple and the beginning of transmembrane domain is shaded in grey. The red box marks the conserved L^{1072} V^{1073} (in *C. elegans*) residues. Clustal Omega was used for the alignment. And the accession number for the sequences are as follows: *C. brenneri*_UNC-40: EGT46408.1; *C. elegans*_UNC-40: AAB17088.1; *C. briggsae*_UNC-40: XP_002639098.1; *C. remanei*_UNC-40: XP_003111323.1; Human_DCC: NP_005206.2; Zebrafish_Neogenin: AAL92552.1; Chick_Neogenin: Q90610.1; Human_Neogenin: AAC51287.1; Mouse_Neogenin: AAH54540.1.

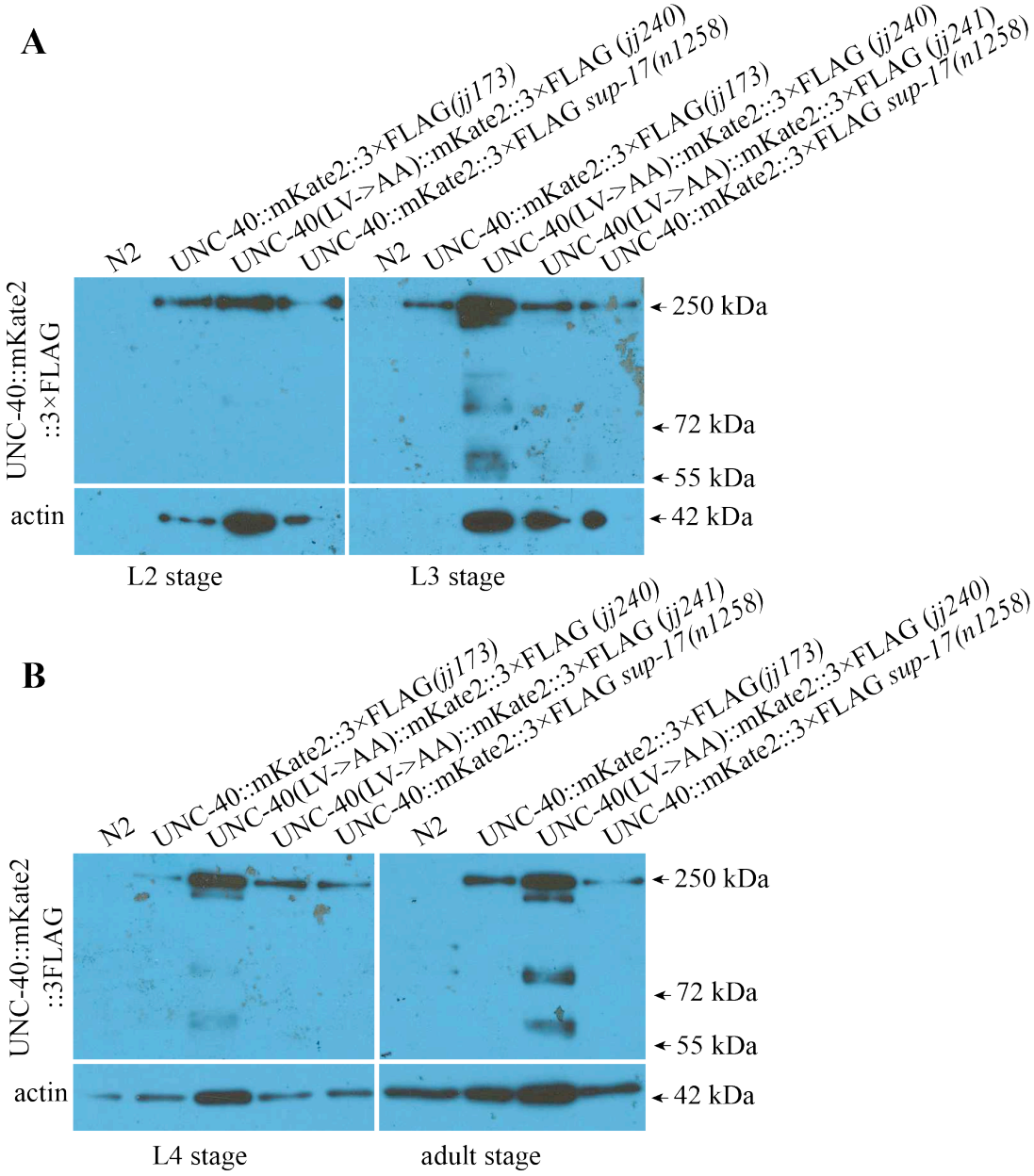

Figure 4.5 Leu[1072] and Val[1073] do not appear to affect the steady state UNC-40 protein level.

Western Blotting of wildtype adult *C. elegans* carrying UNC-40(LV to AA)::mKate2::3×FLAG, or UNC-40::mKate2::3×FLAG, or *sup-17(n1258ts)* mutant animals carrying UNC-40::mKate2::3×FLAG. L2 and L3 stage (A) and in L4 and adult stage (B). All worms were cultured at 25℃ under the same condition. 50 worms were used in each lane of L4 and adult stages, while 300 worms were used for L2 and L3 stages.

4.4.7 Behavior of UNC-40/Neogenin in tetraspanin mutants

We have previously shown that TSP-12 and TSP-14 regulate the subcellular localization of SUP-17 [80], and that UNC-40 is likely a substrate of SUP-17 (Chapters 2 and 3). I therefore asked whether UNC-40 localization or protein level is affected in *tsp-12(0)* and *tsp-14(0)* mutants. Using an integrated functional UNC-40::GFP transgene [143], I found that the fluorescence signal of UNC-40::GFP (Figure 4.2 G) is reduced in *sup-17(n1258ts)*, *tsp-12(ok239)*, *tsp-14(jj95)* and *tsp-12(ok239); tsp-14(jj95)* mutants. These observations are preliminary. Additional experiments are needed to examine the expression pattern of this UNC-40::GFP transgene as well as the endogenously tagged UNC-40::GFP::3xFLAG in various mutants.

I also examined by western blotting, whether the level of the endogenously tagged UNC-40 (UNC-40::mKate2::3×FLAG) is altered in *tsp-12(ok239)*, *tsp-14(jj95)*, *tsp-21(jj168)* and *tsp-12(ok239); tsp-14(jj95)* mutants. As shown in figure 4.6, the amount of the 250 kDa UNC-40 band appears to be slightly increased in adult stage but not in L4 stage *tsp-12(ok239)* mutants compared to wild-type animals. This difference was observed one more time in adult animals (data not shown), suggesting a possible role of TSP-12 in regulating UNC-40 protein level in adults. The amount of UNC-40 in *tsp-14(jj95)* or *tsp-21(jj168)* mutants did not appear to be significantly different from that in wild-type animals at both the L4 and adult stage (Figure 4.6). Further analysis is required to determine if UNC-40 level alters in *tsp-12(ok239); tsp-14(jj95)* double mutants.

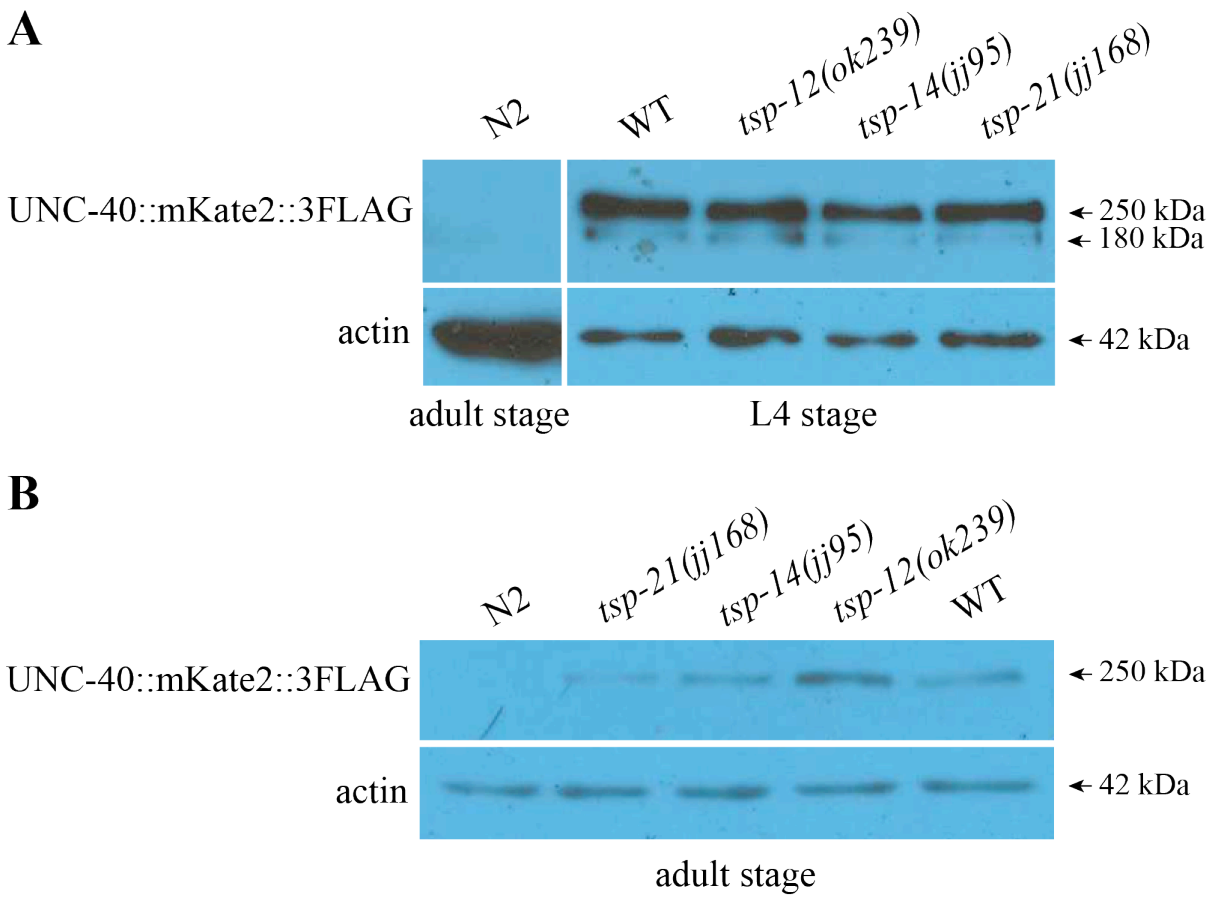

Figure 4.6 Western Blotting of UNC-40 in wild-type and tetraspanin mutants.

Endogenous UNC-40::mKate2::3×FLAG protein level in L4 stage (A) and adult stage (B) wild type and tetraspanin mutants. Fifty worms were picked for each sample.

4.4.8 Possible regulation of UNC-40/Neogenin protein level by other BMP pathway components

UNC-40/Neogenin is a positive modulator of BMP signaling, however it is not known if BMP signaling regulates the level or distribution of UNC-40. Kelly Liu and Herong Shi crossed the endogenous UNC-40::GFP::3×FLAG into various BMP pathway mutants, including null mutants of the type I receptor *sma-6(jj1)*, the R-Smad *sma-3(jj3)*, the negative regulators *lon-1(jj67)* and *lon-2(e678),* and the positive regulators *drag-1(tm3773)* and *sma-10(jj235)*, respectively. I performed western blot analysis using these various strains. I performed the experiments twice, and found no significant change of UNC-40 protein level in *sma-6(jj1)*, *sma-3(jj3)*, *lon-1(jj67)*, *lon-2(e678)* and *sma-10(jj235)* L4 or adult staged worms (Figure 4.7 A-C). However, I found, in two independent experiments, that the UNC-40 protein level appears to be lower in *drag-1(tm3773)* mutants in both L4 and adult worms (Figure 4.7 A-C). This observation suggests that DRAG-1 may play a role in regulating UNC-40 protein level. I have crossed UNC-40::GFP::3×FLAG into another null allele of *drag-1*, *jj4*. I will perform similar experiments as described here to determine if my conclusion holds true in this mutant background.

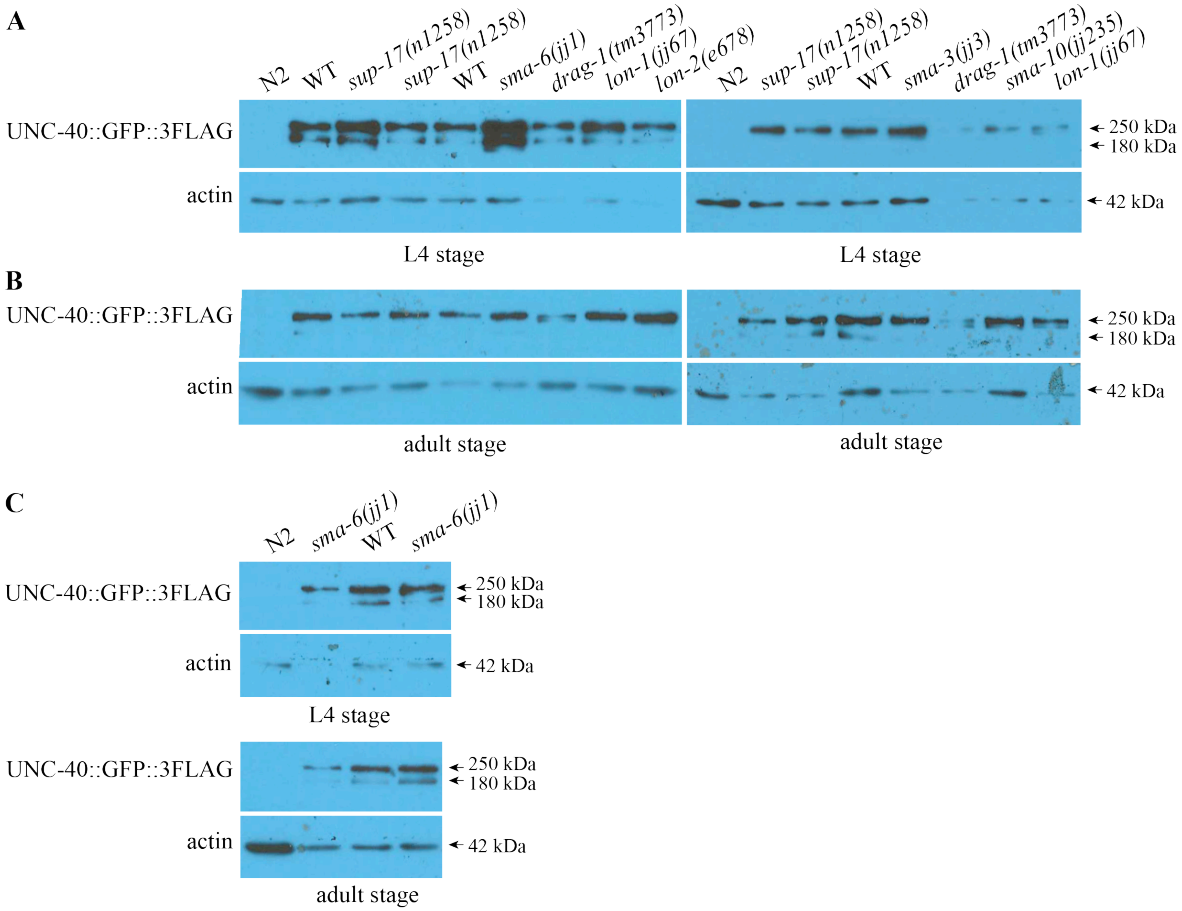

Figure 4.7 Western Blotting of UNC-40 protein in various BMP pathway member mutants.

Endogenous UNC-40::GFP::3×FLAG protein level in wide type and various BMP pathway mutants at the L4 stage (A) or adult stage (B). (C) UNC-40 protein level in wild type and *sma-6(jj1)* mutants. All worms were cultured at 25℃ under the same conditions and each gel lane contains picked 50 worms.

4.5 Discussion

SUP-17/ADAM10 belongs to the ADAM protease family, and ADAM17 (also called TACE, TNFα-converting enzyme) cleaves some of the same substrates as ADAM10 [43] . ADAM17 is known in rat embryonic cortical neurons to bind and cleave off the extracellular domain of Neogenin, whose homolog is UNC-40 in *C. elegans* [84]. I have found that both genetic mutations that are predicted to produce truncated UNC-40 without the intracellular domain and transgenes that only express the extracellular domain of UNC-40 can partially rescue the Susm phenotypes of *sup-17(n1258ts)* ([80] and this Chapter), implicating UNC-40 is one substrate of SUP-17 in BMP signaling. One of the goals of this study is to determine if SUP-17 indeed cleaves UNC-40 to regulate its function in BMP signaling. By studying the cleavage sites of known ADAM10 substrates, we have identified $Leu^{1072}Val^{1073}$ to be the putative cleavage site in UNC-40. However, mutations of both residues to Ala did not appear to cause any defects associated with *unc-40* loss-of-function mutations, suggesting that Leu^{1072} and Val^{1073} are not important for UNC-40 function. One possible explanation is that UNC-40 is not cleaved. Alternatively, other residues might serve as the cleavage sites. Quantitative proteomics studies revealed that murine ADAM10 is more likely to cleave at the N-terminus of Leucine or aromatic amino acids [144]. In addition to the L^{1072} residue I tested in this chapter, there are 5 more candidate sites that are conserved and worth trying: Y^{1021}, F^{1022}, F^{1023}, Y^{1042} and L^{1050}.

I also performed western blotting analysis to try to visualize any possible cleavage products of UNC-40. I did the experiments using L3, L4 and adult worms carrying either UNC-40::GFP::3×FLAG or UNC-40::mKate2::3×FLAG in the wildtype and *sup-17(n1258ts)* mutant background. These western blots did not reproducibly demonstrate accumulation of any full length UNC-40 in *sup-17(n1258ts)* mutants. While the experiments are worth repeating, it might

not be possible to detect any cleavage event of UNC-40 due to the following reasons: 1). Only a portion of total UNC-40 may be cleaved in specific tissues and at specific development stages. This is likely because UNC-40 has multiple roles in addition to its role in BMP signaling, and for its role as the Netrin receptor, the intracellular domain of UNC-40 is indispensable [145]. In this case, the small portion of UNC-40 cleavage in BMP signaling may not be sufficient to be detectable on western blots. Along the same line, L4 and adult may not be the ideal developmental stages for studying UNC-40 cleavage. Future experiments are needed using worms of L2 and L3 stages; 2). The intracellular domain of UNC-40 may be unstable after cleavage because it is dispensable in BMP signaling. Both the endogenously tagged versions of UNC-40, UNC-40::GFP::3×FLAG and UNC-40::mKate2::3×FLAG, have FLAG at the C-terminus. I did try to use transgenes expressing the extracellular N- or M- FLAG tagged UNC-40 to bypass the possible instability of the UNC-40 intracellular domain. However, these FLAG tagged UNC-40 is only partially functional and are produced by transgenes; 3). *sup-17* is essential for embryonic viability. All my experiments relied on the strongest allele of *sup-17(n1258ts)* that allowed viability. But because it is a partial loss-of-function allele, UNC-40 cleavage may not be severely enough affected in *sup-17(n1258ts)* mutants to be detectable by western; 4). UNC-40 is not cleaved.

RGMs are identified as structural bridges between BMP and Neogenin [146]. In *C. elegans*, the RGM protein DRAG-1 also interacts with UNC-40, and the interaction is crucial for the functions of both DRAG-1 and UNC-40 in BMP signaling [38]. I showed that UNC-40 protein level might be reduced in *drag-1(tm3773)* mutants. To further investigate the role of DRAG-1 on UNC-40, I introduced UNC-40::GFP::3×FLAG into another null allele of *drag-1*, *jj4.* Western blot analysis needs be done using this allele to validate the role of DRAG-1 in

regulating the protein level of UNC-40. In mouse cortical neurons, binding of RGM to Neogenin facilitates the cleavage of Neogenin by ADAM17 [84, 128]. It would be interesting to determine if DRAG-1 interacts with SUP-17 and regulates its localization or protein level.

In addition to DRAG-1, tetraspanins may also play a role in regulating the protein level of UNC-40. I have shown that in *tsp-12(ok239)* mutants, the cell surface localization of SUP-17::GFP is decreased and that there is a decrease in the amount of the putative mature form of SUP-17 protein (Chapter 3). Here, I also saw evidence of possible accumulation of the full length UNC-40 protein. I therefore propose the following model: TSP-12 promotes SUP-17 trafficking and maturation, thus regulating its cleavage of UNC-40. Future work is needed to test this model.

CHAPTER 5

SUMMARY AND FUTURE DIRECTIONS

5.1 Characterizing a novel modulator SUP-17 in the C. elegans BMP-like signaling pathway

I have shown in Chapter 2 that SUP-17, the *C. elegans* ortholog of ADAM10, functions in BMP signaling. However, its close homolog ADM-4, the *C. elegans* ortholog of ADAM17, is not involved in BMP signaling (Chapter 2). Two partial loss of function alleles of *sup-17*, *n1258ts* and *n316*, exhibit BMP signaling defects. Genetic epistasis analysis based on the body size phenotype showed that SUP-17 functions in the BMP pathway to regulate body size.

I have used CRISPR and generated a line expressing a functional SUP-17::GFP and shown that SUP-17::GFP is expressed in many tissues throughout development. Moreover, SUP-17 is expressed and functions in BMP-signal receiving cells: in hypodermal cells to regulate body size and in M lineage cells to regulate M lineage development. In *C. elegans* embryos, endogenous SUP-17::GFP is localized both to the cell surface and in intracellular vesicles, including the ER, the early and late endosomes.

Split-ubiquitin yeast two hybrid assay revealed that both TSP-12 and TSP-14 can interact with SUP-17 (Herong Shi and Kelly Liu). Zhiyu Liu in our lab has shown that TSP-12, the TspanC8 tetraspanin in *C. elegans*, is also localized both to the cell surface and in intracellular vesicles, and that it shares a similar expression pattern with SUP-17. Additionally, both TSP-12 and SUP-17 are localized and function in BMP signal-receiving cells to promote BMP signaling. Zhiyu Liu has also shown that TSP-14, a paralog of TSP-12, is localized in early endosomes, late

endosomes and recycling endosomes (personal communication). I have shown in chapter 2 and 3 that mutations in *tsp-12* caused reduced cell surface localization of SUP-17 and increased accumulation in early and late endosomes in embryos. Additionally, TSP-12 may promote the cleavage of SUP-17's pro-domain. TSP-14 on its own does not seem to regulate SUP-17 localization to the cell surface, although a redundant role with TSP-12 has not been ruled out (see below).

The above findings raise many unanswered questions. For instance, is SUP-17 mis-localized in other organelles in *tsp-12(0)* mutant, such as the Golgi apparatus? Golgi markers, *dkIs767* and *dkIs91* available from Ken Sato's lab [147], can be used for this study. Whether the mis-localization of SUP-17 caused by mutations in *tsp-12* affects the protease activity of SUP-17 is another interesting question to ask. To answer this question, one may compare via western blotting the cleavage of known SUP-17 substrates between *tsp-12* mutants and wild-type, if any SUP-17 substrates are identified.

SUP-17 can bind to both TSP-12 and TSP-14, but the corresponding domains in ADAM10 and in tetraspanins that are mediating the interaction have not been identified. Also, whether TSP-14 regulates the localization of SUP-17 in intracellular organelles is still not clear. The same intracellular markers as in Chapter 3 can be used to study endogenous SUP-17::GFP localization in *tsp-14* mutants. TSP-12 and TSP-14 share functional redundancy in regulating ventral enclosure in the embryo, in additional to regulating Notch and BMP signaling [39]. Zhiyu Liu recently showed that TSP-12 and TSP-14 also function redundantly to regulate the localization of the type II receptor DAF-4. Whether these two paralogous tetraspanins regulate SUP-17 localization in subcellular vesicles in similar ways and regulate SUP-17 protein

maturation would also be interesting to investigate. For this purpose, similar strategies as those described in Chapter 3 can be used.

ADAM10 plays many important roles in human diseases due to the versatility of its wide spread substrates. However, targeting ADAM10 for potential therapeutic purposes would not be very successful because of side-effects. So understanding the regulation of SUP-17/ADAM10 in and beyond BMP signaling may shed light on treatment of ADAM10-related diseases.

5.2 Role(s) of SUP-17 in BMP signaling

ADAM10 functions to cleave many cell surface proteins through 'ectodomain shedding'. The cleavage products are fated either to be degraded or to transduce signals, such as in the case of Notch cleavage in the Notch signaling pathway. Through genetic study using the *sma-9* suppression assay, I identified UNC-40/Neogenin as one substrate of SUP-17 in BMP signaling because the extracellular domain of UNC-40 can partially rescue the Susm phenotype of *sup-17(n1258)* mutants [80]. Biochemical analysis of endogenous UNC-40 protein using western blotting suggests that UNC-40 may be cleaved by SUP-17; however, additional biochemical experiments need to be conducted to further test this hypothesis, and the cleavage site in UNC-40 needs to be identified. Western blotting showed that mutations in *tsp-12* may increase UNC-40 protein level whereas mutations in the RGM protein DRAG-1 may reduce UNC-40 protein level (Chapter 4). These experiments also need to be repeated.

Future directions for the studying the roles of SUP-17 in BMP signaling fall into two parts: one is to identify additional substrates in BMP signaling, and the other is to determine the regulation and biological functions of the cleavage events.

The genetic finding that UNC-40 is not the only substrate of SUP-17 in BMP signaling urges us to discover additional substrates of SUP-17. SUP-17/ADAM10-mediated protein processing can occur both in *cis* and in *trans* [41, 148]. Among the known membrane or membrane-associated proteins in Sma/Mab signaling, the following factors are more likely to be substrates. 1) The type I receptor SMA-6. The ADAM protease ADAM17 cleaves TGFβ type I receptor in human prostate cancer (PC-3U) cells [124]. 2) The modulator SMA-10. SMA-10 is a transmembrane protein that belongs to the LRIG family and physically interacts with both type I and type II receptors [31]. LRIG1 is shed by ADAM17 in the African green money kidney cell line COS-7 [149], and the interaction between LRIG2 and Neogenin prevents its cleavage by ADAM17 in E14.5 mouse cortical neurons [128]. 3) The modulator LON-2. LON-2 is a glypican that negatively regulates BMP signaling [33]. Glypican-1 is revealed to be a substrate of ADAM17 through mass spectrometry-based proteomics in the squamous cell carcinoma (SCC-9) cell line derived from tongue [150], suggesting that LON-2/Glypican may be another candidate. To examine if any one of the above molecules is a substrate of SUP-17 in BMP signaling, the following experiments may be done: 1) endogenously tag the candidates and study for alternations of the protein level between wild-type and *sup-17(n1258ts)* worms using western blotting; 2) study their interactions with SUP-17 using co-IP or the split ubiquitin yeast two hybrid system [38, 103]; 3) analyze and mutate possible cleavage sites on those putative substrates, and look for phenotypes in BMP signaling as well as alteration at the protein level via western blotting.

In addition to unveiling more substrates of SUP-17 in Sma/Mab signaling, it would also be interesting to determine in which intracellular compartments and in which tissues the cleavages happen. Blocking the protein trafficking pathway at various steps in cell culture can be

used to answer in which intracellular vesicle are the substrates cleaved. To study for in which cell-type SUP-17 is catalytically competent of cleaving BMP pathway components, tissue-specific rescue can be performed using cleavage product of the substrate *sup-17(n1258ts)* mutants. If it is the extracellular domain that is functional after cleavage and if the fragment can diffuse, tissue-specific knockout is needed to answer this question.

I would also like to propose the following interesting long-term research topics: If multiple substrates of SUP-17 in the BMP pathway are identified, are there spatiotemporal differences of cleavage of the different substrates? If yes, how does SUP-17 make the decisions as to when and where to cleave each substrate? Are there other BMP components involved in regulating the cleavage events by binding to the substrates or to SUP-17? What are the biological consequences when the substrates get cleaved by SUP-17 in BMP signaling? What happens to the cleavage products, are they degraded or released to transmit subsequent signals?

References

1. Massague J, Blain SW, Lo RS. TGFbeta signaling in growth control, cancer, and heritable disorders. Cell. 2000;103(2):295-309. PubMed PMID: 11057902.

2. Heldin CH, Miyazono K, ten Dijke P. TGF-beta signalling from cell membrane to nucleus through SMAD proteins. Nature. 1997;390(6659):465-71. doi: 10.1038/37284. PubMed PMID: 9393997.

3. De Crescenzo G, Grothe S, Zwaagstra J, Tsang M, O'Connor-McCourt MD. Real-time monitoring of the interactions of transforming growth factor-beta (TGF-beta) isoforms with latency-associated protein and the ectodomains of the TGF-beta type II and III receptors reveals different kinetic models and stoichiometries of binding. J Biol Chem. 2001;276(32):29632-43. doi: 10.1074/jbc.M009765200. PubMed PMID: 11382746.

4. Sengle G, Ono RN, Sasaki T, Sakai LY. Prodomains of transforming growth factor beta (TGFbeta) superfamily members specify different functions: extracellular matrix interactions and growth factor bioavailability. J Biol Chem. 2011;286(7):5087-99. doi: 10.1074/jbc.M110.188615. PubMed PMID: 21135108; PubMed Central PMCID: PMCPMC3037620.

5. Sopory S, Nelsen SM, Degnin C, Wong C, Christian JL. Regulation of bone morphogenetic protein-4 activity by sequence elements within the prodomain. J Biol Chem. 2006;281(45):34021-31. doi: 10.1074/jbc.M605330200. PubMed PMID: 16966322.

6. Wrana JL, Attisano L, Wieser R, Ventura F, Massague J. Mechanism of activation of the TGF-beta receptor. Nature. 1994;370(6488):341-7. doi: 10.1038/370341a0. PubMed PMID: 8047140.

7. Macias-Silva M, Abdollah S, Hoodless PA, Pirone R, Attisano L, Wrana JL. MADR2 is a substrate of the TGFbeta receptor and its phosphorylation is required for nuclear accumulation and signaling. Cell. 1996;87(7):1215-24. PubMed PMID: 8980228.

8. Souchelnytskyi S, Tamaki K, Engstrom U, Wernstedt C, ten Dijke P, Heldin CH. Phosphorylation of Ser465 and Ser467 in the C terminus of Smad2 mediates interaction with Smad4 and is required for transforming growth factor-beta signaling. J Biol Chem. 1997;272(44):28107-15. PubMed PMID: 9346966.

9. Shi Y, Wang YF, Jayaraman L, Yang H, Massague J, Pavletich NP. Crystal structure of a Smad MH1 domain bound to DNA: insights on DNA binding in TGF-beta signaling. Cell. 1998;94(5):585-94. PubMed PMID: 9741623.

10. Urist MR. Bone: formation by autoinduction. Science. 1965;150(3698):893-9. PubMed PMID: 5319761.

11. Wozney JM, Rosen V, Celeste AJ, Mitsock LM, Whitters MJ, Kriz RW, et al. Novel regulators of bone formation: molecular clones and activities. Science. 1988;242(4885):1528-34. PubMed PMID: 3201241.

12. Wang RN, Green J, Wang Z, Deng Y, Qiao M, Peabody M, et al. Bone Morphogenetic Protein (BMP) signaling in development and human diseases. Genes Dis. 2014;1(1):87-105. doi: 10.1016/j.gendis.2014.07.005. PubMed PMID: 25401122; PubMed Central PMCID: PMCPMC4232216.

13. Senta H, Park H, Bergeron E, Drevelle O, Fong D, Leblanc E, et al. Cell responses to bone morphogenetic proteins and peptides derived from them: biomedical applications and limitations. Cytokine Growth Factor Rev. 2009;20(3):213-22. doi: 10.1016/j.cytogfr.2009.05.006. PubMed PMID: 19493693.

14. Scheufler C, Sebald W, Hulsmeyer M. Crystal structure of human bone morphogenetic protein-2 at 2.7 A resolution. J Mol Biol. 1999;287(1):103-15. doi: 10.1006/jmbi.1999.2590. PubMed PMID: 10074410.

15. ten Dijke P, Yamashita H, Sampath TK, Reddi AH, Estevez M, Riddle DL, et al. Identification of type I receptors for osteogenic protein-1 and bone morphogenetic protein-4. J Biol Chem. 1994;269(25):16985-8. PubMed PMID: 8006002.

16. Shi Y, Hata A, Lo RS, Massague J, Pavletich NP. A structural basis for mutational inactivation of the tumour suppressor Smad4. Nature. 1997;388(6637):87-93. doi: 10.1038/40431. PubMed PMID: 9214508.

17. Wagner DO, Sieber C, Bhushan R, Borgermann JH, Graf D, Knaus P. BMPs: from bone to body morphogenetic proteins. Sci Signal. 2010;3(107):mr1. doi: 10.1126/scisignal.3107mr1. PubMed PMID: 20124549.

18. Zakin L, De Robertis EM. Extracellular regulation of BMP signaling. Curr Biol. 2010;20(3):R89-92. doi: 10.1016/j.cub.2009.11.021. PubMed PMID: 20144774; PubMed Central PMCID: PMCPMC3034644.

19. Groppe J, Greenwald J, Wiater E, Rodriguez-Leon J, Economides AN, Kwiatkowski W, et al. Structural basis of BMP signalling inhibition by the cystine knot protein Noggin. Nature. 2002;420(6916):636-42. doi: 10.1038/nature01245. PubMed PMID: 12478285.

20. Lin SJ, Lerch TF, Cook RW, Jardetzky TS, Woodruff TK. The structural basis of TGF-beta, bone morphogenetic protein, and activin ligand binding. Reproduction. 2006;132(2):179-90. doi: 10.1530/rep.1.01072. PubMed PMID: 16885528.

21. Sedlmeier G, Sleeman JP. Extracellular regulation of BMP signaling: welcome to the matrix. Biochem Soc Trans. 2017;45(1):173-81. doi: 10.1042/BST20160263. PubMed PMID: 28202671.

22. Peterson RS, Andhare RA, Rousche KT, Knudson W, Wang W, Grossfield JB, et al. CD44 modulates Smad1 activation in the BMP-7 signaling pathway. J Cell Biol. 2004;166(7):1081-91. doi: 10.1083/jcb.200402138. PubMed PMID: 15452148; PubMed Central PMCID: PMCPMC2172010.

23. Luo N, Knudson W, Askew EB, Veluci R, Knudson CB. CD44 and hyaluronan promote the bone morphogenetic protein 7 signaling response in murine chondrocytes. Arthritis Rheumatol. 2014;66(6):1547-58. doi: 10.1002/art.38388. PubMed PMID: 24497488; PubMed Central PMCID: PMCPMC4070509.

24. Oelgeschlager M, Larrain J, Geissert D, De Robertis EM. The evolutionarily conserved BMP-binding protein Twisted gastrulation promotes BMP signalling. Nature. 2000;405(6788):757-63. doi: 10.1038/35015500. PubMed PMID: 10866189; PubMed Central PMCID: PMCPMC2292104.

25. Sawala A, Sutcliffe C, Ashe HL. Multistep molecular mechanism for bone morphogenetic protein extracellular transport in the Drosophila embryo. Proc Natl Acad Sci U S A. 2012;109(28):11222-7. doi: 10.1073/pnas.1202781109. PubMed PMID: 22733779; PubMed Central PMCID: PMCPMC3396515.

26. Winstanley J, Sawala A, Baldock C, Ashe HL. Synthetic enzyme-substrate tethering obviates the Tolloid-ECM interaction during Drosophila BMP gradient formation. Elife. 2015;4. doi: 10.7554/eLife.05508. PubMed PMID: 25642644; PubMed Central PMCID: PMCPMC4337604.

27. Savage C, Das P, Finelli AL, Townsend SR, Sun CY, Baird SE, et al. Caenorhabditis elegans genes sma-2, sma-3, and sma-4 define a conserved family of transforming growth factor beta pathway components. Proc Natl Acad Sci U S A. 1996;93(2):790-4. PubMed PMID: 8570636; PubMed Central PMCID: PMCPMC40134.

28. Foehr ML, Lindy AS, Fairbank RC, Amin NM, Xu M, Yanowitz J, et al. An antagonistic role for the C. elegans Schnurri homolog SMA-9 in modulating TGFbeta signaling during mesodermal patterning. Development. 2006;133(15):2887-96. doi: 10.1242/dev.02476. PubMed PMID: 16790477.

29. Patterson GI, Padgett RW. TGF beta-related pathways. Roles in Caenorhabditis elegans development. Trends Genet. 2000;16(1):27-33. PubMed PMID: 10637628.

30. Savage-Dunn C. TGF-beta signaling. WormBook. 2005:1-12. doi: 10.1895/wormbook.1.22.1. PubMed PMID: 18050404; PubMed Central PMCID: PMCPMC4781025.

31. Gumienny TL, Macneil L, Zimmerman CM, Wang H, Chin L, Wrana JL, et al. Caenorhabditis elegans SMA-10/LRIG is a conserved transmembrane protein that enhances bone morphogenetic protein signaling. PLoS Genet. 2010;6(5):e1000963. doi: 10.1371/journal.pgen.1000963. PubMed PMID: 20502686; PubMed Central PMCID: PMCPMC2873917.

32. Fung WY, Fat KF, Eng CK, Lau CK. crm-1 facilitates BMP signaling to control body size in Caenorhabditis elegans. Dev Biol. 2007;311(1):95-105. doi: 10.1016/j.ydbio.2007.08.016. PubMed PMID: 17869238.

33. Gumienny TL, MacNeil LT, Wang H, de Bono M, Wrana JL, Padgett RW. Glypican LON-2 is a conserved negative regulator of BMP-like signaling in Caenorhabditis elegans. Curr Biol. 2007;17(2):159-64. doi: 10.1016/j.cub.2006.11.065. PubMed PMID: 17240342.

34. Maduzia LL, Gumienny TL, Zimmerman CM, Wang H, Shetgiri P, Krishna S, et al. lon-1 regulates Caenorhabditis elegans body size downstream of the dbl-1 TGF beta signaling pathway. Dev Biol. 2002;246(2):418-28. doi: 10.1006/dbio.2002.0662. PubMed PMID: 12051826.

35. Morita K, Flemming AJ, Sugihara Y, Mochii M, Suzuki Y, Yoshida S, et al. A Caenorhabditis elegans TGF-beta, DBL-1, controls the expression of LON-1, a PR-related protein, that regulates polyploidization and body length. EMBO J. 2002;21(5):1063-73. doi: 10.1093/emboj/21.5.1063. PubMed PMID: 11867534; PubMed Central PMCID: PMCPMC125886.

36. Liang J, Lints R, Foehr ML, Tokarz R, Yu L, Emmons SW, et al. The Caenorhabditis elegans schnurri homolog sma-9 mediates stage- and cell type-specific responses to DBL-1 BMP-related signaling. Development. 2003;130(26):6453-64. doi: 10.1242/dev.00863. PubMed PMID: 14627718.

37. Tian C, Sen D, Shi H, Foehr ML, Plavskin Y, Vatamaniuk OK, et al. The RGM protein DRAG-1 positively regulates a BMP-like signaling pathway in Caenorhabditis elegans. Development. 2010;137(14):2375-84. doi: 10.1242/dev.051615. PubMed PMID: 20534671; PubMed Central PMCID: PMCPMC2889605.

38. Tian C, Shi H, Xiong S, Hu F, Xiong WC, Liu J. The neogenin/DCC homolog UNC-40 promotes BMP signaling via the RGM protein DRAG-1 in C. elegans. Development.

2013;140(19):4070-80. doi: 10.1242/dev.099838. PubMed PMID: 24004951; PubMed Central PMCID: PMCPMC3775419.

39. Liu Z, Shi H, Szymczak LC, Aydin T, Yun S, Constas K, et al. Promotion of bone morphogenetic protein signaling by tetraspanins and glycosphingolipids. PLoS Genet. 2015;11(5):e1005221. doi: 10.1371/journal.pgen.1005221. PubMed PMID: 25978409; PubMed Central PMCID: PMCPMC4433240.

40. Gould RJ, Polokoff MA, Friedman PA, Huang TF, Holt JC, Cook JJ, et al. Disintegrins: a family of integrin inhibitory proteins from viper venoms. Proc Soc Exp Biol Med. 1990;195(2):168-71. PubMed PMID: 2236100.

41. Dreymueller D, Pruessmeyer J, Groth E, Ludwig A. The role of ADAM-mediated shedding in vascular biology. Eur J Cell Biol. 2012;91(6-7):472-85. doi: 10.1016/j.ejcb.2011.09.003. PubMed PMID: 22138087.

42. Seals DF, Courtneidge SA. The ADAMs family of metalloproteases: multidomain proteins with multiple functions. Genes Dev. 2003;17(1):7-30. doi: 10.1101/gad.1039703. PubMed PMID: 12514095.

43. Pruessmeyer J, Ludwig A. The good, the bad and the ugly substrates for ADAM10 and ADAM17 in brain pathology, inflammation and cancer. Semin Cell Dev Biol. 2009;20(2):164-74. doi: 10.1016/j.semcdb.2008.09.005. PubMed PMID: 18951988.

44. Escrevente C, Morais VA, Keller S, Soares CM, Altevogt P, Costa J. Functional role of N-glycosylation from ADAM10 in processing, localization and activity of the enzyme. Biochim Biophys Acta. 2008;1780(6):905-13. doi: 10.1016/j.bbagen.2008.03.004. PubMed PMID: 18381078.

45. Van Wart HE, Birkedal-Hansen H. The cysteine switch: a principle of regulation of metalloproteinase activity with potential applicability to the entire matrix metalloproteinase gene family. Proc Natl Acad Sci U S A. 1990;87(14):5578-82. PubMed PMID: 2164689; PubMed Central PMCID: PMCPMC54368.

46. Anders A, Gilbert S, Garten W, Postina R, Fahrenholz F. Regulation of the alpha-secretase ADAM10 by its prodomain and proprotein convertases. FASEB J. 2001;15(10):1837-9. PubMed PMID: 11481247.

47. Wong E, Maretzky T, Peleg Y, Blobel CP, Sagi I. The Functional Maturation of A Disintegrin and Metalloproteinase (ADAM) 9, 10, and 17 Requires Processing at a Newly Identified Proprotein Convertase (PC) Cleavage Site. J Biol Chem. 2015;290(19):12135-46. doi: 10.1074/jbc.M114.624072. PubMed PMID: 25795784; PubMed Central PMCID: PMCPMC4424348.

48. Lolis E, Petsko GA. Transition-state analogues in protein crystallography: probes of the structural source of enzyme catalysis. Annu Rev Biochem. 1990;59:597-630. doi: 10.1146/annurev.bi.59.070190.003121. PubMed PMID: 2197984.

49. Wolfsberg TG, Primakoff P, Myles DG, White JM. ADAM, a novel family of membrane proteins containing A Disintegrin And Metalloprotease domain: multipotential functions in cell-cell and cell-matrix interactions. J Cell Biol. 1995;131(2):275-8. PubMed PMID: 7593158; PubMed Central PMCID: PMCPMC2199973.

50. Noy PJ, Yang J, Reyat JS, Matthews AL, Charlton AE, Furmston J, et al. TspanC8 Tetraspanins and A Disintegrin and Metalloprotease 10 (ADAM10) Interact via Their Extracellular Regions: EVIDENCE FOR DISTINCT BINDING MECHANISMS FOR DIFFERENT TspanC8 PROTEINS. J Biol Chem. 2016;291(7):3145-57. doi:

10.1074/jbc.M115.703058. PubMed PMID: 26668317; PubMed Central PMCID: PMCPMC4751363.

51. Parra LM, Hartmann M, Schubach S, Li Y, Herrlich P, Herrlich A. Distinct Intracellular Domain Substrate Modifications Selectively Regulate Ectodomain Cleavage of NRG1 or CD44. Mol Cell Biol. 2015;35(19):3381-95. doi: 10.1128/MCB.00500-15. PubMed PMID: 26217011; PubMed Central PMCID: PMCPMC4561721.

52. Marcello E, Gardoni F, Di Luca M, Perez-Otano I. An arginine stretch limits ADAM10 exit from the endoplasmic reticulum. J Biol Chem. 2010;285(14):10376-84. doi: 10.1074/jbc.M109.055947. PubMed PMID: 20100836; PubMed Central PMCID: PMCPMC2856244.

53. Maretzky T, Evers A, Le Gall S, Alabi RO, Speck N, Reiss K, et al. The cytoplasmic domain of a disintegrin and metalloproteinase 10 (ADAM10) regulates its constitutive activity but is dispensable for stimulated ADAM10-dependent shedding. J Biol Chem. 2015;290(12):7416-25. doi: 10.1074/jbc.M114.603753. PubMed PMID: 25605720; PubMed Central PMCID: PMCPMC4367251.

54. Wild-Bode C, Fellerer K, Kugler J, Haass C, Capell A. A basolateral sorting signal directs ADAM10 to adherens junctions and is required for its function in cell migration. J Biol Chem. 2006;281(33):23824-9. doi: 10.1074/jbc.M601542200. PubMed PMID: 16777847.

55. Qi H, Rand MD, Wu X, Sestan N, Wang W, Rakic P, et al. Processing of the notch ligand delta by the metalloprotease Kuzbanian. Science. 1999;283(5398):91-4. PubMed PMID: 9872749.

56. Gutwein P, Mechtersheimer S, Riedle S, Stoeck A, Gast D, Joumaa S, et al. ADAM10-mediated cleavage of L1 adhesion molecule at the cell surface and in released membrane vesicles. FASEB J. 2003;17(2):292-4. doi: 10.1096/fj.02-0430fje. PubMed PMID: 12475894.

57. Lammich S, Kojro E, Postina R, Gilbert S, Pfeiffer R, Jasionowski M, et al. Constitutive and regulated alpha-secretase cleavage of Alzheimer's amyloid precursor protein by a disintegrin metalloprotease. Proc Natl Acad Sci U S A. 1999;96(7):3922-7. PubMed PMID: 10097139; PubMed Central PMCID: PMCPMC22396.

58. Altmeppen HC, Prox J, Krasemann S, Puig B, Kruszewski K, Dohler F, et al. The sheddase ADAM10 is a potent modulator of prion disease. Elife. 2015;4. doi: 10.7554/eLife.04260. PubMed PMID: 25654651; PubMed Central PMCID: PMCPMC4346534.

59. Chen C, Lv Y, Zhang BY, Zhang J, Shi Q, Wang J, et al. Apparent reduction of ADAM10 in scrapie-infected cultured cells and in the brains of scrapie-infected rodents. Mol Neurobiol. 2014;50(3):875-87. doi: 10.1007/s12035-014-8708-7. PubMed PMID: 24771043.

60. Parkin ET, Watt NT, Turner AJ, Hooper NM. Dual mechanisms for shedding of the cellular prion protein. J Biol Chem. 2004;279(12):11170-8. doi: 10.1074/jbc.M312105200. PubMed PMID: 14711812.

61. Taylor DR, Parkin ET, Cocklin SL, Ault JR, Ashcroft AE, Turner AJ, et al. Role of ADAMs in the ectodomain shedding and conformational conversion of the prion protein. J Biol Chem. 2009;284(34):22590-600. doi: 10.1074/jbc.M109.032599. PubMed PMID: 19564338; PubMed Central PMCID: PMCPMC2755666.

62. Pasciuto E, Ahmed T, Wahle T, Gardoni F, D'Andrea L, Pacini L, et al. Dysregulated ADAM10-Mediated Processing of APP during a Critical Time Window Leads to Synaptic

Deficits in Fragile X Syndrome. Neuron. 2015;87(2):382-98. doi: 10.1016/j.neuron.2015.06.032. PubMed PMID: 26182420.

63. Lo Sardo V, Zuccato C, Gaudenzi G, Vitali B, Ramos C, Tartari M, et al. An evolutionary recent neuroepithelial cell adhesion function of huntingtin implicates ADAM10-Ncadherin. Nat Neurosci. 2012;15(5):713-21. doi: 10.1038/nn.3080. PubMed PMID: 22466506.

64. Hartmann M, Parra LM, Ruschel A, Lindner C, Morrison H, Herrlich A, et al. Inside-out Regulation of Ectodomain Cleavage of Cluster-of-Differentiation-44 (CD44) and of Neuregulin-1 Requires Substrate Dimerization. J Biol Chem. 2015;290(28):17041-54. doi: 10.1074/jbc.M114.610204. PubMed PMID: 25925953; PubMed Central PMCID: PMCPMC4498042.

65. Wen C, Metzstein MM, Greenwald I. SUP-17, a Caenorhabditis elegans ADAM protein related to Drosophila KUZBANIAN, and its role in LIN-12/NOTCH signalling. Development. 1997;124(23):4759-67. PubMed PMID: 9428412.

66. Rooke J, Pan D, Xu T, Rubin GM. KUZ, a conserved metalloprotease-disintegrin protein with two roles in Drosophila neurogenesis. Science. 1996;273(5279):1227-31. PubMed PMID: 8703057.

67. Sotillos S, Roch F, Campuzano S. The metalloprotease-disintegrin Kuzbanian participates in Notch activation during growth and patterning of Drosophila imaginal discs. Development. 1997;124(23):4769-79. PubMed PMID: 9428413.

68. Tax FE, Thomas JH, Ferguson EL, Horvitz HR. Identification and characterization of genes that interact with lin-12 in Caenorhabditis elegans. Genetics. 1997;147(4):1675-95. PubMed PMID: 9409830; PubMed Central PMCID: PMCPMC1208340.

69. Jarriault S, Greenwald I. Evidence for functional redundancy between C. elegans ADAM proteins SUP-17/Kuzbanian and ADM-4/TACE. Dev Biol. 2005;287(1):1-10. doi: 10.1016/j.ydbio.2005.08.014. PubMed PMID: 16197940; PubMed Central PMCID: PMCPMC1805470.

70. Charrin S, Jouannet S, Boucheix C, Rubinstein E. Tetraspanins at a glance. J Cell Sci. 2014;127(Pt 17):3641-8. doi: 10.1242/jcs.154906. PubMed PMID: 25128561.

71. Yang X, Claas C, Kraeft SK, Chen LB, Wang Z, Kreidberg JA, et al. Palmitoylation of tetraspanin proteins: modulation of CD151 lateral interactions, subcellular distribution, and integrin-dependent cell morphology. Mol Biol Cell. 2002;13(3):767-81. doi: 10.1091/mbc.01-05-0275. PubMed PMID: 11907260; PubMed Central PMCID: PMCPMC99597.

72. Charrin S, Manie S, Oualid M, Billard M, Boucheix C, Rubinstein E. Differential stability of tetraspanin/tetraspanin interactions: role of palmitoylation. FEBS Lett. 2002;516(1-3):139-44. PubMed PMID: 11959120.

73. Lineberry N, Su L, Soares L, Fathman CG. The single subunit transmembrane E3 ligase gene related to anergy in lymphocytes (GRAIL) captures and then ubiquitinates transmembrane proteins across the cell membrane. J Biol Chem. 2008;283(42):28497-505. doi: 10.1074/jbc.M805092200. PubMed PMID: 18713730; PubMed Central PMCID: PMCPMC2568916.

74. Termini CM, Gillette JM. Tetraspanins Function as Regulators of Cellular Signaling. Front Cell Dev Biol. 2017;5:34. doi: 10.3389/fcell.2017.00034. PubMed PMID: 28428953; PubMed Central PMCID: PMCPMC5382171.

75. Dornier E, Coumailleau F, Ottavi JF, Moretti J, Boucheix C, Mauduit P, et al. TspanC8 tetraspanins regulate ADAM10/Kuzbanian trafficking and promote Notch activation in flies and

mammals. J Cell Biol. 2012;199(3):481-96. doi: 10.1083/jcb.201201133. PubMed PMID: 23091066; PubMed Central PMCID: PMCPMC3483123.

76. Haining EJ, Yang J, Bailey RL, Khan K, Collier R, Tsai S, et al. The TspanC8 subgroup of tetraspanins interacts with A disintegrin and metalloprotease 10 (ADAM10) and regulates its maturation and cell surface expression. J Biol Chem. 2012;287(47):39753-65. doi: 10.1074/jbc.M112.416503. PubMed PMID: 23035126; PubMed Central PMCID: PMCPMC3501075.

77. Jouannet S, Saint-Pol J, Fernandez L, Nguyen V, Charrin S, Boucheix C, et al. TspanC8 tetraspanins differentially regulate the cleavage of ADAM10 substrates, Notch activation and ADAM10 membrane compartmentalization. Cell Mol Life Sci. 2016;73(9):1895-915. doi: 10.1007/s00018-015-2111-z. PubMed PMID: 26686862; PubMed Central PMCID: PMCPMC4819958.

78. Xu D, Sharma C, Hemler ME. Tetraspanin12 regulates ADAM10-dependent cleavage of amyloid precursor protein. FASEB J. 2009;23(11):3674-81. doi: 10.1096/fj.09-133462. PubMed PMID: 19587294; PubMed Central PMCID: PMCPMC2775005.

79. Seipold L, Damme M, Prox J, Rabe B, Kasparek P, Sedlacek R, et al. Tetraspanin 3: A central endocytic membrane component regulating the expression of ADAM10, presenilin and the amyloid precursor protein. Biochim Biophys Acta. 2017;1864(1):217-30. doi: 10.1016/j.bbamcr.2016.11.003. PubMed PMID: 27818272.

80. Wang L, Liu Z, Shi H, Liu J. Two Paralogous Tetraspanins TSP-12 and TSP-14 Function with the ADAM10 Metalloprotease SUP-17 to Promote BMP Signaling in Caenorhabditis elegans. PLoS Genet. 2017;13(1):e1006568. doi: 10.1371/journal.pgen.1006568. PubMed PMID: 28068334; PubMed Central PMCID: PMCPMC5261805.

81. Dunn CD, Sulis ML, Ferrando AA, Greenwald I. A conserved tetraspanin subfamily promotes Notch signaling in Caenorhabditis elegans and in human cells. Proc Natl Acad Sci U S A. 2010;107(13):5907-12. doi: 10.1073/pnas.1001647107. PubMed PMID: 20220101; PubMed Central PMCID: PMCPMC2851858.

82. Gad JM, Keeling SL, Wilks AF, Tan SS, Cooper HM. The expression patterns of guidance receptors, DCC and Neogenin, are spatially and temporally distinct throughout mouse embryogenesis. Dev Biol. 1997;192(2):258-73. doi: 10.1006/dbio.1997.8756. PubMed PMID: 9441666.

83. Hong M, Schachter KA, Jiang G, Krauss RS. Neogenin regulates Sonic Hedgehog pathway activity during digit patterning. Dev Dyn. 2012;241(3):627-37. doi: 10.1002/dvdy.23745. PubMed PMID: 22275192; PubMed Central PMCID: PMCPMC3424067.

84. Okamura Y, Kohmura E, Yamashita T. TACE cleaves neogenin to desensitize cortical neurons to the repulsive guidance molecule. Neurosci Res. 2011;71(1):63-70. doi: 10.1016/j.neures.2011.05.012. PubMed PMID: 21645559.

85. Galko MJ, Tessier-Lavigne M. Function of an axonal chemoattractant modulated by metalloprotease activity. Science. 2000;289(5483):1365-7. PubMed PMID: 10958786.

86. Cai J, Pardali E, Sanchez-Duffhues G, ten Dijke P. BMP signaling in vascular diseases. FEBS Lett. 2012;586(14):1993-2002. doi: 10.1016/j.febslet.2012.04.030. PubMed PMID: 22710160.

87. Katagiri T, Watabe T. Bone Morphogenetic Proteins. Cold Spring Harb Perspect Biol. 2016;8(6). doi: 10.1101/cshperspect.a021899. PubMed PMID: 27252362.

88. Massague J. TGF-beta signaling in development and disease. FEBS Lett. 2012;586(14):1833. doi: 10.1016/j.febslet.2012.05.030. PubMed PMID: 22651913.

89. Brazil DP, Church RH, Surae S, Godson C, Martin F. BMP signalling: agony and antagony in the family. Trends Cell Biol. 2015;25(5):249-64. doi: 10.1016/j.tcb.2014.12.004. PubMed PMID: 25592806.

90. Massague J. TGFbeta signalling in context. Nat Rev Mol Cell Biol. 2012;13(10):616-30. doi: 10.1038/nrm3434. PubMed PMID: 22992590; PubMed Central PMCID: PMCPMC4027049.

91. Gleason RJ, Akintobi AM, Grant BD, Padgett RW. BMP signaling requires retromer-dependent recycling of the type I receptor. Proc Natl Acad Sci U S A. 2014;111(7):2578-83. doi: 10.1073/pnas.1319947111. PubMed PMID: 24550286; PubMed Central PMCID: PMCPMC3932876.

92. Tian C, Liu J. Repulsive guidance molecules (RGMs) and neogenin in bone morphogenetic protein (BMP) signaling. Mol Reprod Dev. 2013;80(9):700-17. doi: 10.1002/mrd.22199. PubMed PMID: 23740870; PubMed Central PMCID: PMCPMC4440832.

93. Prox J, Willenbrock M, Weber S, Lehmann T, Schmidt-Arras D, Schwanbeck R, et al. Tetraspanin15 regulates cellular trafficking and activity of the ectodomain sheddase ADAM10. Cell Mol Life Sci. 2012;69(17):2919-32. doi: 10.1007/s00018-012-0960-2. PubMed PMID: 22446748.

94. Gumienny TL, Savage-Dunn C. TGF-beta signaling in C. elegans. WormBook. 2013:1-34. doi: 10.1895/wormbook.1.22.2. PubMed PMID: 23908056.

95. Brenner S. The genetics of Caenorhabditis elegans. Genetics. 1974;77(1):71-94. PubMed PMID: 4366476; PubMed Central PMCID: PMCPMC1213120.

96. Schindelin J, Arganda-Carreras I, Frise E, Kaynig V, Longair M, Pietzsch T, et al. Fiji: an open-source platform for biological-image analysis. Nat Methods. 2012;9(7):676-82. doi: 10.1038/nmeth.2019. PubMed PMID: 22743772; PubMed Central PMCID: PMCPMC3855844.

97. Rual JF, Ceron J, Koreth J, Hao T, Nicot AS, Hirozane-Kishikawa T, et al. Toward improving Caenorhabditis elegans phenome mapping with an ORFeome-based RNAi library. Genome Res. 2004;14(10B):2162-8. doi: 10.1101/gr.2505604. PubMed PMID: 15489339; PubMed Central PMCID: PMCPMC528933.

98. Frokjaer-Jensen C, Davis MW, Hopkins CE, Newman BJ, Thummel JM, Olesen SP, et al. Single-copy insertion of transgenes in Caenorhabditis elegans. Nat Genet. 2008;40(11):1375-83. doi: 10.1038/ng.248. PubMed PMID: 18953339; PubMed Central PMCID: PMCPMC2749959.

99. Friedland AE, Tzur YB, Esvelt KM, Colaiacovo MP, Church GM, Calarco JA. Heritable genome editing in C. elegans via a CRISPR-Cas9 system. Nat Methods. 2013;10(8):741-3. doi: 10.1038/nmeth.2532. PubMed PMID: 23817069; PubMed Central PMCID: PMCPMC3822328.

100. Dickinson DJ, Ward JD, Reiner DJ, Goldstein B. Engineering the Caenorhabditis elegans genome using Cas9-triggered homologous recombination. Nat Methods. 2013;10(10):1028-34. doi: 10.1038/nmeth.2641. PubMed PMID: 23995389; PubMed Central PMCID: PMCPMC3905680.

101. Arribere JA, Bell RT, Fu BX, Artiles KL, Hartman PS, Fire AZ. Efficient marker-free recovery of custom genetic modifications with CRISPR/Cas9 in Caenorhabditis elegans. Genetics. 2014;198(3):837-46. doi: 10.1534/genetics.114.169730. PubMed PMID: 25161212; PubMed Central PMCID: PMCPMC4224173.

102. Dickinson DJ, Pani AM, Heppert JK, Higgins CD, Goldstein B. Streamlined Genome Engineering with a Self-Excising Drug Selection Cassette. Genetics. 2015;200(4):1035-49. doi: 10.1534/genetics.115.178335. PubMed PMID: 26044593; PubMed Central PMCID: PMCPMC4574250.

103. Grefen C, Lalonde S, Obrdlik P. Split-ubiquitin system for identifying protein-protein interactions in membrane and full-length proteins. Curr Protoc Neurosci. 2007;Chapter 5:Unit 5 27. doi: 10.1002/0471142301.ns0527s41. PubMed PMID: 18428659.

104. Yoshida S, Morita K, Mochii M, Ueno N. Hypodermal expression of Caenorhabditis elegans TGF-beta type I receptor SMA-6 is essential for the growth and maintenance of body length. Dev Biol. 2001;240(1):32-45. doi: 10.1006/dbio.2001.0443. PubMed PMID: 11784045.

105. Wang J, Tokarz R, Savage-Dunn C. The expression of TGFbeta signal transducers in the hypodermis regulates body size in C. elegans. Development. 2002;129(21):4989-98. PubMed PMID: 12397107.

106. Watanabe N, Ishihara T, Ohshima Y. Mutants carrying two sma mutations are super small in the nematode C. elegans. Genes Cells. 2007;12(5):603-9. doi: 10.1111/j.1365-2443.2007.01077.x. PubMed PMID: 17535251.

107. Cai Q, Wang W, Gao Y, Yang Y, Zhu Z, Fan Q. Ce-wts-1 plays important roles in Caenorhabditis elegans development. FEBS Lett. 2009;583(19):3158-64. doi: 10.1016/j.febslet.2009.09.002. PubMed PMID: 19737560.

108. Greenwald I. Notch and the awesome power of genetics. Genetics. 2012;191(3):655-69. doi: 10.1534/genetics.112.141812. PubMed PMID: 22785620; PubMed Central PMCID: PMCPMC3389966.

109. Li X, Greenwald I. HOP-1, a Caenorhabditis elegans presenilin, appears to be functionally redundant with SEL-12 presenilin and to facilitate LIN-12 and GLP-1 signaling. Proc Natl Acad Sci U S A. 1997;94(22):12204-9. PubMed PMID: 9342387; PubMed Central PMCID: PMCPMC23751.

110. Levitan D, Greenwald I. Facilitation of lin-12-mediated signalling by sel-12, a Caenorhabditis elegans S182 Alzheimer's disease gene. Nature. 1995;377(6547):351-4. doi: 10.1038/377351a0. PubMed PMID: 7566091.

111. Arduengo PM, Appleberry OK, Chuang P, L'Hernault SW. The presenilin protein family member SPE-4 localizes to an ER/Golgi derived organelle and is required for proper cytoplasmic partitioning during Caenorhabditis elegans spermatogenesis. J Cell Sci. 1998;111 (Pt 24):3645-54. PubMed PMID: 9819355.

112. Reiss K, Saftig P. The "a disintegrin and metalloprotease" (ADAM) family of sheddases: physiological and cellular functions. Semin Cell Dev Biol. 2009;20(2):126-37. doi: 10.1016/j.semcdb.2008.11.002. PubMed PMID: 19049889.

113. Alexander M, Chan KK, Byrne AB, Selman G, Lee T, Ono J, et al. An UNC-40 pathway directs postsynaptic membrane extension in Caenorhabditis elegans. Development. 2009;136(6):911-22. doi: 10.1242/dev.030759. PubMed PMID: 19211675.

114. Pan D, Rubin GM. Kuzbanian controls proteolytic processing of Notch and mediates lateral inhibition during Drosophila and vertebrate neurogenesis. Cell. 1997;90(2):271-80. PubMed PMID: 9244301.

115. van Tetering G, van Diest P, Verlaan I, van der Wall E, Kopan R, Vooijs M. Metalloprotease ADAM10 is required for Notch1 site 2 cleavage. J Biol Chem. 2009;284(45):31018-27. doi: 10.1074/jbc.M109.006775. PubMed PMID: 19726682; PubMed Central PMCID: PMCPMC2781502.

116. Greenwald IS, Sternberg PW, Horvitz HR. The lin-12 locus specifies cell fates in Caenorhabditis elegans. Cell. 1983;34(2):435-44. PubMed PMID: 6616618.

117. Foehr ML, Liu J. Dorsoventral patterning of the C. elegans postembryonic mesoderm requires both LIN-12/Notch and TGFbeta signaling. Dev Biol. 2008;313(1):256-66. doi: 10.1016/j.ydbio.2007.10.027. PubMed PMID: 18036582; PubMed Central PMCID: PMCPMC2213558.

118. Chisholm AD, Hardin J. Epidermal morphogenesis. WormBook. 2005:1-22. doi: 10.1895/wormbook.1.35.1. PubMed PMID: 18050408; PubMed Central PMCID: PMCPMC4781537.

119. Berditchevski F, Odintsova E. Tetraspanins as regulators of protein trafficking. Traffic. 2007;8(2):89-96. doi: 10.1111/j.1600-0854.2006.00515.x. PubMed PMID: 17181773.

120. Kopan R, Ilagan MX. The canonical Notch signaling pathway: unfolding the activation mechanism. Cell. 2009;137(2):216-33. doi: 10.1016/j.cell.2009.03.045. PubMed PMID: 19379690; PubMed Central PMCID: PMCPMC2827930.

121. Hori K, Sen A, Artavanis-Tsakonas S. Notch signaling at a glance. J Cell Sci. 2013;126(Pt 10):2135-40. doi: 10.1242/jcs.127308. PubMed PMID: 23729744; PubMed Central PMCID: PMCPMC3672934.

122. Greenwald I, Kovall R. Notch signaling: genetics and structure. WormBook. 2013:1-28. doi: 10.1895/wormbook.1.10.2. PubMed PMID: 23355521.

123. Liu C, Xu P, Lamouille S, Xu J, Derynck R. TACE-mediated ectodomain shedding of the type I TGF-beta receptor downregulates TGF-beta signaling. Mol Cell. 2009;35(1):26-36. doi: 10.1016/j.molcel.2009.06.018. PubMed PMID: 19595713; PubMed Central PMCID: PMCPMC2740991.

124. Mu Y, Sundar R, Thakur N, Ekman M, Gudey SK, Yakymovych M, et al. TRAF6 ubiquitinates TGFbeta type I receptor to promote its cleavage and nuclear translocation in cancer.

Nat Commun. 2011;2:330. doi: 10.1038/ncomms1332. PubMed PMID: 21629263; PubMed Central PMCID: PMCPMC3113296.

125. Gudey SK, Sundar R, Mu Y, Wallenius A, Zang G, Bergh A, et al. TRAF6 stimulates the tumor-promoting effects of TGFbeta type I receptor through polyubiquitination and activation of presenilin 1. Sci Signal. 2014;7(307):ra2. doi: 10.1126/scisignal.2004207. PubMed PMID: 24399296.

126. Kawasaki K, Freimuth J, Meyer DS, Lee MM, Tochimoto-Okamoto A, Benzinou M, et al. Genetic variants of Adam17 differentially regulate TGFbeta signaling to modify vascular pathology in mice and humans. Proc Natl Acad Sci U S A. 2014;111(21):7723-8. doi: 10.1073/pnas.1318761111. PubMed PMID: 24812125; PubMed Central PMCID: PMCPMC4040598.

127. Jackson LF, Qiu TH, Sunnarborg SW, Chang A, Zhang C, Patterson C, et al. Defective valvulogenesis in HB-EGF and TACE-null mice is associated with aberrant BMP signaling. EMBO J. 2003;22(11):2704-16. doi: 10.1093/emboj/cdg264. PubMed PMID: 12773386; PubMed Central PMCID: PMCPMC156761.

128. van Erp S, van den Heuvel DM, Fujita Y, Robinson RA, Hellemons AJ, Adolfs Y, et al. Lrig2 Negatively Regulates Ectodomain Shedding of Axon Guidance Receptors by ADAM Proteases. Dev Cell. 2015;35(5):537-52. doi: 10.1016/j.devcel.2015.11.008. PubMed PMID: 26651291.

129. Mochizuki S, Okada Y. ADAMs in cancer cell proliferation and progression. Cancer Sci. 2007;98(5):621-8. doi: 10.1111/j.1349-7006.2007.00434.x. PubMed PMID: 17355265.

130. Saftig P, Reiss K. The "A Disintegrin And Metalloproteases" ADAM10 and ADAM17: novel drug targets with therapeutic potential? Eur J Cell Biol. 2011;90(6-7):527-35. doi: 10.1016/j.ejcb.2010.11.005. PubMed PMID: 21194787.

131. Wetzel S, Seipold L, Saftig P. The metalloproteinase ADAM10: A useful therapeutic target? Biochim Biophys Acta. 2017;1864(11 Pt B):2071-81. doi: 10.1016/j.bbamcr.2017.06.005. PubMed PMID: 28624438.

132. Marcello E, Gardoni F, Mauceri D, Romorini S, Jeromin A, Epis R, et al. Synapse-associated protein-97 mediates alpha-secretase ADAM10 trafficking and promotes its activity. J Neurosci. 2007;27(7):1682-91. doi: 10.1523/JNEUROSCI.3439-06.2007. PubMed PMID: 17301176.

133. Hemler ME. Tetraspanin functions and associated microdomains. Nat Rev Mol Cell Biol. 2005;6(10):801-11. doi: 10.1038/nrm1736. PubMed PMID: 16314869.

134. Yanez-Mo M, Barreiro O, Gordon-Alonso M, Sala-Valdes M, Sanchez-Madrid F. Tetraspanin-enriched microdomains: a functional unit in cell plasma membranes. Trends Cell Biol. 2009;19(9):434-46. doi: 10.1016/j.tcb.2009.06.004. PubMed PMID: 19709882.

135. Sato K, Norris A, Sato M, Grant BD. C. elegans as a model for membrane traffic. WormBook. 2014:1-47. doi: 10.1895/wormbook.1.77.2. PubMed PMID: 24778088; PubMed Central PMCID: PMCPMC4096984.

136. Amin NM, Hu K, Pruyne D, Terzic D, Bretscher A, Liu J. A Zn-finger/FH2-domain containing protein, FOZI-1, acts redundantly with CeMyoD to specify striated body wall muscle fates in the Caenorhabditis elegans postembryonic mesoderm. Development. 2007;134(1):19-29. doi: 10.1242/dev.02709. PubMed PMID: 17138663.

137. Audhya A, Desai A, Oegema K. A role for Rab5 in structuring the endoplasmic reticulum. J Cell Biol. 2007;178(1):43-56. doi: 10.1083/jcb.200701139. PubMed PMID: 17591921; PubMed Central PMCID: PMCPMC2064419.

138. Mezyk-Kopec R, Bzowska M, Stalinska K, Chelmicki T, Podkalicki M, Jucha J, et al. Identification of ADAM10 as a major TNF sheddase in ADAM17-deficient fibroblasts. Cytokine. 2009;46(3):309-15. doi: 10.1016/j.cyto.2009.03.002. PubMed PMID: 19346138.

139. Suzuki Y, Yandell MD, Roy PJ, Krishna S, Savage-Dunn C, Ross RM, et al. A BMP homolog acts as a dose-dependent regulator of body size and male tail patterning in Caenorhabditis elegans. Development. 1999;126(2):241-50. PubMed PMID: 9847238.

140. Morita K, Chow KL, Ueno N. Regulation of body length and male tail ray pattern formation of Caenorhabditis elegans by a member of TGF-beta family. Development. 1999;126(6):1337-47. PubMed PMID: 10021351.

141. Stefanakis N, Carrera I, Hobert O. Regulatory Logic of Pan-Neuronal Gene Expression in C. elegans. Neuron. 2015;87(4):733-50. doi: 10.1016/j.neuron.2015.07.031. PubMed PMID: 26291158; PubMed Central PMCID: PMCPMC4545498.

142. Brou C, Logeat F, Gupta N, Bessia C, LeBail O, Doedens JR, et al. A novel proteolytic cleavage involved in Notch signaling: the role of the disintegrin-metalloprotease TACE. Mol Cell. 2000;5(2):207-16. PubMed PMID: 10882063.

143. Chan SS, Zheng H, Su MW, Wilk R, Killeen MT, Hedgecock EM, et al. UNC-40, a C. elegans homolog of DCC (Deleted in Colorectal Cancer), is required in motile cells responding to UNC-6 netrin cues. Cell. 1996;87(2):187-95. PubMed PMID: 8861903.

144. Tucher J, Linke D, Koudelka T, Cassidy L, Tredup C, Wichert R, et al. LC-MS based cleavage site profiling of the proteases ADAM10 and ADAM17 using proteome-derived peptide

libraries. J Proteome Res. 2014;13(4):2205-14. doi: 10.1021/pr401135u. PubMed PMID: 24635658.

145. Stavoe AK, Colon-Ramos DA. Netrin instructs synaptic vesicle clustering through Rac GTPase, MIG-10, and the actin cytoskeleton. J Cell Biol. 2012;197(1):75-88. doi: 10.1083/jcb.201110127. PubMed PMID: 22451697; PubMed Central PMCID: PMCPMC3317799.

146. Healey EG, Bishop B, Elegheert J, Bell CH, Padilla-Parra S, Siebold C. Repulsive guidance molecule is a structural bridge between neogenin and bone morphogenetic protein. Nat Struct Mol Biol. 2015;22(6):458-65. doi: 10.1038/nsmb.3016. PubMed PMID: 25938661; PubMed Central PMCID: PMCPMC4456160.

147. Sakaguchi A, Sato M, Sato K, Gengyo-Ando K, Yorimitsu T, Nakai J, et al. REI-1 Is a Guanine Nucleotide Exchange Factor Regulating RAB-11 Localization and Function in C. elegans Embryos. Dev Cell. 2015;35(2):211-21. doi: 10.1016/j.devcel.2015.09.013. PubMed PMID: 26506309.

148. Janes PW, Saha N, Barton WA, Kolev MV, Wimmer-Kleikamp SH, Nievergall E, et al. Adam meets Eph: an ADAM substrate recognition module acts as a molecular switch for ephrin cleavage in trans. Cell. 2005;123(2):291-304. doi: 10.1016/j.cell.2005.08.014. PubMed PMID: 16239146.

149. Yi W, Holmlund C, Nilsson J, Inui S, Lei T, Itami S, et al. Paracrine regulation of growth factor signaling by shed leucine-rich repeats and immunoglobulin-like domains 1. Exp Cell Res. 2011;317(4):504-12. doi: 10.1016/j.yexcr.2010.11.005. PubMed PMID: 21087604.

150. Kawahara R, Granato DC, Yokoo S, Domingues RR, Trindade DM, Paes Leme AF. Mass spectrometry-based proteomics revealed Glypican-1 as a novel ADAM17 substrate. J Proteomics. 2017;151:53-65. doi: 10.1016/j.jprot.2016.08.017. PubMed PMID: 27576135.